EUSKAL HERRIKO UNIBERTSITATEA
UNIVERSITY OF THE BASQUE COUNTRY

Department of Electricity and Electronics

CAMPUS OF INTERNATIONAL EXCELLENCE

Space-time symmetries in classical and quantum electromagnetic scattering theory

Thesis by

Jon Lasa Alonso

Supervised by

Dr. Gabriel Molina Terriza

and

Dr. Aitzol García Etxarri

Donostia, December 2023

(Page intentionally left blank)

A las personas que alimentaron mi interés por la Física. A las que me han acompañado en estos años. Este trabajo es también vuestro.

(Page intentionally left blank)

ACKNOWLEDGEMENTS

Una tesis es un pedazo de la vida. Un tiempo en el que los estudiantes ponemos literalmente el cuerpo y el alma por hacer una aportación al conocimiento. Corazón y, también, tripas. Por eso creo que, así como es fundamental tener unos buenos referentes técnicos y científicos, es absolutamente crucial favorecer un acompañamiento personal y humano a lo largo de todo el proceso. En estos años, siento que he tenido el privilegio de haber conocido a personas que me han acompañado tanto técnica como personalmente.

Aitzol, tú que me has visto crecer científicamente (acuérdate de aquellas prácticas de verano en 2017), has sido un referente respecto de la gestión de las personas y, sobre todo, de los estudiantes. Creo que los doctorandos que hemos estado bajo tu supervisión estaríamos de acuerdo en esto. Desde que comenzamos a trabajar juntos, tu implicación personal me ha reforzado en momentos difíciles y ha contribuido a que siguiera avanzando. Gracias.

Gabriel, acerté de pleno al elegir el laboratorio y, en definitiva, tu grupo para desarrollar la tesis. Siento que hay dos aspectos de tu personalidad que han marcado mi trabajo a lo largo de estos años. Primero, la pasión por lo que hacemos y la determinación por hacerlo bien. Y, segundo, la libertad para decidir desarrollar los proyectos que consideremos que son más relevantes. Sin duda, esta tesis no hubiera sido posible sin tus enseñanzas y reflexiones. Gracias.

También quisiera agradecer a otros investigadores que, aunque no hayan estado directamente relacionados con la supervisión de mi tesis, sí creo que han jugado un papel importante en diferentes partes del proceso. Mole, gracias por enseñarme que la buena ciencia puede hacerse en una pizarra y que las conversaciones más interesantes pueden darse en cualquier esquina. Geza, thanks for pushing the projects during the first years of my PhD. It was not an easy moment, the pandemic was around, and, still, we managed to reach our goals. I really appreciate it. Finally, Iwo and Zofia, it was a real pleasure to share with you a few weeks in Warsaw. Thanks for sharing your thoughts and your knowledge, you are an inspiring example for the coming generations.

En lo personal, quiero agradecer primero el apoyo de mis compañeros. La gente con la que he aprendido que para embarcarse en un proyecto a largo plazo, como es una tesis, es fundamental echar raíces. Primero, a los titanes que me abrieron las puertas del CFM allá por Mayo de 2018, Álvaro y Antton. Vuestra hospitalidad fue fundamental para que me sintiera bienvenido en aquel lugar que aún era extraño para mí. Después Txemikel, que en Junio de aquel mismo año supimos que, en aquel cuarto lleno de radiadores en el techo, íbamos a tener que montar un laboratorio. Gracias por tu disposición y, sobre todo, gracias por pedir que te armaran un chulengo con una bombona de nitrógeno líquido. 2018 fue un año especial también porque,

después de 2 años, me reencontraría con un antiguo compañero de la carrera. Martín, eres un grande. Gracias por tu cariño y por ese humor absurdo con el que tan buenos ratos hemos pasado. ¡Ánimo en la recta final! Carlitos, valiente y luchador. Creo que has sido una de las personas con las que más he aprendido durante el doctorado. Te deseo lo mejor y que las lecciones que hemos aprendido en estos años nos sirvan también para la vida.

En general, he tenido mucha suerte de comenzar la tesis junto con la camada de los primeros *juegos del hambre*. Carmen, Cris, Marina, Miguel Ángel, Joseba, Rodrigo, Fer, Auguste, Thomas, Jorgito, Mikel, Raulillo. A los que muy rápidamente se unirían Cris, Jorge, Iker, Rober y Bruno. Muchos ratos buenos juntos y, sobre todo, mucha comprensión y desahogo en algunos momentos complicados. Siento que el núcleo que formamos en esos primeros años ha servido como red de apoyo en los años posteriores. Lo bueno, además, es que el grupo siempre ha estado abierto a los nuevos estudiantes que iban progresivamente llegando al CFM. Creo que se generó un ambiente muy permeable y amigable, que permitió que personas como Alberto, Josu, Adrian o Johnny, se incorporaran con facilidad. La verdad es que ha sido un placer poder compartir este camino con todos vosotros. Ha habido momentos especiales que merecen especial mención y, sin duda, los cumples de Carmen se llevan la palma. Los pintxopotes de los lunes, martes, miércoles, jueves y viernes fueron también divertidos, mientras aguantamos... Incluso las semanas de conferencia en Benasque o los asados argentinos, presentes desde el primer día en que la mayoría de nosotros nos conocimos en Arrokaundieta. ¡Gracias por todos estos buenos momentos!

Por otro lado, las personas que poco a poco han ido construyendo lo que hoy en día es el Laboratorio de Nanofotónica Cuántica. Las reuniones de los viernes creo que son un buen ejemplo de cómo se puede compartir el conocimiento científico de una forma sana y participativa. Rubén, eres un ejemplo a seguir, gracias por tu amabilidad y contagiosa curiosidad. Miriam, ¡suerte en tu nueva aventura alpina! María, la persona que más rápidamente he visto adaptarse a un nuevo lugar. Ha sido un placer compartir este último año contigo. El laboratorio queda en buenas manos: Jason, Ángel, Pablo, Rubén, Isaac, Mikel, Alexey, Sha, Quimey. Las dinámicas de grupo creo que han tenido la virtud de que en algún momento hayamos podido intercambiar comentarios o consejos, por muy distintos que a veces hayan sido nuestros temas de investigación. Como teórico he aprendido mucho de vuestras explicaciones sobre los experimentos, creo que ha sido una parte fundamental de mi formación en estos años. Gracias por vuestras enseñanzas. Por otro lado, también quisiera agradecer a los *Etxarri's children* por su afabilidad y alegría: María, Teresa, Javi, Carol, Edurne, Nuno, Antonio. In particular, I would like to acknowledge Chiara, for letting me learn from your incredible skills for science. It has been a pleasure to work along with you!

Además, me gustaría mencionar el trabajo del personal del CFM y el DIPC. Personas como Mari Mar, Ane y Marta en las administraciones, cuyo trabajo es completamente necesario para que nosotros

desenpeñemos el nuestro. Y, también, Juan, una persona clave en la construcción del laboratorio. También quisiera agradecer a Dani su trabajo al frente de la dirección del CFM en estos últimos 4 años. Gestionar una institución con tantos trabajadores a cargo no es fácil y siento que, en lo que respecta a los investigadores predoctorales, has jugado un papel muy importante. En este sentido, también cabe mencionar a Idoia. Gracias por tu apoyo laboral y humano, haces una labor necesaria (y, a veces, no remunerada) en el CFM.

A parte de los *cefemitos*, hay personas sin las que este camino tampoco hubiera sido posible. Sara, gracias por acompañarme en los primeros pasos del doctorado. Tu apoyo y sensibilidad contribuyeron a que encontrara mi senda y finalmente, mira, ¡llegamos al final! Eskerrik asko, benetan, emandako laguntza guztiagatik. Kuadrillari, orokorrean, beti presente izateagatik. Partikularmente, Txegus azkeneko urte eta erdian sortu dugun dupla padelero izugarri horrengatik eta Tross plan berriak egiteko prest egoteagatik. Manri, gran remero y mejor farrero, echaré de menos tus dominadas en el Aurresku. Petri, por el picantito que le pones a las conversaciones. Perma, por amenizar las tardes con tus siempre puntuales links de AceStream. Algarra, por advertirme de que el patín eléctrico va a tener problemas en subir las cuestas conmigo encima. Kepa, por tu cariño, dedicación y lealtad a la Real. Goe, por poner el listón de deportista lo suficientemente alto como para que el resto lo podamos pasar por debajo. Txintxe, por enseñarme que no hace falta ir de traje a una boda. Arrieta, por tener abiertas las puertas de Isla en verano y de Isaba en invierno. Y, por último, a Carrillo por tu presencia involuntaria en casi todos los planes de la kuadrilla.

También, quiero agradecer a los *Mariachis* los ratos que hemos seguido pasando incluso años después de habernos marchado de Salamanca. Primero, en esa época intermedia donde el campamento base se mudó a Madrid. Edu y Juan, fue siempre un placer visitaros en la capital y ponernos al día con las novedades. Después, también en Barcelona, visitando a Rodri y al Tomate. Y, finalmente, en Cáceres, eterna morada de Fran, Estévez y Rudi. ¡Gracias por seguir manteniendo viva la llama!

Por último, a la familia. Ama, por ser un referente de lucha y dignidad, y por enseñarme el valor del trabajo y la autonomía. Gracias. Aita, bidea ibiltzen bakarrik egin daitekeela erakusteagatik. Urteetan eman didazun sostengu hori gabe tesi hau ez litzateke posible izango. Eskerrik asko. Amaya eta Kizkitza, emandako laguntzagatik, zuek egindako bideek nirea ere argitzen laguntzen dutelako. Finalmente, Diana, gracias por tu amor y cariño.

¡Esta tesis es también vuestra!

Jon Lasa Alonso
Donostia, 1 de Diciembre de 2023

(Page intentionally left blank)

LABURPENA

XVII. mendean metodo zientifikoa ezarri zenetik, natur zientzien ikerketa lege axiomatikoetan oinarritu izan da. Proposamen arrakastatsu honen aitzindaria Newton izan zen. 1687an argitaratu zuen Principia liburuan, Mekanikaren diziplina lege matematikoetan (gaur egun Newtonen legeak deitzen ditugunak) oinarritzea proposatu zuen. Honako hau dio bere liburuan: *Gainerako fenomeno naturalak printzipio mekanikoetatik eta arrazoiketa mota berberetik ulertu ahal izatea nahiko nuke*. Bestela esanda, Newtonek gaur egun erabiltzen dugun eskema zientifikoaren oinarriak ezarri zituen. Bere bizitzan zehar, penduluen higidura periodikoa, jaurtigaien ibilbide parabolikoa eta gorputz astronomikoen orbita eliptikoak azaldu ahal izan zituen bere legeak abiapuntutzat hartuz. Ikerlari inglesari esker ere ulertzen dugu, adibidez, Lurrera erakartzen gaituen indar hori dela planetek Eguzkiaren inguruan egiten duten mugimenduaren arduraduna. Azkeneko honi grabitazio unibertsalaren legea deritzogu eta naturaren funtsezko lau interakzioetako bat kodifikatzen du. Newtonen arrakastak zientziaren garapena baldintzatu zuen hurrengo belaunaldietan. Harrezkero, fenomeno fisikoen azterketa matematikoa axiomatzat hartu beharreko ekuazio dinamikoetan oinarritu zen.

XVIII eta XIX. mendeetan hurbilketa axiomatikoaren beste hainbat adibide aurki ditzakegu. Kasu paradigmatikoena ziurrenik teoria elektromagnetikoaren eraikuntza da. Teoria honen ezarpena lan esperimentaletan oinarritu zen, bereziki, Coulomb, Ampère eta Faradayk egin zituzten behaketetan. Esperimentu hauetako gehienak korronte elektrikoa zeramaten kableen elkarreraginak aztertzen egin ziren. Faradayren lanetan oinarrituta, Maxwellek eremuaren kontzeptua proposatu zuen arte ez ziren eraiki elektromagnetismoaren lege matematikoak. Bere omenez, lege hauek Maxwellen ekuazioak deitzen dira eta fenomeno elektromagnetiko guztien sintesia osatzen dute. Hau da, ekuazio hauek axiomatzat hartuz, Maxwellek aurretik aurkitutako fenomeno elektriko eta magnetiko guztiak azaldu ahal izan zituen. Gainera, lege horietan oinarrituta, Maxwellek berak proposatu zuen lehen aldiz argia uhin elektromagnetiko bat izan zitekeela. Bere iragarpena 1887an baieztatu zuen Hertzek, irrati uhinen izaera elektromagnetikoa esperimentalki frogatu zuenean. XX. mende hasieran ere, zientziaren perspektiba axiomatikoa nagusi zen eta erabateko influentzia izan zuen, adibidez, teoria kuantikoan. Mekanika kuantikoan dinamika determinatzen duen lege matematikoa, Schrödingeren ekuazioa, postulatu gisa asimilatua izan zen.

Testuinguru honetan, 1930 eta 1940ko hamarkadetan, Eugene Wigner eta Valentine Bargmannen ekarpen nagusienak argitaratu ziren. Ikerlari hauen lanek eragin handia izan zuten zientziaren adar ezberdinetan, baina tesi honen egiturarekin bat datozen bi aipa ditzagun. Alde batetik, natur zientziek 250 urteetan zehar aintzat hartu izandako ikuspegi axiomatikoa zalantzan jarri zuten. Izan ere, zeinbat

ekuazio dinamiko, tartean Klein-Gordonen ekuazioa edota Diracen ekuazioa, espazio-denboraren simetrien ondorio zirela erakutsi zuten. Honela, lege naturalekiko hurbilketa berri bat sortu zen, non ekuazio dinamikoak postulatu gisa onartzea ez zen beharrezkoa. Erlatibitate bereziak ezartzen zituen kondizioen ondorio ziren, besterik ez. Bestetik, Wigner eta Bargmannek Maxwellen ekuazioak (espazio hutsean) ere simetria erlatibisten ondorio zirela erakutsi zuten. Wignerren klasifikazioan, eremu elektromagnetikoaren ekuazioak masarik gabeko eta spin bateko partikula batekin erlazionaturik agertzen ziren, hau da, fotoiarekin. Honela, Wigner eta Bargmannen lanek teoria elektromagnetikoa ikuspegi alternatibo batetik aztertzeko esparrua ezarri zuten. Ikuspegi alternatibo honi jarraipena eman dioten hainbat ikerlari daude, baina azpimarratzekoa da Iwo Bialynicki-Birula eta Zofia Bialynicka-Birulak egin duten lana. Riemann-Silberstein bektorearen inguruan egin dituzten ikerketekin, Wigner eta Bargmannen kontribuzioak gaur egungo zientzilariei transmititzea lortu dute.

Tesi honetan, Wigner eta Bargmannen lanetan inspiratuta, uhin elektromagnetikoen dinamika aztertzeko beste ikuspegi bat proposatuko dugu. Talde teoriaren aplikazio sistematikoak ongi ikertuta dauden gaietan emaitza berriak lortzera eraman gaitzakela erakutsiko dugu. Gure tresna nagusiena Riemann-Silberstein bektorea izango da, Iwo Bialynicki-Birulak eta Zofia Bialynicka-Birulak ekarpen ugaritan aurkeztu eta eztabaidatu dutena. Lehenik, Riemann-Silberstein bektoreak simetria taldeekin duen erlazioaz hitz egingo dugu, eta ondoren, teoria elektromagnetiko klasiko eta kuantikoko barreiatze problemak ebazteko erabiliko dugu. Beraz, tesi honen helburua bi adar ezberdinetan banatu genezakeen. Alde batetik, Riemann-Silberstein bektorearen ezaugarri matematiko nagusienak aztertuko ditugu talde teoria erabiliz. Analisi honek elektromagnetismoak beste teoria fisiko erlatibista eta ez-erlatibistekin duen erlazioa ikertzera eramango gaitu. Eta, bestetik, Riemann-Silberstein bektorea problema praktikoetan nola erabili dezakegun aztertuko dugu. Tesiaren kapituluak honela daude egituratuta:

1. kapituluan, gaiaren sarrera historiko bat egingo dugu. Wigner eta Bargmannen lanak bere kontextuan jarriko ditugu eta teoria elektromagnetikoaren inguruan egin zituzten ekarpen funtsezkoenak aipatuko ditugu. Horretaz gain, tesian jorratuko ditugun gaien estruktura orokorra azalduko dugu.

2. kapituluan, lehenik eta behin, Maxwellen ekuazioak forma kanonikoan aurkeztuko ditugu eta tesian zehar erabiliko ditugun erlazio konstitutiboak azalduko ditugu. Gainera, Riemann-Silberstein bektorearen hainbat bertsio aurkeztuko ditugu: espazio hutsean, inguru homogeneotan eta inguru inhomogeneotan. Ikusiko dugunez, Maxwellen ekuazioek forma oso bereizgarria hartzen dute Riemann-Silberstein bektorea erabiltzen dugunean. Hurbilketa alternatibo honek eremu elektromagnetikoaren helizitatea sakonki aztertzen lagunduko digu, Riemann-Silberstein bektorea helizitate operadorean bektore propioa delako hain zuzen. Azkenik, talde teoriako oinarrizko kontzeptu batzuk aipatuko ditugu. Uhin elektromagnetikoek bektore espazio bat osatzen dutenez, espazio-denborako simetria taldeen errepresen-

tazioak sor ditzakegula ikusiko dugu. Honela, adibide modura, Poincaré simetria taldearen posizio errepresentazioaren berezitasunak aztertuko ditugu.

3. kapituluan, helizitateak simetria talde ezberdinekin duen erlazioa aztertuko dugu. Alde batetik, erlatibitate espezialeko Poincaré simetria taldearekin duen erlazioa aztertuko dugu. Kasu honetan, helizitatearen balioak masarik gabeko partikulen errepresentazio laburtezinak ezberdintzen dituela ikusiko dugu. Hau da, Poincaré taldeko errepresentazio laburtezin batzuentzako, helizitatea Casimir operadore bat dela ikusiko dugu. Gainera, Bialynicki-Birulak proposatutako fotoiaren uhin funtzioa ere Poincaré taldearen errepresentazio laburtezinekin erlazionaturik dagoela aurkituko dugu. Honetaz gain, helizitateak simetria talde euklideoarekin, hau da, ez-erlatibistarekin, duen erlazioa aztertuko dugu. Kasu honetan ere Casimir operadore bat dela ikusiko dugu, momentu linealaren moduloarekin batera. Beraz, helizitateak talde euklideoaren errepresentazio laburtezinak bereizten dituela ikusiko dugu. Gainera, Riemann-Silberstein bektorearen bertsio monokromatikoa talde euklideoaren errepresentazio laburtezinekin erlazionatuta dagoela ikusiko dugu. Azkenik, talde teoriako argumentuak erabiliz, uhin elektromagnetiko monokromatiko batzuen expresio matematikoak eraikiko ditugu. Tartean, uhin lauak, Bessel uhinak edota uhin esferikoak.

4. kapituluan, Riemann-Silberstein bektore monokromatikoa barreiatze elektromagnetikoko problemak ebazteko erabiliko dugu. Horretarako, aurreko kapituluan definituriko uhin esferikoak erabiliko ditugu. Hasteko, barreiatze klasikoko magnitude garrantzitsuenak Riemann-Silberstein bektorea erabiliz aurkeztuko ditugu. Besteak beste, barreiatutako eta iraungitutako energia elektromagnetikoaren formulak helizitate konponenteekin emango ditugu. Ondoren, partikula dual eta partikula antidualen propietate optikoak aztertuko ditugu. Hauek, hurrenez hurren, barreiatze prozesuan uhin elektromagnetikoen helizitatea mantendu eta guztiz aldatzen duten laginak dira. Ikusiko dugunez, dualak eta antidualak diren partikulak sortu ahal izateko materialek kondizio berezi batzuk bete behar dituzte energiari dagokionez. Partikula dual dielektrikoek ezin dute absortzio optikorik izan eta partikula antidualak sortzeko materialei energia ponpatu egin behar zaie. Azkenik, partikula zilindrikoen ezaugarri optikoak neurtzeko erabilgarriak izan daitezkeen erlazio batzuk aztertuko ditugu. Konkretuki, Single Characterization Angle (SCA) metodoa aurkeztuko dugu, etorkizunean partikula zilindriko batzuen propietateak foto-detektore batekin bakarrik neurtzea ahal bidetu dezakeen metodoa.

5. kapituluan, uhin elektromagnetikoen hedapena inguru magnetiko eta inhomogeneotan aztertuko dugu. Lehenik, Riemann-Silberstein bektore monokromatikoa erabiliz, Maxwellen ekuazioek inguru hauetan hartzen duten forma aztertuko dugu. Ikusiko dugunez, analisi honen ondorioz, errefrakzio indizea eta inpedantzia konstantea duten inguru inhomogeneoak era naturalean agertuko zaizkigu. Bi inguru mota hauek soluzio analitikoa duten problema batzuetan aztertuko ditugu: Fresnel eta Mieren barreiatze problemetan; hau da, uhin elek-

tromagnetiko lau batek azalera infinitu batekin edo esfera batekin elkareragiten duen problemetan hain zuzen. Ondoren, errefrakzio indizea konstantea duten inguruak gertuagotik ikertuko ditugu. Horretarako, mekanika kuantikoan sarritan erabili ohi den perturbazio teoria aplikatuko dugu. Azkenik, errefrakzio indizea eta inpedantzia konstante duten inguruetan kontserbatzen diren magnitude fisikoak aztertuko ditugu. Ikusiko dugunez, 3. kapituluan azaldutako talde teorian oinarrituta, analisi honek Kerkeren fenomenoen interpretazio alternatibo bat ahal bidetuko du.

6. kapituluan, barreiatze kuantikoko problemak aztertuko ditugu. Horretarako, lehenik eta behin, eremu elektromagnetikoa bigarren kuantizazioaren formalismoan adieraziko dugu. Beam splitter kuantikoaren deskripzioan oinarriturik, fotoien barreiatzea *input-output* erako erlazio linealekin deskribatuko dugu. Ondoren, partikula zilindrikoetan zentratuko gara. Fotoi egoera batzuk, simetriaz-babesturiko egoerak deritzogunak, forma honetako laginekin elkareragitean aldatu gabe gelditzen direla ikusiko dugu. Simetriaz-babesturiko fotoi egoera hauek, gainera, fotoi bakar batez edo fotoi askoz osaturik egon daitezkeela ikusiko dugu. Horretaz gain, simetriaz-babesturiko egoerak momentu angeluarraren balio ezberdinak dituzten fotoiekin osatu daitezkeela ikusiko dugu ere bai. Azkenik, simetriaz-babesturiko fotoi egoerak dekoherentziaz libre dauden azpiespazioak sortzeko baliagarriak izan daitezkela ikusiko dugu.

7. kapituluan, tesi honetako ondorio nagusienak azalduko ditugu. Alde batetik, lortu izan ditugun lorpen garrantzitsuenak azpimarratu eta, bestetik, etorkizunera begira egin daitezkeen aurrera pausuak ere aztertuko ditugu.

Gure analisiarekin, simetria printzipioak beste problema elektromagnetiko batzuk ikertzeko ere erabilgarriak izan daitezkeela ikusiko dugu. Konkretuki, Riemann-Silbertein bektorearen aplikazio sistematikoak ongi aztertuta dauden beste hainbat gaietan emaitza eta ikuspegi berriak ekarri ditzakeela uste dugu. Tesi honetan egingo dugun ikerketa magnitude elektromagnetiko zehatz batzuetan zentratuko da, baina Riemann-Silberstein bektorearen aplikazio eremua askozez haratago joan daitekeela uste dugu. Adibidez, barreiatze problema klasikoetan indar eta torke elektromagnetikoak aztertzeko ere erabili daitekeela ikusi izan dugu. Horretaz gain, partikula dual eta antidualei dagokienez, materialen propietateekiko menpekotasun garrantzitsuak dituztela ikusiko dugu. Horregatik, diseinu esperimentalek partikula mota horiek zein baldintzatan eraiki daitezkeen (edo ezin daitezkeen) izan beharko dute kontutan. Azkenik, Single Characterization Angle (SCA) metodoak potentzial argia du laborategietan egiten diren neurketa espektroskopikoak sinplifikatzeko. Ikerketa talde batzuk jada metodo hau zein baldintza esperimentaletan aplikatu daitekeen aztertzen ari dira.

Bestalde, azkeneko bi kapituluetan egindako ekarpenek inpaktu kontzeptualago bat izango dutela uste dugu. Alde batetik, errefrakzio indize konstanteko eta impedantzia konstanteko inguru inhomogeneoak elektromagnetismoko hainbat kontextutan paraleloki agertzen direla ikusiko dugu. Gainera, errefrakzio indize konstanteko ingu-

ruetan eremu elektromagnetikoaren helizitate konponenteen nahaste erresonantea gertatzen dela aurkituko dugu ere bai. Fenomeno hau beste partikula fundamentaletan aztertu izan da, adibidez, neutrinoetan. Gure ustetan, partikula ezberdinen arteko antzekotasun matematiko hauek modu sakonago batean ikertzea interesgarria litzateke. Honetaz gain, errefrakzio indize konstanteko inguru inhomogeneoen analisiak duela 40 urte Kerker, Wang eta Gilesek aurkitu zituzten fenomenoen jatorria argitzen duela uste dugu. Bestetik, simetria argudioak barreiatze kuantikoko problemetan ere erabil daitezkeela erakutsiko dugu. Ildo honetan, sistema optiko ugari daude simetria zilindrikoa dutenak, tartean, fibra optiko zirkularrak. Riemann-Silberstein bektorearen aplikazioa sistema hauetan ere erabilgarria izan daitekeela esan genezake.

Oro har, gure ekarpenek aurrera pausu kontzeptualak eta praktikoak dakartzatela uste dugu. Teoriaren arloan eginiko ekarpen zientifikoek indar handia hartzen dute kasu praktikoetan erabilgarri direla aurkitzen denean eta, bestalde, ekarpen praktikoek indarra hartzen dute ere bai paradigma teoriko berriak bultzatzen dituztenean. Tesi honetan, zientzaren bi noranzko horietan ibiltzen saiatu gara. Emandako pausuak datozen ikerlarientzat erabilgarriak eta inspiratzaileak izatea espero dugu.

(Page intentionally left blank)

LIST OF CONTRIBUTIONS

Publications closely related to this thesis:

I **J. Lasa-Alonso**, M. Molezuelas-Ferreras, J. J. M. Varga, A. García-Etxarri, G. Giedke and G. Molina-Terriza. "Symmetry protection of multiphoton states of light", New Journal of Physics 22, 123010 (2020).

II J. Olmos-Trigo, C. Sanz-Fernández, D. R. Abujetas, **J. Lasa-Alonso**, N. de Sousa, A. García-Etxarri, J. A. Sánchez-Gil, G. Molina-Terriza and J. J. Sáenz. "Kerker conditions upon lossless, absorption and optical gain regimes", Physical Review Letters 125, 073205 (2020).

III **J. Lasa-Alonso**, J. Olmos-Trigo, A. García-Etxarri and G. Molina-Terriza. "Correlations between helicity and optical losses within general electromagnetic scattering theory", Materials Advances, 3, 4179-4185 (2022).

IV **J. Lasa-Alonso**, J. Olmos-Trigo, C. Devescovi, P. Hernández, A. García-Etxarri and G. Molina-Terriza. "Resonant helicity mixing of electromagnetic waves propagating through matter", Physical Review Research 5, 023116 (2023).

V J. Olmos-Trigo, **J. Lasa-Alonso**, I. Gómez-Viloria, G. Molina-Terriza and A. García-Etxarri. "Capturing near-field circular dichroism enhancements from measurements in the far-field", arXiv:2301.01248 (2023).

VI **J. Lasa-Alonso**, I. Gómez-Viloria, Á. Nodar, A. García-Etxarri, G. Molina-Terriza and J. Olmos-Trigo. "Characterizing cylindrical particles upon local measurements of two Stokes parameters", arXiv:2304.02762 (2023).

VII **J. Lasa-Alonso**, C. Devescovi, C. Maciel-Escudero, A. García-Etxarri and G. Molina-Terriza. "On the origin of the Kerker phenomena", arXiv:2306.12762 (2023).

Other relevant publications:

VIII **J. Lasa-Alonso**, D. R. Abujetas, Á. Nodar, J. A. Dionne, J. J. Sáenz, G. Molina-Terriza, J. Aizpurua and A. García-Etxarri. "Surface-enhanced circular dichroism on periodic dual nanostrucutures", ACS Photonics 7, 11, 2978–2986 (2020).

IX C. Sanz-Fernández, M. Molezuelas-Ferreras, **J. Lasa-Alonso**, N. de Sousa, X. Zambrana-Puyalto and J. Olmos-Trigo. "Multiple Kerker anapoles in dielectric microspheres", Laser & Photonics Reviews 15, 7, 2100035 (2021).

X C. Devescovi, M. García-Díez, I. Robredo, M. Blanco de Paz, **J. Lasa-Alonso**, B. Bradlyn, J. L. Mañes, M. G. Vergniory and A. García-Etxarri. "Cubic 3D Chern photonic insulators with orientable large Chern vectors", Nature Communications 12, 7330 (2021).

XI J. J. Miguel Varga, **Jon Lasa-Alonso**, Martín Molezuela-Ferreras, Nora Tischler and Gabriel Molina-Terriza. "Bandwidth control of the biphoton wave function exploiting spatio-temporal correlations", Optics Communications 505, 127461 (2022).

XII Á. Nodar, R. Esteban, C. Maciel-Escudero, **J. Lasa-Alonso**, J. Aizpurua and G. Molina-Terriza. "Preservation and destruction of entanglement of two-photon states in the interaction with a nanoscatterer", arXiv:2211.14244 (2022).

XIII M. Molezuelas-Ferreras, Á. Nodar, M. Barra-Burillo, J. Olmos-Trigo, **J. Lasa-Alonso**, I. Gómez-Viloria, E. Posada, J. J. M. Varga, R. Esteban, J. Aizpurua, L. E. Hueso, C. López and G. Molina-Terriza. "Characterizing the backscattered spectrum of Mie spheres", (accepted in Laser & Photonics Reviews).

CONTENTS

1

INTRODUCTION

In this Chapter, we provide some historical guidelines about how modern physics has been structured along the past 350 years. We particularly highlight the axiomatic approach implemented by Newton in his *Principia* and how it influenced physical sciences until the beginning of the twentieth century. In this framework, we put forward the works by Wigner and Bargmann, who showed that symmetry principles could replace the equations of motion under some circumstances. Finally, we introduce the structure of this thesis.

A BRIEF HISTORY OF MODERN PHYSICS

Medieval western philosophers defended that the comprehension of the universe could be addressed either by religious faith or by rational thought, commonly subjecting the latter to the former. However, at the beginning of the Modern era, a new epistemological scheme emerged: science. This new paradigm is based upon two fundamental pillars: experimental observation and the description of natural phenomena through mathematical laws. From the scientific point of view, the understanding of nature requires, on the one hand, a systematic empiric analysis of a particular phenomenon. Importantly, such an analysis has to be carried out quantitatively in terms of physical magnitudes such as time, position, velocity and so on. To complete the scientific understanding, such observations need to match a set of mathematical laws which relate the physical magnitudes in a particular way. One of the first achievements of the scientific method is the experimental observations of Tycho Brahe and the determination of Kepler's laws of the planetary motion around the sun. Brahe dedicated a great part of his lifetime to take accurate measurements of the motion of Mars. Based on his work, Kepler tried first to fit the data considering circular orbits, but he did not succeed. The deviations were above the experimental uncertainty. Finally, Kepler found that the curve which best fit Brahe's experimental data was not a circle, but an ellipse, leading to what is currently regarded as Kepler's first law of planetary motion.

A few decades after Kepler died, Newton put forward an axiomatic approach to Physics. In his *Principia*, published in 1687, he proposed that the discipline of Mechanics should be based on the assumption, a priori, of certain mathematical laws (currently regarded as Newton's laws) such that all the particular phenomena regarding the motion of bodies may be derived from them. He literally states: *I wish we could derive the rest of the phenomena of nature by the same kind of reasoning from mechanical principles*. In other words, it was Newton who implemented the scientific scheme that we still employ nowadays. Such an approach has barely 350 years and its validity has persisted in time due to the colossal predictions that have been corroborated since then. Only in his lifetime, Newton demonstrated that experimental observations such as the periodic motion of pendula, the parabolic trajectories of projectiles and the orbits of celestial bodies could be all explained taking as a starting point his laws. These findings lead to the idea that the same force that makes objects be attracted to the Earth is also responsible of the motion of the Moon around the Earth and the planets around the Sun. This is the so-called law of universal gravitation and supposes the codification of one of the four fundamental interactions of nature. Newton's success conditioned the conception of science in the coming generations. Since then, the mathematical study of physical phenomena was established in terms of dynamical equations that must be taken as axioms. And, of course, the scientific validity of such equations was, and it is still, subjected to experimental corroboration.

We find many other examples of this modern approach to science during the XVIII and XIX centuries. A paradigmatic case is the building of the electromagnetic theory. It begun with the experimental works of scientists such as Cavendish and Coulomb, who determined that electric charges suffer an attractive or repulsive force which is inversely proportional to the square of the distances [1, 2]. Their findings lead to the so-called Coulomb's law, which is one of the founding laws of electromagnetic theory. The settling of this theory is also based on experimental work developed during the XIX century, in particular, on the observations carried out by Ampère and Faraday. Most of these experiments were performed by studying the forces and interactions of conducting wires which carried electric currents [3]. It was not until Maxwell introduced the notion of a field, based on Faraday's observations, that the mathematical laws of electromagnetism were consistently built [4]. These laws, commonly regarded as Maxwell's equations, are not only a collection of previously reported laws, but constitute the synthesis of all electromagnetic phenomena in a handful of equations. In other words, taking these equations as axioms, Maxwell was able to explain all previously reported electric and magnetic phenomena. Furthermore, based on those same laws, Maxwell himself proposed, for the first time, the existence of electromagnetic waves (including light). His prediction was confirmed in 1887 by Hertz, who experimentally demonstrated the electromagnetic character of radio waves.

By the end of the XIX century Newton's laws and Maxwell's equations were somehow thought to constitute the final synthesis of scientific knowledge. On the one hand, light had been shown to be an electromagnetic wave and, thus, all the optical phenomena was comprehensible from Maxwell's equations. Also, thermodynamics had been explained in terms of statistical mechanics, i.e. the microscopic motion of gas molecules, which made it derivable from Newton's principles. As a result, in the last part of the XIX century, almost all the physical observations of many different branches could be explained with a handful of mathematical laws. However, there were a few experiments which did not match either of the two theories, in particular, the optical spectrum of hydrogen and the so-called black bodies. The resolution to the latter was given by Planck, who introduced the notion of quantization. On the other hand, the understanding of the hydrogen atom had to wait until the 1920s, when Schrödinger showed that its spectrum could be computed from the newly proposed quantum theory. These and other findings led to the theory of Quantum Mechanics, which overcame the difficulties of Newton's laws to describe particle dynamics at the atomic scale. Finally, the mathematical law that determines the dynamics within the quantum theory, i.e. the Schrödinger equation, was also assimilated as a postulate and its validity lied (and still lies) in its power to give account of a great deal of experimental observations.

Despite of many experimental corroborations, the quantum theory based on Schrödinger's equation was not fully satisfactory at the time because it does not follow the principle of relativity introduced by

Einstein in 1905. As a result, it is only valid to describe the dynamics of microscopic particles moving at velocities small compared to the speed of light. This particular feature lead scientists to search for alternative ways of making the quantum theory compatible with special relativity. There was a variety of proposals. For instance, Klein and Gordon proposed an equation derived from the relativistic energy-momentum relation for massive particles, which in the massless case lead to the conventional wave equation. Then, Dirac proposed a relativistic equation which was of first order in the time derivatives and accounted for the hyperfine structure of the hydrogen spectra. Also, Weyl proposed an equation which described the relativistic dynamics of massless particles with spin $S = 1/2$ and so on. In short, by the end of the 1930s, a wide set of relativistic wave equations had been proposed, each of them applying to different types of particles. It is in this context that the seminal contributions by Wigner and Bargmann were published. First, in 1939 Wigner showed that the emergence of fundamental properties of elementary particles such as mass and spin could be understood in terms of group theoretical arguments [5]. Indeed, he provided a classification of all possible elementary particles in terms of the unitary irreducible representations of the Poincaré group. Then, in 1948, Bargmann and Wigner showed that the relativistic equations proposed by Klein, Gordon, Dirac, Weyl and so on could be associated with particular types of elementary particles that had previously been classified by Wigner [6].

The contributions of Wigner and Bargmann had an impact in many different aspects and branches of science, but let us highlight two which particularly concern the structure of this thesis. First, their work challenged the perspective in which Physics had been structured in the past 250 years. Particularly, the assumption that dynamical equations must be accepted as axioms. Indeed, they showed that the emergence of such a variety of dynamical equations was a consequence of the underlying symmetries of space-time. Thus, a different approach to natural laws emerged, where one needed not to assume the equations of motion as postulates, but only as a result of the constrains imposed by special relativity [7]. Second, they showed that, apart from the reported relativistic quantum equations, Maxwell's equations (in vacuum) also emerged as a result of their group theoretical analysis. In particular, within Wigner's classification, the equations of the electromagnetic field emerged as being associated with a massless particle of spin $S = 1$, i.e. the photon. Therefore, not only did their group theoretical approach unify the quantum mechanical equations of elementary particles, but it also included the laws of electromagnetism as part of the classification. In this line, the works of Wigner and Bargmann provided a framework to study the electromagnetic theory from an alternative point of view [8].

Symmetries and the introduction of group theory as a mathematical tool conditioned the development of science during the second half of the twentieth century. For instance, Wigner himself proposed a group theoretical approach to analyze and predict the spectrum of atoms and molecules taking into account their continuous and dis-

crete symmetries [9]. These same tools were extended in condensed matter physics to classify crystals, i.e. periodic arrangements of atoms, providing crucial insights about their band structure. On the other hand, symmetries were also central in the development of the Standard Model. Indeed, by the end of the 1970s, the study of gauge symmetries within the framework of quantum field theory led to the unification of the electromagnetic interaction with the nuclear weak and strong interactions into a single theory [10]. More recently, symmetries and group theory have served as a platform for the development of new research lines. An example which is, in a sense, related with this thesis is the field of photonic crystals which settled in the 1990s [11]. Inspired by the success of the mathematical framework in Quantum Mechanics, group theory has been systematically applied to study a variety of electromagnetic systems. The result has been remarkable as it has lead to completely new lines of research such as topological photonics or symmetry based electromagnetic scattering analysis.

MOTIVATION AND STRUCTURE OF THIS THESIS

The structure of this thesis is deeply inspired by the works of Wigner and Bargmann. Based on their seminal contributions on Maxwell's equations and relativistic wave equations, we propose a different approach to study electromagnetic wave dynamics. We show that the systematic application of some group theoretical concepts leads to new insights on well-studied topics such as linear electromagnetic scattering theory or the emergence of the Kerker phenomena. Our principal tool is the so-called Riemann-Silberstein vector which has been introduced and discussed by Iwo Bialynicki-Birula and Zofia Bialynicka-Birula in their seminal contributions to both classical and quantum electrodynamics. In this line, we first discuss the link of the Riemann-Silberstein vector with space-time symmetry groups and, then, we employ it to solve problems of classical and quantum electromagnetic scattering theory. This thesis is structured as follows:

> In Chapter 2, we introduce Maxwell's equations in the conventional form and discuss the type of fields and constitutive relations we will be dealing with during this thesis. Then, we define various forms of the Riemann-Silberstein vector in vacuum, in homogeneous media and in inhomogeneous media. Finally, we introduce some notions of group theory which will be useful for the next Chapter.
>
> In Chapter 3, we discuss the form of Maxwell's equations as given in the works by Wigner and Bargmann. We also show how the Riemann-Silberstein vector and Bialynicki-Birula's photon wave function is linked to Wigner's classification of elementary particles. Then, we apply group theoretical arguments to study the propagation of electromagnetic waves in infinitely homogeneous media. Finally,

we construct monochromatic electromagnetic wave solutions based on similar group theoretical arguments.

In Chapter 4, we put forward a few different applications of the monochromatic Riemann-Silberstein vector in classical electromagnetic scattering theory. After some general considerations and definitions, we delve into the study of dual and antidual scatterers. We show that the construction of these types of samples is subjected to some properties of the materials they are constituted from. Finally, we introduce the Single Characterization Angle (SCA) method that permits the characterization of cylindrical samples in favourable experimental conditions.

In Chapter 5, we extend the analysis to the propagation of electromagnetic waves through inhomogeneous media. After discussing the form of Maxwell's equations in terms of the monochromatic Riemann-Silberstein vector, we analyze the impedance and refractive index matching conditions. We employ perturbation theory to get an insight about these two conditions, leading to a quite instructive analogy with quantum two-level systems. Finally, we study the conserved quantities associated with such matching conditions and we provide an alternative interpretation of the emergence of the Kerker phenomena.

In Chapter 6, we adapt some of previously discussed concepts of classical scattering theory to study the interaction of quantum states of light with optical samples. Based on the framework of post-selected scattering matrices, we show that there are states which remain invariant through the interaction, i.e. the so-called symmetry-protected states. Finally, we show that symmetry-protection can be extended to the multi photon regime and, also, that it enables the construction of decoherence free subspaces.

In Chapter 7, we wrap up the main conclusions of this thesis and propose the lines in which our work may be developed in the future.

2

MAXWELL'S EQUATIONS AND ELECTROMAGNETIC WAVES

In this Chapter, we first present the canonical form of Maxwell's equations and the constitutive relations. Then, we introduce the usual definition of the Riemann-Silberstein vector in vacuum. We also make use of the monochromatic version of the Riemann-Silberstein vector to present an alternative form of Maxwell's equations in homogeneous and inhomogeneous media. Finally, we introduce some basic notions of group theory which will be useful for future discussions. In particular, we introduce relevant physical magnitudes, such as linear momentum or angular momentum, as the generators of continuous symmetry groups.

2.1 MAXWELL'S EQUATIONS

This thesis studies particular features of the electromagnetic field. As a result, the canonical starting point cannot be other than Maxwell's equations.

2.1.1 *General form and constitutive relations*

The most general form of Maxwell's equations is [12, 13]:

$$\nabla \times \mathcal{E}(\mathbf{r}, t) = -\partial_t \mathcal{B}(\mathbf{r}, t) \tag{2.1}$$

$$\nabla \times \mathcal{H}(\mathbf{r}, t) = \mathcal{J}(\mathbf{r}, t) + \partial_t \mathcal{D}(\mathbf{r}, t) \tag{2.2}$$

$$\nabla \cdot \mathcal{D}(\mathbf{r}, t) = \rho(\mathbf{r}, t) \tag{2.3}$$

$$\nabla \cdot \mathcal{B}(\mathbf{r}, t) = 0 \tag{2.4}$$

where $\mathcal{D}(\mathbf{r}, t)$ is the electric displacement, $\mathcal{B}(\mathbf{r}, t)$ is the magnetic induction, $\mathcal{E}(\mathbf{r}, t)$ is the electric field and $\mathcal{H}(\mathbf{r}, t)$ the magnetic field. Moreover, $\rho(\mathbf{r}, t)$ represents electric charge density and $\mathcal{J}(\mathbf{r}, t)$ the electric current density. In short, Eqs. (2.1)-(2.4) describe the local behaviour of the electromagnetic field in presence of electric charges and currents, which are the sources. Note that all the fields and magnitudes expressed in Eqs. (2.1)-(2.4) are real. In addition, such a set of equations already contains the charge conservation law implicitly. Indeed, taking the divergence of Eq. (2.2) and employing Eq. (2.3) we arrive to:

$$\partial_t \rho(\mathbf{r}, t) + \nabla \cdot \mathcal{J}(\mathbf{r}, t) = 0. \tag{2.5}$$

The mathematical relation given above is usually denoted as the continuity equation and it implies that electric charge is locally conserved at every time and point in space.

In this thesis, however, we do not study the behaviour of electromagnetic fields in charged media and, thus, we fix $\rho(\mathbf{r}, t) = 0$ and $\mathcal{J}(\mathbf{r}, t) = 0$. In turn, we will deal with macroscopic linear media, i.e. environments in which the relations between $\mathbf{D}(\mathbf{r}, \omega)$, $\mathbf{B}(\mathbf{r}, \omega)$, $\mathbf{E}(\mathbf{r}, \omega)$ and $\mathbf{H}(\mathbf{r}, \omega)$ are linear. In our notation, the vector field $\mathbf{V}(\mathbf{r}, \omega)$ represents the time Fourier transform of $\mathcal{V}(\mathbf{r}, t)$:

$$\mathcal{V}(\mathbf{r}, t) = \frac{1}{\sqrt{2\pi}} \int_{-\infty}^{+\infty} d\omega \, \mathbf{V}(\mathbf{r}, \omega) e^{-i\omega t}. \tag{2.6}$$

Given the relation between real fields and their Fourier transform specified by Eq. (2.6), we may express Maxwell's equations without charges, in the following form:

$$\nabla \times \mathbf{E}(\mathbf{r}, \omega) = i\omega \mathbf{B}(\mathbf{r}, \omega) \tag{2.7}$$

$$\nabla \times \mathbf{H}(\mathbf{r}, \omega) = -i\omega \mathbf{D}(\mathbf{r}, \omega) \tag{2.8}$$

$$\nabla \cdot \mathbf{D}(\mathbf{r}, \omega) = 0 \tag{2.9}$$

$$\nabla \cdot \mathbf{B}(\mathbf{r}, \omega) = 0. \tag{2.10}$$

This form of the equations applies to physical phenomena that may be well-described in terms of a single angular frequency, ω. As a result, the equations given by Eqs. (2.7)-(2.10) are usually called the monochromatic or time-independent Maxwell's equations (without charges and currents). Interestingly, note that, whenever $\omega \neq 0$, Faraday and Ampère's laws encoded in Eqs. (2.7)-(2.8) already contain Gauss' laws specified in Eqs. (2.9)-(2.10).

Finally, in this thesis we focus on isotropic media which are local in space and non-local in time. In plain words, space locality implies that relations between the different fields depend on the spatial coordinate, $\mathbf{r}$, whereas temporal non-locality implies that they depend on the frequency of the field, ω. Under these constrains, the constitutive relations between the electric and magnetic field vectors can most generally be written as [14]:

$$\mathbf{D}(\mathbf{r},\omega) = \varepsilon(\mathbf{r},\omega)\left[\mathbf{E}(\mathbf{r},\omega) + \gamma(\mathbf{r},\omega)\nabla\times\mathbf{E}(\mathbf{r},\omega)\right] \tag{2.11}$$

and

$$\mathbf{B}(\mathbf{r},\omega) = \mu(\mathbf{r},\omega)\left[\mathbf{H}(\mathbf{r},\omega) + \beta(\mathbf{r},\omega)\nabla\times\mathbf{H}(\mathbf{r},\omega)\right]. \tag{2.12}$$

In the expression above, $\varepsilon(\mathbf{r},\omega)$ is the electric permittivity, $\mu(\mathbf{r},\omega)$ is the magnetic permeability and, on the other hand, $\gamma(\mathbf{r},\omega)$ and $\beta(\mathbf{r},\omega)$ determine the chiral or bianisotropic response of the medium. During this thesis we will mostly deal with non-chiral media for which $\gamma = 0$ and $\beta = 0$, except in Chapter 4 where we will study the response of isotropic chiral spheres. Finally, we do not deal with anisotropic media, which means that constitutive relations are determined by scalar functions.

2.1.2 *Boundary conditions*

As we have just mentioned, we exclusively study the response of linear isotropic media, i.e. systems for which the constitutive relations are determined by Eqs. (2.11)-(2.12). More specifically, many practical examples we discuss along the thesis deal with piecewise homogeneous media. This type of optical environments are composed of various regions or domains in which the constitutive relations are constant in $\mathbf{r}$. For instance, a non-chiral piecewise homogeneous medium is an optical system for which $\varepsilon(\mathbf{r},\omega) = \varepsilon_j(\omega)$ and $\mu(\mathbf{r},\omega) = \mu_j(\omega)$ for $\mathbf{r} \in V_j$, where V_j represents a particular region of space. As a result, this type of media are characterized for having sharp boundaries.

Due to the presence of such boundaries, the electromagnetic field may have discontinuities. In this context, the boundary conditions determine exactly the effect of those discontinuities in the field components. Let us consider the discontinuities of the electromagnetic field at some point $\mathbf{r}_0$ within the interface between V_1 and V_2 domains. Let us also consider that, at that point, the normal vector pointing from region V_1 to region V_2 is denoted as $\hat{\mathbf{n}}$. As we do not consider the

presence of charges or currents, the boundary conditions acquire a relatively simple form [12]:

$$\hat{n} \cdot [\mathbf{D}_2(\mathbf{r},\omega) - \mathbf{D}_1(\mathbf{r},\omega)]\Big|_{\mathbf{r}=\mathbf{r}_0} = 0 \tag{2.13}$$

$$\hat{n} \cdot [\mathbf{B}_2(\mathbf{r},\omega) - \mathbf{B}_1(\mathbf{r},\omega)]\Big|_{\mathbf{r}=\mathbf{r}_0} = 0 \tag{2.14}$$

$$\hat{n} \times [\mathbf{E}_2(\mathbf{r},\omega) - \mathbf{E}_1(\mathbf{r},\omega)]\Big|_{\mathbf{r}=\mathbf{r}_0} = 0 \tag{2.15}$$

$$\hat{n} \times [\mathbf{H}_2(\mathbf{r},\omega) - \mathbf{H}_1(\mathbf{r},\omega)]\Big|_{\mathbf{r}=\mathbf{r}_0} = 0. \tag{2.16}$$

These expressions are employed in many situations such as the scattering of electromagnetic waves by spheres or planar surfaces, which we discuss in Chapters 4 and 5. Also, the same relations are useful to solve other relevant physical problems such as finding the guided modes in optical fibers, among many others. In all these situations, boundary conditions permit the determination of the amplitude of the electromagnetic field in the different regions V_j.

2.2 RIEMANN-SILBERSTEIN (RS) VECTOR

After introducing the general form of Maxwell's equations, we would like to present the Riemann-Silberstein (RS) vector. The interest of introducing this field is closely related with the effects we study along this thesis. Indeed, the RS vector is fundamental in the description of the internal degrees of freedom of electromagnetic waves. Electromagnetic waves are of transverse nature and, as such, oscillations of the fields can only happen in two specific directions, i.e. the two orthogonal directions to the direction of propagation. This degree of freedom has commonly been related to the spin angular momentum of the waves, however, as it has been shown by some authors, the intrinsic characteristic of a field representing a massless particle is not the spin, but its helicity [8, 15]. This is the main reason to consider a description of electromagnetic waves based on the RS vector, because it naturally splits the two helicity components of the electromagnetic field.

2.2.1 *Vacuum*

The RS vector is usually defined in terms of the electric displacement, $\mathcal{D}(\mathbf{r},t)$, and magnetic induction, $\mathcal{B}(\mathbf{r},t)$. In vacuum, it is most commonly constructed as [8]:

$$\mathcal{F}^{\lambda}(\mathbf{r},t) = \frac{1}{\sqrt{2}}\left[\frac{\mathcal{D}(\mathbf{r},t)}{\sqrt{\varepsilon_0}} + \lambda i \frac{\mathcal{B}(\mathbf{r},t)}{\sqrt{\mu_0}}\right], \tag{2.17}$$

where $\lambda = \pm 1$, ε_0 is the electric permittivity in vacuum and μ_0 the magnetic permeability in vacuum. Please note that the fields $\mathcal{D}(\mathbf{r},t)$ and $\mathcal{B}(\mathbf{r},t)$ are real and, thus, one has that $\mathcal{F}^{-\lambda}(\mathbf{r},t) = [\mathcal{F}^{\lambda}(\mathbf{r},t)]^*$. As we will see, λ represents the helicity of the electromagnetic field. However, for the time being, we can just take it as a parameter that allows

us express the electromagnetic field as a superposition of electric and magnetic fields.

In terms of the RS vector, Maxwell's equations in vacuum can be expressed as:

$$i\partial_t \mathcal{F}^\lambda(\mathbf{r},t) = \lambda \nabla \times \mathcal{F}^\lambda(\mathbf{r},t) \tag{2.18}$$

$$\nabla \cdot \mathcal{F}^\lambda(\mathbf{r},t) = 0, \tag{2.19}$$

where we have set the speed of light in vacuum $c = 1/\sqrt{\varepsilon_0 \mu_0} = 1$. The form of Maxwell's equations written above has been regarded as the "hamiltonian" formulation of electrodynamics. This follows from the analogy between Eq. (2.18) and the Schrödinger's equation. Indeed, the time-evolution equation for a quantum massive particle is: $i\partial_t \Psi(\mathbf{r},t) = H\Psi(\mathbf{r},t)$, where $\Psi(\mathbf{r},t)$ is the wave function of the particle and H is the hamiltonian of the system. As we will show in the following Chapter, the RS vector plays, in some sense, the role of the wave function in electrodynamics, which makes the analogy with Schrödinger's equation even sounder. In this line, it can also be checked that the RS vector in vacuum may also fulfill the wave equation. In other words, starting from Eqs. (2.18)-(2.19), we can build electromagnetic fields which are also solutions to the wave equation:

$$\nabla^2 \mathcal{F}^\lambda(\mathbf{r},t) - \partial_t^2 \mathcal{F}^\lambda(\mathbf{r},t) = 0. \tag{2.20}$$

The expression above represents the wave equation in terms of the RS vector. We denote as *electromagnetic waves* the electromagnetic fields which, apart from Maxwell's equations, also fulfill Eq. (2.20).

Let us now look for solutions of electromagnetic waves in terms of the RS vector. In what follows, we just consider the field $\mathcal{F}(\mathbf{r},t) = \mathcal{F}^+(\mathbf{r},t)$ and assume that $\mathcal{F}^-(\mathbf{r},t)$ can be obtained by complex conjugation. The natural way of solving Maxwell's equations as expressed in Eqs. (2.18)-(2.19) is by applying the space Fourier transform [16]. Defining the spatial Fourier transform as:

$$\mathcal{V}(\mathbf{r},t) = \frac{1}{(2\pi)^{3/2}} \int_{-\infty}^{+\infty} d\mathbf{k}\, \mathbf{V}(\mathbf{k},t) e^{i\mathbf{k}\cdot\mathbf{r}}, \tag{2.21}$$

we arrive to the following form of Eqs. (2.18)-(2.19):

$$\partial_t \mathbf{F}(\mathbf{k},t) = \mathbf{k} \times \mathbf{F}(\mathbf{k},t) \tag{2.22}$$

$$\mathbf{k} \cdot \mathbf{F}(\mathbf{k},t) = 0. \tag{2.23}$$

These relations imply that the RS vector, in reciprocal space, is contained in a plane orthogonal to $\mathbf{k}$, which allows us to express it in the very general form:

$$\mathbf{F}(\mathbf{k},t) = \alpha^+(\mathbf{k},t)\hat{e}^+(\mathbf{k}) + \alpha^-(\mathbf{k},t)\hat{e}^-(\mathbf{k}), \tag{2.24}$$

where the two unitary vectors, $\hat{e}^\pm(\mathbf{k})$, are orthogonal to $\mathbf{k}$ and the amplitude functions $\alpha^\pm(\mathbf{k},t)$ are complex. These few constrains permit the election of the unitary vectors in a quite free manner, concretely, Bialynicki-Birula chooses them such that [16]:

$$i\mathbf{k} \times \hat{e}^\pm(\mathbf{k}) = \pm|\mathbf{k}|\hat{e}^\pm(\mathbf{k}), \tag{2.25}$$

which also fulfill $\hat{e}^{-}(\mathbf{k}) = [\hat{e}^{+}(\mathbf{k})]^{*} = \hat{e}^{+}(-\mathbf{k})$ and $[\hat{e}^{\mp}(\mathbf{k})]^{*} \cdot \hat{e}^{\pm}(\mathbf{k}) = \hat{e}^{\pm}(\mathbf{k}) \cdot \hat{e}^{\pm}(\mathbf{k}) = 0$. The explicit form of $\hat{e}^{\pm}(\mathbf{k})$, such that Eq. (2.25) is fulfilled, had previously been derived by a few authors [16, 17]:

$$\hat{e}^{\pm}(\mathbf{k}) = -\frac{\mathbf{k} \times (\hat{m} \times \mathbf{k}) \mp ik(\hat{m} \times \mathbf{k})}{\sqrt{2}k|\hat{m} \times \mathbf{k}|}, \tag{2.26}$$

where $\hat{m}$ is an arbitrary unit vector.

As we see, the role of the polarization vector $\hat{e}^{\pm}(\mathbf{k})$ is central when representing electromagnetic fields in terms of the RS vector. It fixes a basis to represent the polarization of the Fourier components. In particular, if we choose $\hat{m} = \hat{z}$ and employ spherical coordinates in reciprocal space, i.e. $k_x = k \sin\theta_{\mathbf{k}} \cos\phi_{\mathbf{k}}$, $k_y = k \sin\theta_{\mathbf{k}} \sin\phi_{\mathbf{k}}$ and $k_z = k \cos\theta_{\mathbf{k}}$, then, we are lead to the following form of the polarization vector:

$$\hat{e}^{\pm}(\mathbf{k}) = \frac{1}{\sqrt{2}} \begin{pmatrix} \cos\phi_{\mathbf{k}} \cos\theta_{\mathbf{k}} \mp i \sin\phi_{\mathbf{k}} \\ \sin\phi_{\mathbf{k}} \cos\theta_{\mathbf{k}} \pm i \cos\phi_{\mathbf{k}} \\ -\sin\theta_{\mathbf{k}}. \end{pmatrix} \tag{2.27}$$

For instance, if we fix that our wave is propagating in the OZ direction, i.e. $\theta_{\mathbf{k}} = 0$ and $\phi_{\mathbf{k}} = 0$, we retrieve the form: $\hat{e}^{\pm} = (1, \pm i, 0)/\sqrt{2}$, which is the usual circular polarization vector associated with a plane-wave propagating in the positive OZ direction. The polarization vector given by Eq. (2.27) constitutes a general expression of a circular polarization vector associated with a plane-wave that propagates in an arbitrary direction. Note that the $\pm$ sign determines whether the unitary vector is left or right polarized. In our convention, the left polarized unitary vector, $\hat{e}^{+}(\mathbf{k})$, has positive helicity, whereas the right polarized vector, $\hat{e}^{-}(\mathbf{k})$, has negative helicity.

With this election of the unitary vectors, we are ready to obtain a general expression of the RS vector in reciprocal space. Introducing the expression in Eq. (2.24) into Eq. (2.22) and using the algebraic property given in Eq. (2.25) we arrive to:

$$\partial_t \alpha_{+}(\mathbf{k}, t) = -i|\mathbf{k}|\alpha_{+}(\mathbf{k}, t) \tag{2.28}$$

$$\partial_t \alpha_{-}(\mathbf{k}, t) = +i|\mathbf{k}|\alpha_{-}(\mathbf{k}, t), \tag{2.29}$$

which results in $\alpha_{\pm}(\mathbf{k}, t) = \alpha_{\pm}(\mathbf{k}) e^{\mp i\omega_k t}$, where $\omega_{\mathbf{k}} = |\mathbf{k}|$ (recall that $c = 1$). In conclusion, the RS vector in reciprocal space can be written as:

$$\mathbf{F}(\mathbf{k}, t) = f^{+}(\mathbf{k})\hat{e}^{+}(\mathbf{k})e^{-i\omega_k t} + [f^{-}(-\mathbf{k})\hat{e}^{-}(-\mathbf{k})]^{*} e^{i\omega_k t}, \tag{2.30}$$

where we have defined a new set of complex amplitudes $f^{+}(\mathbf{k}) = \alpha^{+}(\mathbf{k})$ and $[f^{-}(-\mathbf{k})]^{*} = \alpha^{-}(\mathbf{k})$. Finally, if we undo the spatial Fourier transform, we are left with the following form of the RS vector in real space:

$$\mathcal{F}(\mathbf{r}, t) = \frac{1}{(2\pi)^{3/2}} \int_{-\infty}^{+\infty} d\mathbf{k} \left\{ f^{+}(\mathbf{k})\hat{e}^{+}(\mathbf{k}) e^{i\mathbf{k}\cdot\mathbf{r} - i\omega_k t} + [f^{-}(\mathbf{k})\hat{e}^{-}(\mathbf{k})]^{*} e^{-i\mathbf{k}\cdot\mathbf{r} + i\omega_k t} \right\}. \tag{2.31}$$

where we have changed the integration variable of the second term of the integral as $\mathbf{k} \to -\mathbf{k}$. Importantly, note that the expression of the RS vector given in Eq. (2.31) is not only a solution to Maxwell's equations specified in Eqs. (2.18)-(2.19), but also to the wave equation given by Eq. (2.20).

From the result obtained in Eq. (2.31) we observe that the RS vector naturally splits the positive helicity components associated with positive frequencies and negative helicity components with negative frequencies. Here, however, we only deal with positive frequencies, i.e. with the so-called analytic signal of the fields [13]. As a result, we may define a new field, $\boldsymbol{\Psi}^{\lambda}(\mathbf{r}, t)$, which precisely takes on the positive energy parts of the RS vector and its complex conjugate [18]:

$$\boldsymbol{\Psi}^{\lambda}(\mathbf{r}, t) = \frac{1}{(2\pi)^{3/2}} \int_{-\infty}^{+\infty} d\mathbf{k}\, f^{\lambda}(\mathbf{k}) \hat{e}^{\lambda}(\mathbf{k}) e^{i\mathbf{k}\cdot\mathbf{r} - i\omega_k t}. \tag{2.32}$$

Note that $\boldsymbol{\Psi}^{+}(\mathbf{r}, t)$ takes the positive frequency component of $\mathcal{F}^{+}(\mathbf{r}, t)$ field given by Eq. (2.31), while $\boldsymbol{\Psi}^{-}(\mathbf{r}, t)$ takes the positive energy component of $\mathcal{F}^{-}(\mathbf{r}, t)$. Such a representation of an electromagnetic field is nothing but the statement that one can construct any propagating electromagnetic wave as a superposition of circularly polarized plane-waves with different frequencies and propagation directions. This, might seem quite obvious at this stage, but we will see that the expansion of electromagnetic waves in helicity Fourier components has interesting applications. In particular, this representation of the fields is useful in situations in which one aims to split the two polarization degrees of freedom. As we infer from Eq. (2.32), $\boldsymbol{\Psi}^{\lambda}(\mathbf{r}, t)$ naturally separates the Fourier components which are left ($\lambda = 1$) or right ($\lambda = -1$) polarized. Thus, employing $\boldsymbol{\Psi}^{\lambda}(\mathbf{r}, t)$ to describe electromagnetic waves, instead of the usual electric and magnetic fields, permits the separation of the helicity components in coordinate space.

2.2.2 *Homogeneous media*

Following the construction of Eq. (2.17), the monochromatic RS vector in an infinitely homogeneous medium may be defined as:

$$\mathbf{F}^{\lambda}(\mathbf{r}, \omega) = \frac{1}{\sqrt{2}} \left[\frac{\mathbf{D}(\mathbf{r}, \omega)}{\sqrt{\varepsilon}} + \lambda i \frac{\mathbf{B}(\mathbf{r}, \omega)}{\sqrt{\mu}} \right]. \tag{2.33}$$

With respect to the previous definition of the RS vector, we see that in this case we consider the electric permittivity, ε, and magnetic permeabilities, μ, different from those of vacuum. In addition, note that the monochromatic version of the RS vector is built from the complex displacement, $\mathbf{D}(\mathbf{r}, \omega)$, and magnetic induction, $\mathbf{B}(\mathbf{r}, \omega)$, fields. This implies that, unlike $\mathcal{F}^{\lambda}(\mathbf{r}, t)$, the two helicity components of the monochromatic RS vector, $\mathbf{F}^{\lambda}(\mathbf{r}, \omega)$, contain different information of the electromagnetic field, i.e. $\mathbf{F}^{-\lambda}(\mathbf{r}, \omega) \neq [\mathbf{F}^{\lambda}(\mathbf{r}, \omega)]^{*}$.

In an infinitely homogeneous medium, time-independent Maxwell's equations can be expressed in a very compact form with the aid of the monochromatic RS vector:

$$\frac{1}{\omega n}\nabla \times \mathbf{F}^{\lambda}(\mathbf{r},\omega) = \lambda \mathbf{F}^{\lambda}(\mathbf{r},\omega) \tag{2.34}$$

$$\nabla \cdot \mathbf{F}^{\lambda}(\mathbf{r},\omega) = 0, \tag{2.35}$$

where $n = \sqrt{\varepsilon\mu}$ is the refractive index of the medium and we have again set the speed of light in vacuum $c = 1$. Note that, as we have previously indicated, the four time-independent Maxwell's equations are fully contained in Eq. (2.34). In other words, Gauss' laws expressed in Eq. (2.35) can be derived just by taking the divergence of Faraday-Ampère's laws in Eq. (2.34). In addition, we may also consider electromagnetic wave solutions propagating in infinitely homogeneous environments. In this case, as we are dealing with monochromatic fields, the wave equation is expressed in a particular form:

$$-\nabla^2 \mathbf{F}^{\lambda}(\mathbf{r},\omega) = k^2 \mathbf{F}^{\lambda}(\mathbf{r},\omega), \tag{2.36}$$

with $k = \omega n$. The expression above represents Helmholtz's equation and it is the monochromatic version of the wave equation presented in Eq. (2.20).

Even though we will properly introduce the helicity operator in the following Chapter, let us now qualitatively show that the curl operator is directly related to the helicity of the electromagnetic field. Helicity, Λ, is defined to be proportional to the projection of the total angular momentum onto the linear momentum, i.e. $\Lambda \propto \mathbf{J}\cdot\mathbf{P}$, where the total angular momentum is $\mathbf{J} = \mathbf{L} + \mathbf{S}$. Here, $\mathbf{L}$ represents the orbital angular momentum and $\mathbf{S}$ is the spin angular momentum. However, as it is known from classical and quantum mechanics, the orbital angular momentum is orthogonal to the linear momentum, i.e. $\mathbf{L} = \mathbf{r}\times\mathbf{P}$. This simplifies the expression of the helicity and one is left with the equivalent relation $\Lambda \propto \mathbf{S}\cdot\mathbf{P}$. Now, the action of the linear momentum over wave type solutions is known to be represented as $\mathbf{P} \to -i(\partial_x, \partial_y, \partial_z)$. And, on the other hand, the representation of the $\mathbf{S}$ operator is made in electrodynamics through the three dimensional matrices of spin $S = 1$. In other words, one considers the spin of the electromagnetic field through the mapping $\mathbf{S} \to (\hat{S}_x, \hat{S}_y, \hat{S}_z)$, where the Cartesian components of the spin operator are given by:

$$\hat{S}_x = \begin{pmatrix} 0 & 0 & 0 \\ 0 & 0 & -i \\ 0 & i & 0 \end{pmatrix}, \quad \hat{S}_y = \begin{pmatrix} 0 & 0 & i \\ 0 & 0 & 0 \\ -i & 0 & 0 \end{pmatrix}, \quad \hat{S}_z = \begin{pmatrix} 0 & -i & 0 \\ i & 0 & 0 \\ 0 & 0 & 0 \end{pmatrix}. \tag{2.37}$$

Strictly speaking, we will show that such maps are associated with the representations of continuous group generators in specific vector spaces, but for the time being one can just take them as a "natural" correspondence.

Thus, from one side, we have that the helicity operator in electrodynamics is represented by the matrix:

$$\hat{\Lambda}\mathbf{V}(\mathbf{r}) \propto \hat{\mathbf{S}} \cdot \hat{\mathbf{P}}\, \mathbf{V}(\mathbf{r}) = \begin{pmatrix} 0 & -\partial_z & \partial_y \\ \partial_z & 0 & -\partial_x \\ -\partial_y & \partial_x & 0 \end{pmatrix} \begin{pmatrix} V_x(\mathbf{r}) \\ V_y(\mathbf{r}) \\ V_z(\mathbf{r}) \end{pmatrix}. \tag{2.38}$$

On the other hand, let us now show how the curl operator acts over a generic vector field expressed in Cartesian coordinates:

$$\begin{aligned} \nabla \times \mathbf{V}(\mathbf{r}) = \hat{x}[\partial_y V_z[\mathbf{r}) - \partial_z V_y(\mathbf{r})] - \hat{y}[\partial_x V_z(\mathbf{r}) - \partial_z V_x(\mathbf{r})] + \\ + \hat{z}[\partial_x V_y(\mathbf{r}) - \partial_y V_x(\mathbf{r})]. \end{aligned} \tag{2.39}$$

By comparing Eq. (2.38) and (2.39), we can conclude that the curl operator is very closely related to the helicity of the electromagnetic field, i.e. we have just shown that $\hat{\Lambda}\mathbf{V}(\mathbf{r}) \propto \nabla \times \mathbf{V}(\mathbf{r})$. Through this first intuitive derivation, it can be inferred that the monochromatic RS vector has the very specific property of being an eigenfunction of the helicity operator (see Eq. (2.34)). As we show throughout this thesis, such a property is extremely helpful for the study of the internal degrees of freedom in electromagnetic wave solutions.

2.2.3 *Inhomogeneous media*

Another useful application of the monochromatic RS vector deals with the form of Maxwell's equations in inhomogeneous media, i.e. in environments where the electric permittivity and magnetic permeability are functions of position vector $\mathbf{r}$. To derive the RS form of Maxwell's equations in this kind of environments, it is convenient to consider an auxiliary field which is defined in terms of the complex electric and magnetic fields:

$$\mathbf{G}^{\lambda}(\mathbf{r},\omega) = \frac{1}{\sqrt{2}}\left[\frac{\mathbf{E}(\mathbf{r},\omega)}{\sqrt{\mu(\mathbf{r})}} + \lambda i \frac{\mathbf{H}(\mathbf{r},\omega)}{\sqrt{\varepsilon(\mathbf{r})}}\right], \tag{2.40}$$

with $\mathbf{F}^{\lambda}(\mathbf{r},\omega) = n(\mathbf{r})\mathbf{G}^{\lambda}(\mathbf{r},\omega)$ and $n(\mathbf{r}) = \sqrt{\varepsilon(\mathbf{r})\mu(\mathbf{r})}$ is the local refractive index. It can be checked the conventional electromagnetic fields are expressed in terms of the $\mathbf{F}^{\lambda}(\mathbf{r},\omega)$ and $\mathbf{G}^{\lambda}(\mathbf{r},\omega)$ vectors as:

$$\mathbf{D}(\mathbf{r},\omega) = \sqrt{\frac{\varepsilon(\mathbf{r})}{2}}\left[\mathbf{F}^{+}(\mathbf{r},\omega) + \mathbf{F}^{-}(\mathbf{r},\omega)\right] \tag{2.41}$$

$$\mathbf{B}(\mathbf{r},\omega) = -i\sqrt{\frac{\mu(\mathbf{r})}{2}}\left[\mathbf{F}^{+}(\mathbf{r},\omega) - \mathbf{F}^{-}(\mathbf{r},\omega)\right] \tag{2.42}$$

$$\mathbf{E}(\mathbf{r},\omega) = \sqrt{\frac{\mu(\mathbf{r})}{2}}\left[\mathbf{G}^{+}(\mathbf{r},\omega) + \mathbf{G}^{-}(\mathbf{r},\omega)\right] \tag{2.43}$$

$$\mathbf{H}(\mathbf{r},\omega) = -i\sqrt{\frac{\varepsilon(\mathbf{r})}{2}}\left[\mathbf{G}^{+}(\mathbf{r},\omega) - \mathbf{G}^{-}(\mathbf{r},\omega)\right]. \tag{2.44}$$

To construct Maxwell's equations in inhomogeneous media one may start by computing the equivalent Faraday-Ampère's laws for

the $\mathbf{F}^{\lambda}(\mathbf{r},\omega)$ vector. In the derivation steps we explicitly omit the $(\mathbf{r},\omega)$ dependence of the fields, the electric permittivity and magnetic permeability:

$$\begin{aligned}-i\omega\mathbf{F}^{\lambda} &= \frac{-i\omega}{\sqrt{2}}\left[\frac{1}{\sqrt{\varepsilon}}\mathbf{D}+\lambda i\frac{1}{\sqrt{\mu}}\mathbf{B}\right]\\ &= \frac{1}{\sqrt{2}}\left[\frac{1}{\sqrt{\varepsilon}}\nabla\times\mathbf{H}-\lambda i\frac{1}{\sqrt{\mu}}\nabla\times\mathbf{E}\right]\\ &= \frac{1}{\sqrt{2}}\left[\frac{-i}{\sqrt{\varepsilon}}\nabla\times\sqrt{\frac{\varepsilon}{2}}\left[\mathbf{G}^{+}-\mathbf{G}^{-}\right]-\lambda i\frac{1}{\sqrt{\mu}}\nabla\times\sqrt{\frac{\mu}{2}}\left[\mathbf{G}^{+}+\mathbf{G}^{-}\right]\right].\end{aligned}$$

By employing the vector identity $\nabla\times(f\mathbf{V}) = \nabla f\times\mathbf{V}+f(\nabla\times\mathbf{V})$, one obtains the following form of the time derivative of the RS vector:

$$\omega\mathbf{F}^{\lambda} = \lambda\left[\nabla\times\mathbf{G}^{\lambda}+\nabla\ln\sqrt{n}\times\mathbf{G}^{\lambda}+\nabla\ln\sqrt{Z}\times\mathbf{G}^{-\lambda}\right], \tag{2.45}$$

where $Z(\mathbf{r}) = \sqrt{\mu(\mathbf{r})/\varepsilon(\mathbf{r})}$ is the local impedance of the medium and $\nabla\ln f(\mathbf{r}) = \nabla f(\mathbf{r})/f(\mathbf{r})$ for any arbitrary function $f(\mathbf{r})$. Finally, making use of the constitutive relations, we arrive to the form of Faraday-Ampère's laws expressed only in terms of the monochromatic RS vector [8]:

$$\omega\mathbf{F}^{\lambda} = \lambda\left[\frac{1}{\sqrt{n}}\nabla\times\left(\frac{\mathbf{F}^{\lambda}}{\sqrt{n}}\right)+\frac{1}{n}\nabla\ln\sqrt{Z}\times\mathbf{F}^{-\lambda}\right]. \tag{2.46}$$

On the other hand, to build Gauss' laws in inhomogeneous media one should evaluate the divergence of the monochromatic RS vector:

$$\begin{aligned}\nabla\cdot\mathbf{F}^{\lambda} &= \frac{1}{\sqrt{2}}\left[\nabla\cdot\left(\frac{\mathbf{D}}{\sqrt{\varepsilon}}\right)+\lambda i\nabla\cdot\left(\frac{\mathbf{B}}{\sqrt{\mu}}\right)\right]\\ &= \frac{1}{\sqrt{2}}\left[\nabla\left(\frac{1}{\sqrt{\varepsilon}}\right)\cdot\mathbf{D}+\lambda i\nabla\left(\frac{1}{\sqrt{\mu}}\right)\cdot\mathbf{B}\right]\\ &= \frac{1}{2}\left[\sqrt{\varepsilon}\nabla\left(\frac{1}{\sqrt{\varepsilon}}\right)\cdot(\mathbf{F}^{+}+\mathbf{F}^{-})+\lambda\sqrt{\mu}\nabla\left(\frac{1}{\sqrt{\mu}}\right)\cdot(\mathbf{F}^{+}-\mathbf{F}^{-})\right],\end{aligned}$$

where we have used the vectorial identity $\nabla\cdot(f\mathbf{V}) = \nabla f\cdot\mathbf{V}+f(\nabla\cdot\mathbf{V})$. Rearranging the terms, one is finally left with the following expression of Gauss' laws [8]:

$$\nabla\cdot\mathbf{F}^{\lambda} = -\nabla\ln\sqrt{n}\cdot\mathbf{F}^{\lambda}+\nabla\ln\sqrt{Z}\cdot\mathbf{F}^{-\lambda}. \tag{2.47}$$

Let us remark a few properties of the form of Maxwell's equations specified by Eq. (2.46) and Eq. (2.47). Note that when describing Maxwell's equations in terms of the monochromatic RS vector, the relevant medium parameters are not the electric permittivity and the magnetic permeability, but the local refractive index, $n(\mathbf{r})$, and impedance, $Z(\mathbf{r})$. In particular, it can be readily seen that the spatial derivatives of each of these parameters appear associated with the same, λ, or opposite helicity components, $-\lambda$, of the electromagnetic field. We will come back to this in Chapter 5, where we study the helicity properties of electromagnetic waves propagating through inhomogeneous magnetic media.

2.3 SOME NOTIONS OF GROUP THEORY

In the previous Section we have presented the form of Maxwell's equations in terms of the RS vector, both in homogeneous and inhomogeneous environments. We have also shown that electromagnetic wave solutions can be expressed in terms of this vector field. In this line, note that electromagnetic wave solutions fulfill the superposition principle, i.e. a linear combination of electromagnetic waves is also an electromagnetic wave. This fundamental property implies that the set of all electromagnetic wave solutions forms a particular mathematical structure, i.e. a vector space. In this Section, we make use of this fundamental property of electromagnetic wave solutions to introduce group representations.

Even if the approach may not seem natural, it is, in our opinion, the clearest way of introducing the operator form of the physical magnitudes we will be dealing with in this thesis. We start by introducing the notions of a group and a representation of a group in a vector space. We then discuss the concept of irreducible representations and some of their properties. Finally, we delve into the discussion of continuous symmetry groups and, in particular, the Poincaré group. We show that the usual operator forms of frequency, linear momentum, angular momentum and boosts generate a particular representation of the Poincaré group over the vector space of electromagnetic wave solutions.

2.3.1 *Groups and representations*

In this Subsection we introduce some basic definitions of group theory which will aid us in the following Chapter. We employ the definitions as provided in various books of reference and, in particular, we follow Wu-Ki Tung's [19] and Hamermesh's [20] books.

- **Group**: a set of elements $G = \{g_1, g_2, ...\}$ is a group provided that there is a multiplication rule, symbolically denoted by "$\cdot$", so that the product of any two elements of the set, $g_i \cdot g_j$, fulfills:
  1. Multiplication rule is associative, i.e. $g_i \cdot (g_j \cdot g_k) = (g_i \cdot g_j) \cdot g_k$ for any element in the set.
  2. If g_i and g_j are elements of the set, then $g_i \cdot g_j$ is also an element of the set.
  3. The set G contains an element $e \in G$ called the identity, which has the property $e \cdot g_i = g_i \cdot e = g_i$, for every g_i in the set.
  4. For every g_i element of the set there is also an element g_i^{-1} in G such that $g_i \cdot g_i^{-1} = g_i^{-1} \cdot g_i = e$. The element g_i^{-1} is called the inverse of element g_i.
- **Subgroup**: given a group G, we can select from its elements a subset $H \subset G$. If the subset H forms a group, under the same multiplication rule that is used in G, H is said to be a subgroup of the group G.

- **Representation of a group**: a representation of a group is a map of the elements of a group into a set of operators acting over a particular vector space, such that the multiplication rule is preserved. Symbolically we write that a representation is:

$$g_i \in G \rightarrow \hat{O}_i, \tag{2.48}$$

where $\hat{O}_i$ is an operator, such that if $g_i \cdot g_j = g_k$, then, $\hat{O}_i \times \hat{O}_j = \hat{O}_k$. Here, the symbol "$\times$" represents the multiplication rule between operators. A simple way of thinking about a representation is by assigning to each element of a group, g_i, a square matrix, $\hat{M}_i$. A set of matrices $R = \{\hat{M}_1, \hat{M}_2, ...\}$ forms a representation of group G with the matrix multiplication as an operator multiplication rule only if the matrix multiplication respects the group multiplication rule.

Let us consider the dihedral group, D_2, as an specific example. This group consists of four group elements which we will denote as $D_2 = \{e, a, b, c\}$ and the multiplication rule specified by Table 1. A set of Matrices $R = \{\hat{M}_e, \hat{M}_a, \hat{M}_b, \hat{M}_c\}$ may form a representation of D_2 only if by matrix multiplication the relations provided in Table 1 are respected. A particular representation of the D_2 group is constructed by the following set of matrices:

$$\hat{M}_e = \begin{pmatrix} 1 & 0 \\ 0 & 1 \end{pmatrix}, \ \hat{M}_a = \begin{pmatrix} -1 & 0 \\ 0 & 1 \end{pmatrix},$$
$$\hat{M}_b = \begin{pmatrix} 1 & 0 \\ 0 & -1 \end{pmatrix}, \ \hat{M}_c = \begin{pmatrix} -1 & 0 \\ 0 & -1 \end{pmatrix}.$$

Even if matrix representations are common for physical applications, they are not the only ones. In general, to construct a representation, one just requires a set of operators. An important type of operators which are not matrices are differential operators such as time or spatial derivatives. These operators act in vector spaces of functions and will be further discussed when dealing with continuous groups.

Finally, a representation is said to be unitary if the operators associated with the group elements are unitary. As a result, the construction of unitary representations is possible only in vector spaces equipped with a scalar product.

	e	**a**	**b**	**c**
e	e	a	b	c
a	a	e	c	b
b	b	c	e	a
c	c	b	a	e

Table 1: Multiplication table of the dihedral group, D_2. The first row and columns represent all the group elements (in bold) and the rest indicate the results of their multiplications.

- **Invariant subspace**: consider a representation $R = \{\hat{O}_1, \hat{O}_2, ...\}$ of a group $G = \{g_1, g_2, ...\}$ on a vector space V and let us also define a subspace V_1 of V. Now, if for all the operators $\hat{O}_i$ of the representation and for every vector $\mathbf{v}_1 \in V_1$ we have that $\hat{O}_i \mathbf{v}_1 \in V_1$, then, V_1 is said to be an invariant subspace of V. An invariant subspace is said to be proper if it does not contain any further invariant subspaces.

- **Irreducible representation**: a representation R is said to be irreducible on a vector space V if there is no invariant subspace in V with respect to R.

  For instance, in the example given above the representation of the dihedral group, D_2, is not irreducible. This is so because we can easily identify subspaces which are invariant, in particular, the subspace V_1 with basis vector $\mathbf{v}_1 = (1, 0)$ and the subspace V_2 with basis vector $\mathbf{v}_2 = (0, 1)$ are invariant.

- **Schur's lemma**: given $R = \{\hat{O}_1, \hat{O}_2, ...\}$, an irreducible representation of a group G on the vector space V, consider an arbitrary operator $\hat{A}$ on V. If $\hat{A}$ commutes with all the operators of the representation, i.e. $\hat{A}\hat{O}_i = \hat{O}_i\hat{A}$, $\forall\, i$, then $\hat{A}$ must be a multiple of the identity operator $\hat{\mathbb{I}}$, i.e. $\hat{A} = \lambda\hat{\mathbb{I}}$ where λ is a number.

  A close version of this important lemma of group theory will be employed in the next Chapter for the determination of irreducible representations of continuous groups. In particular, for this kind of groups, operators which commute with all the elements of a representation are called Casimir operators and they permit the labelling of inequivalent irreducible representations.

2.3.2 *Continuous groups and physical magnitudes*

In the previous Subsection we have discussed the general notions of a group and a representation. We have seen that group representations are built as a set of operators acting over a particular vector space. Electromagnetic wave solutions form a vector space. In what follows, we show that the canonical operator forms of the frequency (energy), linear momentum, angular momentum and boost operators are associated with a representation of the Poincaré group.

The basic underlying idea is that the magnitudes that we usually evaluate in Physics such as linear momentum, angular momentum and so on are closely related to symmetry groups. Symmetry groups are associated with transformations that we can apply to an "object" such that it remains invariant. For instance, an equilateral triangle is invariant under discrete rotations, i.e. we can rotate it by $\theta = \pi/3$ and the remaining system is exactly the same as the one we started with. Also, a square is invariant under rotations of $\theta = \pi/4$ and so on. In general, we say that a regular polygon of N sides is invariant under rotations of $\theta = \pi/N$. However, a circle, which can be understood as the limit of a regular polygon for $N \to \infty$, is invariant under infinitesimally small rotations. This is what we refer to as a continuous

symmetry. Continuous symmetries are those which can be built out from infinitesimally small changes of a given parameter. As a result, one associates discrete symmetry groups to systems which are invariant under discrete transformations and continuous symmetry groups to systems which are invariant under continuous transformations.

Some of the problems we deal with in Optics are invariant under certain continuous transformations. For instance, the scattering of waves by a plane surface (a problem addressed by Augustin Fresnel in the XIX century) is invariant under translations in two dimensions and rotations in one dimension. On the other hand, the scattering of waves by a sphere (solved by Gustav Mie in 1908 [21]) is invariant under rotations in three dimensions. Also, the propagation of electromagnetic waves through an infinite circular optical fiber is invariant under translations and rotations in one dimension. In addition to this, if the properties of the materials that constitute these optical systems do not change in time, we say that the problem is invariant under continuous time translations. This basically means that the features of the problem do not change if we wait a certain amount of time, i.e. that the constituent materials are static. From this particular examples, we can infer that there is a whole set of continuous transformations under which our problems may remain invariant. In particular, the simpler our system is the larger the set of symmetry transformations under which the system remains invariant.

Continuous symmetry transformations are central in Physics as, through Noether's theorem, they imply the conservation of certain physical magnitudes [22]. More specifically, invariance under space translations is associated with the conservation of linear momentum components, P_i; invariance under rotations with the conservation of total angular momentum components, J_i; invariance under time translations with the conservation of frequency (or energy), P_0; and invariance under Lorentz transformations with the conservation of boost components, K_i. In the language of group theory, these conserved quantities are linked to the generators of the different symmetry transformations. In short, generators are physical magnitudes which, by complex exponentiation, define the elements of the continuous group they are derived from [19]. As the continuous symmetry groups we are interested in are composed of an infinite number of group elements, it is much easier to keep track of a finite number of generators. For instance, we can keep track of all the possible time translations, T_τ, through the association $T_\tau = e^{-i\tau P_0}$, just by considering different values of the parameter $\tau \in \mathbb{R}$. In this line, for each different value of τ, we build a particular element of the time translations group which is infinite. However, note that all the group elements are built from a single generator, P_0.

A prominent example is the Poincaré group, which is the continuous symmetry group under which every relativistic physical theory must be invariant. The Poincaré group is generated by all the generators we have discussed so far, i.e. by the set $\{P_0, P_i, J_i, K_i\}$. This implies that every relativistically invariant theory must be symmetric under spatio-temporal translations, rotations and Lorentz transformations.

$[P_0, P_0] = 0$	$[P_0, P_n] = 0$ $[P_m, P_n] = 0$	$[P_0, J_n] = 0$ $[P_m, J_n] = i\epsilon_{mnl}P_l$ $[J_m, J_n] = i\epsilon_{mnl}J_l$	$[P_0, K_n] = iP_n$ $[P_m, K_n] = i\delta_{mn}P_0$ $[J_m, K_n] = i\epsilon_{mnl}K_l$ $[K_m, K_n] = -i\epsilon_{mnl}J_l$

Table 2: Commutation relations of the generators of the Poincaré group. The indices can have the values $\{m, n, l\} = \{1, 2, 3\}$, each representing a different Cartesian component. ϵ_{mnl} is the Levi-Civita symbol and, by convention, $\epsilon_{123} = 1$. $\epsilon_{mnl} = 1$ if mnl is an even permutation of 123 and $\epsilon_{mnl} = -1$ if it is an odd permutation. ϵ_{mnl} vanishes if two indices are repeated. δ_{mn} is the Kronecker delta such that $\delta_{mn} = 1$ if $m = n$ and $\delta_{mn} = 0$ if $m \neq n$.

An important property of the generators of a continuous group is that they have an associated algebra. The generator algebra, which ultimately is a set of commutation relations, is a central feature of continuous groups because it completely determines the multiplication properties of the group [23]. In the case of the Poincaré group, the algebra is given by the the commutation relations specified by Table 2 [19, 24, 25]. It is important to note that, until this point, all the discussion on continuous groups is general and does not depend on the specific physical system one may be dealing with. However, in this thesis we will deal with electromagnetic wave solutions, which as explained above form a specific vector space. This very particular feature of wave solutions permits us the construction of representations of any group and, in particular, of the Poincaré group.

A representation of a group is technically defined as a map of the elements of a group into a set of operators on a particular vector space, such that the multiplication rule of the group is preserved. As mentioned above, the multiplication rule of a continuous group is completely determined by the commutation relations of the generators. Thus, to find a representation of the Poincaré group on the vector space of electromagnetic wave solutions, we just have to find an appropriate operator form of the generators of the Poincaré group, such that the commutation relations given by Table 2 are preserved. For instance, in what is known as the *position representation*, the generators of the Poincaré group are expressed as [26, 27]:

$$P_0 \to i\partial_t \tag{2.49}$$

$$\mathbf{P} \to -i\nabla \tag{2.50}$$

$$\mathbf{J} \to -i\mathbf{r} \times \nabla + \hat{\mathbf{S}} \tag{2.51}$$

$$\mathbf{K} \to -i[\mathbf{r}\partial_t + t\nabla] + i\hat{\mathbf{S}}, \tag{2.52}$$

where we have chosen natural units, i.e. $c = \hbar = 1$. Note that the relations given by Eqs. (2.49)-(2.52) constitute the canonical correspondence rule employed in quantum mechanics to derive the Schrödinger or Klein-Gordon wave equations from the classical expressions of the energy-momentum relations [28, 29]. In this line, all the operators, except $\hat{\mathbf{S}}$, are already well-defined, i.e. they are differential operators

which act over functions expressed in coordinates $(\mathbf{r}, t)$. This, however, is not the case of the spin operator. $\hat{\mathbf{S}}$ acts on the internal space of the particles that the theory describes.

Electromagnetic wave solutions are associated with photons which can be regarded as particles with spin $S = 1$. Moreover, as the description of electromagnetic waves is usually done in terms of three component vector fields, we shall employ a three dimensional representation of the spin matrices, i.e. exactly the one given by Eq. (2.37). Indeed, it can be checked that that such matrices represent the internal degrees of freedom of a particle of spin $S = 1$ just by computing the $\hat{\mathbf{S}}^2 = S_x^2 + S_y^2 + S_z^2$ operator. This leads $\hat{\mathbf{S}}^2 = 2\mathbb{I}$, where $\mathbb{I}$ is the three dimensional identity matrix. As the spin of a particle is defined through the eigenvalue of the $\hat{\mathbf{S}}^2$ operator, i.e. $2 = S(S+1)$, it gives as a result $S = 1$. In this precise sense we say that the matrices given by Eq. (2.37) represent a particle of spin $S = 1$. Note that this association gives a physical meaning to the vector nature of the electromagnetic field. Frequently, and in analogy with massive particles, the spin angular momentum has been regarded as the fundamental magnitude associated with the internal degrees of freedom of the electromagnetic field. However, we should bear in mind that electromagnetic waves are associated with a massless particle and, thus, the fundamental magnitude representing the internal degrees of freedom is not spin, but helicity.

Helicity as a physical magnitude is defined as $\Lambda = \mathbf{J} \cdot \mathbf{P}/|\mathbf{P}|$, i.e. it is the projection of the total angular momentum in the direction of propagation. However, as the total angular momentum is $\mathbf{J} = \mathbf{L} + \mathbf{S}$ and as the orbital angular momentum, $\mathbf{L}$, is orthogonal to the linear momentum, $\mathbf{P}$, helicity is sometimes defined as the projection of the spin angular momentum onto the direction of propagation. In this thesis, we will stick to the first definition because it defines the helicity in terms of two generators of the Poincaré group. In the position representation, helicity is most naturally defined for monochromatic solutions. This is because there is not an easy representation for the magnitude $|\mathbf{P}|^{-1}$, i.e. the inverse of the linear momentum modulus, in position space. This, of course, would not be a problem if we would have chosen to represent electromagnetic solutions in reciprocal space. However, we prefer to stick to the representation as given by Eqs. (2.49)-(2.52) because it results in the canonical form of the operators. If we further restrict to monochromatic electromagnetic waves, helicity is represented in position space as $\Lambda \to k^{-1}\nabla\times$, where k is the modulus of the wave vector.

Summing up, we have just shown that we can define the usual operators associated with energy, linear momentum or angular momentum as the generators of continuous symmetry groups. Moreover, in Eqs. (2.49)-(2.52) we have presented a representation of the generators of the Poincaré group on the vector space of electromagnetic wave solutions. However, we should take into account that this is not the only possible representation and, as long as the commutation relations given by Table 2 are fulfilled, other representations may be constructed.

2.3.3 *A representation of the Poincaré group*

To end this Section, let us show that the operators given by Eqs. (2.49)-(2.52) actually generate a representation of the Poincaré group. To that end, we must show that the commutation relations given in Table 2 are fulfilled by the operators in Eqs. (2.49)-(2.52). In this line, we will explicitly evaluate a representative example for each of the commutation relations.

- **Time translations**, $[\hat{P}_0, \hat{P}_0]$: the commutation of $\hat{P}_0$ with itself can be proved from the definition of the commutator:

$$[\hat{P}_0, \hat{P}_0] = \hat{P}_0\hat{P}_0 - \hat{P}_0\hat{P}_0 = 0. \tag{2.53}$$

  The same holds for the commutator of any operator with itself.

- **Time and spatial translations**, $[\hat{P}_0, \hat{P}_n]$: the commutation of $\hat{P}_0$ and any Cartesian component of linear momentum $\hat{P}_n$ directly follows if we consider sufficiently smooth functions on variables $(\mathbf{r}, t)$. Let us compute this result explicitly by operating over an arbitrary scalar function $\psi(\mathbf{r}, t)$.

$$(\hat{P}_0\hat{P}_x)\psi = (\partial_t\partial_x)\psi$$
$$(\hat{P}_x\hat{P}_0)\psi = (\partial_x\partial_t)\psi$$

  For the functions we will be dealing with, derivatives over time and space coordinates are interchangeable. In proper mathematical terms, we constrain our analysis to complex functions of real variables that fulfill Clairaut's theorem of second order partial derivatives. Thus, we have that $[\hat{P}_0, \hat{P}_x] = 0$.

- **Spatial translations**, $[\hat{P}_m, \hat{P}_n]$: the commutation of the different components of the linear momentum also follows if we assume functions subjected to Clairaut's theorem. Explicitly, we have that:

$$(\hat{P}_y\hat{P}_z)\psi = -(\partial_y\partial_z)\psi$$
$$(\hat{P}_z\hat{P}_y)\psi = -(\partial_z\partial_y)\psi,$$

  which are equivalent for the functions we will be dealing with. Thus, in the example above, we get that $[\hat{P}_y, \hat{P}_z] = 0$. In the following examples, we will implicitly employ the fact that derivatives in different variables commute.

- **Time translations and rotations**, $[\hat{P}_0, \hat{J}_n]$: the commutation of $\hat{P}_0$ with the angular momentum operator components, $\hat{J}_n$, is based of the commutation of spatial and time derivatives discussed above, but not only. It is also based of the fact that the spin operator, $\hat{\mathbf{S}}$, commutes with all the differential operators acting on the spatial or temporal coordinates. This follows from the fact that $\hat{\mathbf{S}}$ operator is constructed from constant matrix components.

Let us evaluate the example $[\hat{P}_0, \hat{J}_y] = [\hat{P}_0, \hat{L}_y] + [\hat{P}_0, \hat{S}_y]$. For the orbital part, we have:

$$(\hat{P}_0\hat{L}_y)\psi = (\hat{L}_y\hat{P}_0)\psi = (y\partial_t\partial_z - z\partial_t\partial_y)\psi$$

whereas for the spin part we get

$$\hat{P}_0\hat{S}_y = \hat{S}_y\hat{P}_0 = \begin{pmatrix} 0 & 0 & -\partial_t \\ 0 & 0 & 0 \\ \partial_t & 0 & 0 \end{pmatrix}.$$

Thus, we finally have that $[\hat{P}_0, \hat{J}_y] = 0$.

- **Spatial translations and rotations**, $[\hat{P}_m, \hat{J}_n]$: Table 2 indicates that translations and rotations in different Cartesian do not commute. However, note that $\hat{\mathbf{P}}$ and $\hat{\mathbf{S}}$ commute, which implies that we just have to compute the commutator with the orbital angular momentum operator, $\hat{\mathbf{L}}$.

$$(\hat{P}_x\hat{L}_y)\psi = (-z\partial_x^2 + x\partial_x\partial_z + \partial_z)\psi$$
$$(\hat{L}_y\hat{P}_x)\psi = (-z\partial_x^2 + x\partial_x\partial_z)\psi.$$

Thus, we get that $[\hat{P}_x, \hat{J}_y] = [\hat{P}_x, \hat{L}_y] = i\hat{P}_z$, which is in agreement with Table 2. Note that, in this case, $mnl = 123$ and, thus, $\epsilon_{mnl} = \epsilon_{123} = 1$.

- **Rotations**, $[\hat{J}_m, \hat{J}_n]$: the commutator of the total angular momentum components can be split into two contributions, i.e. the orbital and the spin ones. In other words, $[\hat{J}_m, \hat{J}_n] = [\hat{L}_m, \hat{L}_n] + [\hat{S}_m, \hat{S}_n]$. Let us just show a particular example:

$$(\hat{L}_x\hat{L}_z)\psi = (-xy\partial_y\partial_z + y^2\partial_x\partial_z + xz\partial_y^2 - yz\partial_x\partial_y - z\partial_x)\psi$$
$$(\hat{L}_z\hat{L}_x)\psi = (-xy\partial_y\partial_z + y^2\partial_x\partial_z + xz\partial_y^2 - yz\partial_x\partial_y - x\partial_z)\psi.$$

From the orbital angular momentum we, thus, get $[\hat{L}_x, \hat{L}_z] = -i\hat{L}_y$. Regarding the spin contribution we have to compute the matrices:

$$\hat{S}_x\hat{S}_z = \begin{pmatrix} 0 & 0 & 0 \\ 0 & 0 & -i \\ 0 & i & 0 \end{pmatrix}\begin{pmatrix} 0 & -i & 0 \\ i & 0 & 0 \\ 0 & 0 & 0 \end{pmatrix} = \begin{pmatrix} 0 & 0 & 0 \\ 0 & 0 & 0 \\ -1 & 0 & 0 \end{pmatrix}$$
$$\hat{S}_z\hat{S}_x = \begin{pmatrix} 0 & -i & 0 \\ i & 0 & 0 \\ 0 & 0 & 0 \end{pmatrix}\begin{pmatrix} 0 & 0 & 0 \\ 0 & 0 & -i \\ 0 & i & 0 \end{pmatrix} = \begin{pmatrix} 0 & 0 & -1 \\ 0 & 0 & 0 \\ 0 & 0 & 0 \end{pmatrix},$$

which leads that $[\hat{S}_x, \hat{S}_z] = -i\hat{S}_y$. Thus, we have that, $[\hat{J}_x, \hat{J}_z] = -i(\hat{L}_y + \hat{S}_y) = -i\hat{J}_y$. Note that, in this case, $mnl = 132$ which is an odd permutation of 123.

- **Time translations and Lorentz transformations**, $[\hat{P}_0, \hat{K}_n]$: to evaluate this commutator we should first note that time derivatives commute with $\hat{\mathbf{S}}$. Thus, we only have to compute:

$$(\hat{P}_0\hat{K}_y)\psi = (y\partial_t^2 + t\partial_t\partial_y + \partial_y)\psi$$
$$(\hat{K}_y\hat{P}_0)\psi = (y\partial_t^2 + t\partial_t\partial_y)\psi.$$

  The result is $[\hat{P}_0, \hat{K}_y] = i\hat{P}_y$, which is in agreement with the result in Table 2.

- **Spatial translations and Lorentz transformations**, $[\hat{P}_m, \hat{K}_n]$: in this case we should also take into account that $\hat{\mathbf{S}}$ operator does not play a role in the computation of the commutator. As an example we can evaluate:

$$(\hat{P}_z\hat{K}_z)\psi = -(z\partial_t\partial_z + t\partial_z^2 + \partial_t)\psi$$
$$(\hat{K}_z\hat{P}_z)\psi = -(z\partial_t\partial_z + t\partial_z^2)\psi,$$

  which leads to $[\hat{P}_z, \hat{K}_z] = i\hat{P}_0$.

- **Rotations and Lorentz transformations**, $[\hat{J}_m, \hat{K}_n]$: this is the first situation in which we should also take into account the spin part of the boost operator given by Eq. (2.52). We will denote the orbital and spin parts of the boost operators by $\hat{K}_n^o$ and $\hat{K}_n^s$, respectively. Let us give an example:

$$(\hat{L}_x\hat{K}_z^o)\psi = -(yz\partial_t\partial_z + ty\partial_z^2 - z^2\partial_t\partial_y - tz\partial_t\partial_y + y\partial_t)\psi$$
$$(\hat{K}_z^o\hat{L}_x)\psi = -(yz\partial_t\partial_z + ty\partial_z^2 - z^2\partial_t\partial_y - tz\partial_y\partial_z - t\partial_y)\psi.$$

  On the other hand, we should also compute the commutators of the spin parts. This leads to:

$$\hat{S}_x\hat{K}_z^s = \begin{pmatrix} 0 & 0 & 0 \\ 0 & 0 & -i \\ 0 & i & 0 \end{pmatrix}\begin{pmatrix} 0 & 1 & 0 \\ -1 & 0 & 0 \\ 0 & 0 & 0 \end{pmatrix} = \begin{pmatrix} 0 & 0 & 0 \\ 0 & 0 & 0 \\ -i & 0 & 0 \end{pmatrix}$$
$$\hat{K}_z^o\hat{S}_x = \begin{pmatrix} 0 & 1 & 0 \\ -1 & 0 & 0 \\ 0 & 0 & 0 \end{pmatrix}\begin{pmatrix} 0 & 0 & 0 \\ 0 & 0 & -i \\ 0 & i & 0 \end{pmatrix} = \begin{pmatrix} 0 & 0 & -i \\ 0 & 0 & 0 \\ 0 & 0 & 0 \end{pmatrix},$$

  As a result, summing both contributions of the commutator, we obtain $[\hat{J}_x, \hat{K}_z] = -(y\partial_t + t\partial_y) + \hat{S}_y = -i\hat{K}_y$, which is exactly the result given by Table 2. Note that 132 is and odd permutation of 123.

- **Lorentz transformations**, $[\hat{K}_m, \hat{K}_n]$: let us now show that the commutation relations also hold for the Lorentz boosts. Let us first compute the orbital part for a given example:

$$(\hat{K}_y^o\hat{K}_z^o)\psi = -(yz\partial_t^2 + ty\partial_t\partial_z + tz\partial_t\partial_y + t^2\partial_y\partial_z + y\partial_z)\psi$$
$$(\hat{K}_z^o\hat{K}_y^o)\psi = -(yz\partial_t^2 + ty\partial_t\partial_z + tz\partial_t\partial_y + t^2\partial_y\partial_z + z\partial_y)\psi$$

. On the other hand, for the spin contribution we have that:

$$\hat{K}_y^s \hat{K}_z^s = -\begin{pmatrix} 0 & 0 & i \\ 0 & 0 & 0 \\ -i & 0 & 0 \end{pmatrix}\begin{pmatrix} 0 & -i & 0 \\ i & 0 & 0 \\ 0 & 0 & 0 \end{pmatrix} = \begin{pmatrix} 0 & 0 & 0 \\ 0 & 0 & 0 \\ 0 & 1 & 0 \end{pmatrix}$$

$$\hat{K}_z^s \hat{K}_y^s = -\begin{pmatrix} 0 & -i & 0 \\ i & 0 & 0 \\ 0 & 0 & 0 \end{pmatrix}\begin{pmatrix} 0 & 0 & i \\ 0 & 0 & 0 \\ -i & 0 & 0 \end{pmatrix} = \begin{pmatrix} 0 & 0 & 0 \\ 0 & 0 & 1 \\ 0 & 0 & 0 \end{pmatrix}.$$

which implies that this part is exclusively computed in terms of the spin matrix commutation relations that have been previously computed. As a result, we have that $[\hat{K}_y, \hat{K}_z] = -(y\partial_z - z\partial_y) - i\hat{S}_x = -i\hat{J}_x$ and note that 231 is an even permutation of 123.

Finally, the position representation of the Poincaré group is constructed by a complex exponentiation of the generators. For instance, a rotation by angle θ around the OX axis is represented by the action of the operator $\hat{R}_x(\theta) = \exp(-i\theta\hat{J}_x)$ and a Lorentz transformation along the OZ direction is represented by the action of the operator $\hat{L}_z(\xi) = \exp(-i\xi\hat{K}_z)$. This very specific way of constructing the group elements determines whether the representation is or not unitary. Indeed, note that whenever the generators are represented by hermitian operators, the complex exponentiation leads to a unitary operator. However, the hermiticity of an operator depends on the definition of the scalar product, which is not unique. For instance, it can be shown that the operator given by Eq. (2.52) is not hermitian with respect to the usual scalar product $\langle \mathbf{V}_1 | \mathbf{V}_2 \rangle = \int d\mathbf{r}\, \mathbf{V}_1^*(\mathbf{r}, t) \cdot \mathbf{V}_2(\mathbf{r}, t)$ [8, 27]. The most direct way of checking this is by noting that the Cartesian components of the matrix operator $i\hat{\mathbf{S}}$ are not the same if we conjugate and transpose them. In addition, it can also be shown that the orbital part of the boost generators or the generator of time translations are not hermitian either. This implies that, the position representation of the Poincaré group provided by the operators defined in Eqs. (2.49)-(2.52) is not unitary with respect to the usual scalar product.

Unitary representations of the Poincaré group are most commonly built over the vector space of solutions expressed in reciprocal space variables $(\mathbf{k}, \omega)$ [24, 25]. Accordingly, such representations are usually denoted as *momentum representations*. This kind of representations are, for instance, employed in Quantum Field Theory to check that the quantization of free fields is congruent with special relativity [30, 31]. Also, Bialynicki-Birula has proposed a particular representation of the Poincaré group in coordinate space which is unitary with respect to a particular Lorentz invariant scalar product [8]. Importantly, except in some Sections of Chapter 3, we will mainly study systems which are not invariant under Lorentz transformations. In this line, by making a slight modification on the generator of time translations, one can construct a unitary representation of the subgroup of the Poincaré

group which does not contain Lorentz transformations. Indeed, the mapping:

$$\begin{aligned} P_0 &\to \omega \\ \mathbf{P} &\to -i\nabla \\ \mathbf{J} &\to -i\mathbf{r}\times\nabla + \hat{\mathbf{S}} \end{aligned}$$

results in a hermitian form of the generators with respect to the conventional scalar product, provided that ω is a real number. This result anticipates the important role that monochromatic electromagnetic wave solutions are going to play in systems or environments which are not relativistic. Regarding the representation fixed by Eqs. (2.49)-(2.52), we will employ it as a correspondence rule between physical magnitudes and operators acting in the vector space of electromagnetic wave solutions [32, 33] (see also Part I, Chapter II, Section II in Ref. [28]). This will aid us in translating abstract results of group theory into specific systems of partial differential equations.

2.4 SUMMARY

In Section 2.1, we have introduced the canonical form of Maxwell's equations with a quite general form of the constitutive relations which remain valid for chiral media. Then, in Section 2.2, we have introduced various forms of the RS vector. First, we have introduced the conventional RS vector, $\mathcal{F}^{\lambda}(\mathbf{r},t)$, which is built from the real displacement field and real magnetic induction. Second, we have introduced the monochromatic RS vector, $\mathbf{F}^{\lambda}(\mathbf{r},\omega)$, which is built from complex fields. Third, we have employed the monochromatic RS vector to obtain a particular form of Maxwell's equations in inhomogeneous media. Finally, in Section 2.3, we have introduced some basic notions of group theory. Moreover, making use of the linearity of electromagnetic wave solutions, we have introduced the so-called position representation of the Poincaré group in Eqs. (2.49)-(2.52).

3

FOUNDATIONS OF ELECTROMAGNETIC HELICITY

In this Chapter, we introduce the fundamental physical and mathematical concepts associated with electromagnetic helicity. First, we show how the emergence of electromagnetic helicity can be understood in terms of the symmetries of special relativity. Then, we discuss the role of electromagnetic helicity in the presence of material media based on similar symmetry arguments. Finally, we construct particular solutions of monochromatic electromagnetic waves propagating in material media.

Some derivations of Section 3.1 and most of Section 3.2 have been adapted from Contribution VII.

3.1 HELICITY AND RELATIVISTIC SYMMETRIES

In the previous Chapter we have introduced electromagnetic wave solutions and we have seen that one can construct a representation of the Poincaré group on the vector space that they form. Furthermore, we have also shown that if the generators of the group are mapped into hermitian operators, the resulting representation is unitary. Unitary representations of the Poincaré group play a central role in Physics due to a fundamental contribution by Eugene P. Wigner. Indeed, he determined that in every relativistic linear theory without interactions, the unitary representations of the Poincaré group could replace the equations of motion [5]. This might seem quite unnecessary at this point, as we have already introduced in Eqs. (2.18)-(2.19) the form of Maxwell's equations in vacuum. However, we will see that, from the analysis of the Poincaré group and its representations, the notion of helicity emerges in a quite natural manner.

The relevance of the unitary representations of the Poincaré group is due to the fundamental assumption in Physics that all acceptable theories should lead to the same results in different inertial reference frames. This, also known as the relativistic invariance principle, translates into the fact that physical observables cannot be modified when changing from one reference frame to another. In particular, if such observables are associated with the modulus squared of scalar products, then the representation associated with the symmetry transformations must be based on operators that preserve the norm. And, within complex vector spaces, it implies that the symmetry operators must be unitary (or antiunitary). This is a result of the so-called Wigner's theorem [34]. Even if the argument was derived in the context of Quantum Mechanics, it is also known to hold for other linear relativistic theories such as Maxwell's equations in vacuum [5, 18, 35]. In the following Sections, we introduce some basic concepts to study the theory of representations of the Poincaré group applied to electromagnetism.

In particular, we will delve into the study of unitary irreducible representations (UIRs) of the Poincaré group. We do this for two reasons. First, because all the unitary representations of the Poincaré group can be expressed as direct sums of UIRs [5]. Thus, classifying the UIRs leads to an identification of all possible unitary representations of the Poincaré group. Second, according to Wigner's classification, the vector states (or wave functions) of elementary physical systems must transform according to such UIRs [6, 19]. From this algebraic perspective, elementary particle states are defined as vectors that belong to the invariant space associated with an UIR of the Poincaré group. In our case, as we are interested in the description of electromagnetic waves, we will analyze the UIRs that define the photon as an elementary particle. In the upcoming discussion, we closely follow the mathematical prescriptions for the construction of such irreducible representations. Particularly, we will stick to the tools provided by Wu-Ki Tung's book, *Group theory in Physics* [19].

3.1.1 *Electromagnetic waves in vacuum*

For the determination of the UIRs we may employ two results of representation theory. The first one is related to the existence of Casimir invariants. These magnitudes commute with all the generators of a continuous group, i.e. a Casimir element C fulfills $[C, G] = 0$, where G is any generator of a given continuous group. In the case of the Poincaré group, its generators are $\{P_0, P_i, J_i, K_i\}$ and, thus, a Casimir of this group must be an invariant quantity under time and space translations, rotations and relativistic boosts. It is a result of representation theory that every vector belonging to the invariant space of an UIR must be an eigenstate of all the Casimir operators of the group. This result can be understood as the generalization of Schur's lemma to continuous group representations [19] (see also pages 598 and 599 in Ref. [36]). The second one will be introduced later and it is related with the explicit construction of the invariant vector spaces associated with the UIRs.

In the case of the Poincaré group, there are two principal Casimir operators which determine the nature of the irreducible representations [19, 24]:

$$\hat{C}_1 = \hat{\mathbf{P}} \cdot \hat{\mathbf{P}} - \hat{P}_0^2 \tag{3.1}$$

$$\hat{C}_2 = \hat{\mathbf{W}} \cdot \hat{\mathbf{W}} - (\hat{\mathbf{J}} \cdot \hat{\mathbf{P}})^2, \tag{3.2}$$

which are, respectively, the modulus of the 4-momentum, $\hat{P}_\nu = (\hat{P}_0, \hat{\mathbf{P}})$, and the modulus of the Pauli-Lubanski pseudo-vector, $\hat{W}_\nu = (\hat{\mathbf{J}} \cdot \hat{\mathbf{P}}, \hat{\mathbf{W}})$, with the opposite sign. Here, the spatial components of the Pauli-Lubanski pseudovector are $\hat{\mathbf{W}} = \hat{P}_0 \hat{\mathbf{J}} + \hat{\mathbf{K}} \times \hat{\mathbf{P}}$ and we fix the Minkowski metric with the sign convention $(+,-,-,-)$ [26]. As the modulus of the 4-momentum is related to the mass of the particles in the rest frame, M, we conclude that the eigenvalue of the Casimir operator $\hat{C}_1$ is actually $-M^2$. This implies that different values of the rest mass lead to different irreducible representations of the Poincaré group. In particular, the eigenvalue of $\hat{C}_1$ indicates whether the irreducible representation is associated with a massive ($M > 0$) or a massless ($M = 0$) particle. The electromagnetic theory in vacuum is associated with the massless UIRs of the Poincaré group. Note that in this case, the condition $M = 0$ implies that the vector states belonging to a massless irreducible representation fulfill the wave equation in vacuum. This can be more explicitly checked by substituting the operator forms given by Eq. (2.49) and (2.50) in the expression for $\hat{C}_1$ in Eq. (3.1). Indeed, by doing so, one retrieves the differential equation given by (2.20).

The analysis of the second Casimir invariant, $\hat{C}_2$, is straightforward for the massive representations. As this type of particles do not travel at the speed of light, one can always evaluate the expression of the $\hat{C}_2$ operator in the rest frame of the particle. As it is a relativistic invariant, the value of $\hat{C}_2$ cannot depend on the particular reference frame one may choose. Thus, for massive particles we can fix $\hat{\mathbf{P}} = 0$, which implies that, in this case, $\hat{C}_2 = \hat{P}_0^2(\hat{\mathbf{J}} \cdot \hat{\mathbf{J}})$. Moreover, as we have

fixed the reference frame in which the massive particle is in rest, we further have that $\hat{\mathbf{L}} = \hat{\mathbf{r}} \times \hat{\mathbf{P}} = 0$ and, thus, $\hat{\mathbf{J}} = \hat{\mathbf{S}}$. We finally arrive to the form $\hat{C}_2 = \hat{P}_0^2(\hat{\mathbf{S}} \cdot \hat{\mathbf{S}})$ for any irreducible representation of the Poincaré group with $M > 0$. Note that, in the frame in which the particle is in rest the eigenvalue of the $\hat{P}_0^2$ operator is, precisely, the invariant magnitude M^2. Thus, we can conclude that the eigenvalue of the second Casimir operator is $M^2 S(S+1)$, where $S(S+1)$ represents the eigenvalues of the square of the spin angular momentum $\hat{\mathbf{S}}^2 = \hat{\mathbf{S}} \cdot \hat{\mathbf{S}}$. Thus, the derivation above indicates that the second Casimir is proportional to the spin angular momentum of the particles. This implies that massive irreducible representations are further classified by the eigenvalues of the spin angular momentum. However, as it can be noted, this derivation is only possible if there exists a reference frame in which the particle is at rest. And, as a result, this interpretation of the second Casimir invariant is not possible when we consider massless particles.

Massless representations are split into two possibilities which are denoted as the continuous- or discrete-spin representations [6, 24], depending on the eigenvalue of the second Casimir operator, Ξ. The continuous-spin representations are characterized for having $0 < \Xi < \infty$, whereas the discrete-spin representations for having $\Xi = 0$. As we are exclusively interested with the irreducible representations associated with the electromagnetic theory, here we will just discuss the discrete-spin case. Unfortunately, for this specific class, the second Casimir invariant does not provide a complete characterization [6]. In other words, for massless particles with discrete spin, like the photon, $\hat{C}_2$ does not account for the internal degrees of freedom. However, a third Casimir operator emerges for this specific class of UIRs of the Poincaré group [24]: $\hat{\mathbf{J}} \cdot \hat{\mathbf{P}}/\hat{P}_0$. As we are dealing with massless particles $\hat{P}_0^2 = \hat{\mathbf{P}} \cdot \hat{\mathbf{P}}$ and, thus, the expression of the third Casimir is equivalent to the definition of helicity, i.e. $\hat{\Lambda} = \hat{\mathbf{J}} \cdot \hat{\mathbf{P}}/|\hat{\mathbf{P}}|$. In this line, its eigenvalues λ may take on any positive or negative integer or half integer value. Choosing the two representations $\lambda = \pm S$ for a fixed positive value of S, one describes the two internal degrees of freedom of a given massless elementary particle with discrete spin. Bargmann and Wigner showed that the invariant vector spaces associated with the discrete-spin irreducible representations are characterized by the set of operator equations: $\hat{W}_\nu = \lambda \hat{P}_\nu$ [6, 29]. Note that the temporal component of such equation represents exactly that solutions must be eigenstates of the helicity operator.

Furthermore, as H. Bacry explicitly showed (see Eqs. 21a and 21b in Ref. [26]), the set proposed by Bargmann and Wigner in 1948 corresponds to the equations found in 1936 by Dirac for particles of null mass and spin S [32, 33]:

$$\left(S\hat{P}_0 + \hat{S}_x\hat{P}_x + \hat{S}_y\hat{P}_y + \hat{S}_z\hat{P}_z\right)\Psi(\mathbf{r},t) = 0 \tag{3.3}$$

$$\left(S\hat{P}_x + \hat{S}_x\hat{P}_0 - i\hat{S}_y\hat{P}_z + i\hat{S}_z\hat{P}_y\right)\Psi(\mathbf{r},t) = 0 \tag{3.4}$$

$$\left(S\hat{P}_y + \hat{S}_y\hat{P}_0 - i\hat{S}_z\hat{P}_x + i\hat{S}_x\hat{P}_z\right)\Psi(\mathbf{r},t) = 0 \tag{3.5}$$

$$\left(S\hat{P}_z + \hat{S}_z\hat{P}_0 - i\hat{S}_x\hat{P}_y + i\hat{S}_y\hat{P}_x\right)\Psi(\mathbf{r},t) = 0, \tag{3.6}$$

where $\Psi(\mathbf{r}, t)$ is a $2S+1$ component wave function. Now, considering the case $S = 1$, employing the representation of spin matrices as given by Eq. (2.37) and the operator representations for $\hat{P}_0$ and $\hat{\mathbf{P}}$ as given by Eqs. (2.49) and (2.50), it can be checked that the first of these equations leads to Faraday-Ampère equations as given in Eq. (2.18) setting $\lambda = -1$ [33]. Indeed, the derivation is quite direct if we recall the identity: $\hat{\mathbf{S}} \cdot \hat{\mathbf{P}} = \hat{S}_x \hat{P}_x + \hat{S}_y \hat{P}_y + \hat{S}_z \hat{P}_z = \nabla\times$. Furthermore, it can be shown that substituting $\hat{P}_0$ from Eq. (3.3) into Eqs. (3.4)-(3.6), Gauss' laws as expressed in Eq. (2.19) can also be derived [26, 33]. We can, then, state that the constraint $\hat{W}_\nu = \lambda \hat{P}_\nu$ over the massless irreducible representations with spin $S = 1$ is equivalent to requiring that the vector states are solutions of Maxwell's equations in vacuum. Finally, note that the massless irreducible representations are also characterized by the condition $M = 0$, from where the wave equation in vacuum can be derived. Thus, we reach the conclusion that the states belonging to the invariant vector space of the massless and discrete-spin UIRs of the Poincaré group are electromagnetic wave solutions propagating in vacuum.

Let us just remark a few important results we have obtained in this Subsection. First, we have seen that helicity emerges as a Casimir operator for the massless and discrete-spin UIRs of the Poincaré group. For this specific type of UIRs, helicity is shown to be a relativistic invariant regardless of the spin of the particle, which indicates that it is a fundamental magnitude for the description of other massless particles such as the graviton ($S = 2$) or others. Moreover, we have related the electromagnetic wave solutions with the representation theory of the Poincaré group. This provides us with a solid mathematical framework in which further investigations may be structured. In particular, in the next Subsections, we will show that the UIRs of the subgroups of the Poincaré group are related to electromagnetic wave solutions in environments with less symmetries than vacuum. Finally, in the derivation above, we have also found that the $2S+1$ component wave function, $\Psi(\mathbf{r}, t)$, appearing in Dirac's equation for zero rest mass particles naturally relates with the RS vector for the case $S = 1$. As we show next, this is no mere coincidence. Indeed, there are arguments to defend that the field specified in Eq. (2.32) plays the role of the photon wave function in vacuum [8, 37].

3.1.2 *Photon wave function in vacuum*

To finish the discussion of electromagnetic waves in vacuum, let us explicitly show in what sense the RS vector may be considered a good electromagnetic wave function candidate. As we have previously introduced, UIRs of the Poincaré group are commonly employed to classify elementary particles. In particular, we have just seen that such a classification is done in terms of the Casimir invariants of the group. This means that different elementary particles are labelled by the different values of the rest mass, M, and spin or helicity, S/λ. In short, we say that two particles are identical if they share the same labels

or different if they do not. In addition to the Casimir labels, UIRs have an associate invariant vector space which is also related with the description of such fundamental particles. In particular, the vector spaces of the UIRs of the Poincaré group are associated with the wave functions of elementary particles. Citing Wu-Ki Tung's book [19]: *In fact, the natural correspondence between the basis vectors of unitary irreducible representations of the Poincaré group and quantum mechanical states of elementary physical systems stands out as one of the remarkable monuments to unity between mathematics and physics.* Let us now show that the RS vector as expressed in Eq. (2.32) can also be associated with the massless and discrete-spin irreducible representations of the Poincaré group.

In the upcoming derivation, we closely follow the indications dictated by Wu-Ki Tung's book for the construction of invariant vector spaces. As it is indicated by Theorem 10.14 [19], the basis vectors for the "light-like" UIRs of the Poincaré group can be constructed by operating over a standard vector. Such a vector is chosen to be an eigenstate of the 4-momentum operator $\hat{P}_\nu$, i.e. an eigenstate of the $\hat{P}_0$ and $\hat{\mathbf{P}}$ operators. Moreover, as the standard vector belongs to the invariant vector space, it also has to be an eigenstate of the Casimir operators $\hat{C}_1$ and $\hat{\Lambda}$. All these constraints imply that the standard vector is a circularly polarized monochromatic plane-wave. If we fix the direction of propagation to be in the OZ direction, we are finally left with the following explicit form of the standard vector:

$$\mathbf{\Psi}^{\lambda}_{\mathbf{k}_l}(\mathbf{r},t) \equiv k_l \hat{u}^{\lambda} e^{ik_l(z-t)}, \tag{3.7}$$

where $\hat{u}^{\lambda} = (1, \lambda i, 0)/\sqrt{2}$ is a normalized circular polarization vector, with helicity $\lambda = \pm 1$, and wavevector $\mathbf{k}_l = k_l \hat{z}$. Finally, the introduction of k_l in the amplitude of the standard vector makes it transform unitarily under Lorentz transformations [38]. With the definition above and using the expressions of the operators in the position representation specified by Eqs. (2.49)-(2.52), it can be checked that the following relations hold:

$$\hat{P}_0 \; \mathbf{\Psi}^{\lambda}_{\mathbf{k}_l}(\mathbf{r},t) = k_l \mathbf{\Psi}^{\lambda}_{\mathbf{k}_l}(\mathbf{r},t) \tag{3.8}$$

$$\hat{P}_z \; \mathbf{\Psi}^{\lambda}_{\mathbf{k}_l}(\mathbf{r},t) = k_l \mathbf{\Psi}^{\lambda}_{\mathbf{k}_l}(\mathbf{r},t) \tag{3.9}$$

$$\hat{C}_1 \; \mathbf{\Psi}^{\lambda}_{\mathbf{k}_l}(\mathbf{r},t) = 0 \tag{3.10}$$

$$\hat{\Lambda} \; \mathbf{\Psi}^{\lambda}_{\mathbf{k}_l}(\mathbf{r},t) = \lambda \mathbf{\Psi}^{\lambda}_{\mathbf{k}_l}(\mathbf{r},t). \tag{3.11}$$

Now, the basis vectors of the invariant space associated with the massless and discrete-spin UIRs of the Poincaré group are constructed by operating over the state given in Eq. (3.7). We will represent the elements of the basis by the eigenvalue of the helicity and the direction of propagation, i.e. we will denote an element of this set as $\mathbf{\Psi}^{\lambda}_{\mathbf{k}}(\mathbf{r},t)$. Here, superscript λ indicates that the basis vectors all have a well-defined helicity and subscript $\mathbf{k}$ that they propagate in a well-defined direction, which, in general, is going to be different from $\mathbf{k}_l$. In this notation, the construction of a generic basis vector is carried out by

applying a Lorentz transformation and a rotation to the standard vector (see Eq. 10.4-22 and Eq. 7.1-12 in Ref. [19]):

$$\mathbf{\Psi}^{\lambda}_{\mathbf{k}}(\mathbf{r},t) = \left[\hat{R}_z(\phi_{\mathbf{k}})\hat{R}_y(\theta_{\mathbf{k}})\hat{L}_z(\xi)\right]\mathbf{\Psi}^{\lambda}_{\mathbf{k}_l}(\mathbf{r},t). \tag{3.12}$$

We choose to write the rotation angles with a subscript $\mathbf{k}$ because they will actually represent the spherical polar angles of vector $\mathbf{k}$. At this point, we could choose to write the expression of the rotation and Lorentz transformation operators as an exponential of the operators given in Eq. (2.51) and Eq. (2.52). However, a much more convenient approach is just to employ the widely known expressions for the transformations of electromagnetic fields under such operations. The expressions for the rotations can be found in books dealing with vector fields such as Rose (see Eq. 5.40 in Ref. [39]). The expressions for the Lorentz transformations can be found in books of reference in electrodynamics such as Jackson (see Eq. 11.149 in Ref. [12]).

Following the operator order in Eq. (3.12), we should first apply the Lorentz transformation, $\hat{L}_z(\xi)$, to the electromagnetic wave expressed in Eq. (3.7). The way in which an arbitrary electromagnetic field with well-defined helicity, $\mathbf{V}^{\lambda}(\mathbf{r},t)$, transforms under Lorentz transformations can be derived from the usual expressions of the electric and magnetic field transformations [8, 12]:

$$\tilde{\mathbf{V}}^{\lambda}(\mathbf{r}',t') = \gamma\left[\mathbf{V}^{\lambda}(\mathbf{r},t) - \lambda i\mathbf{b}\times\mathbf{V}^{\lambda}(\mathbf{r},t)\right] - \frac{\gamma^2}{\gamma+1}\mathbf{b}\left[\mathbf{b}\cdot\mathbf{V}^{\lambda}(\mathbf{r},t)\right]. \tag{3.13}$$

Here, the Lorentz transformation is generally considered into the direction specified by the $\mathbf{b}$ vector and into a reference frame moving with speed $v = \tanh(\xi)$. The following relations hold between the parameters defining the transformation: $|\mathbf{b}| = v$ and $\gamma = (1-v^2)^{-1/2}$. As the Lorentz transformation specified by Eq. (3.12) is in the OZ direction in our case $\mathbf{b}/|\mathbf{b}| = \hat{z}$. Now, specifying that the electromagnetic field $\mathbf{V}^{\lambda}(\mathbf{r},t)$ is given by the standard vector in Eq. (3.7), we have that $\lambda i\mathbf{b}\times\mathbf{V}^{\lambda}(\mathbf{r},t) = |\mathbf{b}|\mathbf{V}^{\lambda}(\mathbf{r},t)$ and, also, $\mathbf{b}\cdot\mathbf{V}^{\lambda}(\mathbf{r},t) = 0$. To complete the transformation, we just need the specific form in which space-time coordinates $(\mathbf{r},t)$ are transformed into the new $(\mathbf{r}',t')$. This is also given by Jackson (see Eqs. 11.19 and 11.21 in Ref. [12]):

$$\begin{pmatrix} t \\ x \\ y \\ z \end{pmatrix} = \begin{pmatrix} \cosh\xi & 0 & 0 & \sinh\xi \\ 0 & 1 & 0 & 0 \\ 0 & 0 & 1 & 0 \\ \sinh\xi & 0 & 0 & \cosh\xi \end{pmatrix}\begin{pmatrix} t' \\ x' \\ y' \\ z' \end{pmatrix}. \tag{3.14}$$

By substituting all these expressions into the standard vector expression, we are finally left with the following form of the state in the boosted frame of reference:

$$\hat{L}_z(\xi)\mathbf{\Psi}^{\lambda}_{\mathbf{k}_l}(\mathbf{r},t) = [\gamma(1-v)k_l]\hat{u}^{\lambda}e^{i[\gamma(1-v)k_l](z'-t')}. \tag{3.15}$$

Let us discuss this result in detail. First, if we check the transformation rule in Eq. (3.13), the helicity of the monochromatic plane-wave is explicitly shown to be invariant. This, of course, is related with the

fact that helicity is a Casimir operator for particles with zero mass and discrete spin. Also, it can be noted that the modulus of the wavevector, or the frequency, of the plane-wave is modified by the effect of the Lorentz transformation. As rotations do not further modify this parameter, we have that the modulus of the wavevector of the state $\Psi^{\lambda}_{\mathbf{k}}(\mathbf{r}, t)$ is specified by:

$$|\mathbf{k}| = \gamma(1 - v)k_l = (\cosh\xi - \sinh\xi)k_l = e^{-\xi}k_l. \tag{3.16}$$

In other words, parameter $\xi \in (-\infty, \infty)$ modulates the frequency of the monochromatic plane-wave. By choosing different Lorentz transformations into reference frames moving at different speeds in the OZ direction, Eq. (3.16) indicates that one is able to modify the modulus of the wavevector in the range $k \in (0, \infty)$. Finally, it can be checked that the Lorentz transformation affects the amplitude of the standard vector, $\Psi^{\lambda}_{\mathbf{k}_l}(\mathbf{r}, t)$, by a factor $\gamma(1 - v)$. However, the introduction of the k_l amplitude term in Eq. (3.7) absorbs it into a change over the wavevector modulus, recovering the appropriate transformation rules [19, 38].

Let us now analyze the role of the rotations in the construction of the basis vectors of the invariant space. For convenience, here, we will follow the convention that a vector field, $\mathbf{V}(\mathbf{r}, t)$, is rotated through the operation $R\mathbf{V}(R^{-1}\mathbf{r}, t)$, where R is a conventional 3×3 rotation matrix [15]. Following the sign convention of Wu-ki Tung's book, we have that the composition of rotation matrices around the OY and OZ axis can be expressed as (see Eqs. 7.1-13a and 7.1-13b in Ref. [19]):

$$R_z(\phi_{\mathbf{k}})R_y(\theta_{\mathbf{k}}) = \begin{pmatrix} \cos\theta_{\mathbf{k}}\cos\phi_{\mathbf{k}} & -\sin\phi_{\mathbf{k}} & \sin\theta_{\mathbf{k}}\cos\phi_{\mathbf{k}} \\ \cos\theta_{\mathbf{k}}\sin\phi_{\mathbf{k}} & \cos\phi_{\mathbf{k}} & \sin\theta_{\mathbf{k}}\sin\phi_{\mathbf{k}} \\ -\sin\theta_{\mathbf{k}} & 0 & \cos\theta_{\mathbf{k}} \end{pmatrix}. \tag{3.17}$$

As the matrix given above is orthogonal, then, the inverse matrix is just the transpose, i.e. $R^{-1} = R^{T}$. Moreover, in the standard vector expression given by Eq. (3.7), note that the position operator is contained in the exponent in the following form: $\mathbf{k}_l \cdot \mathbf{r}$, with $\mathbf{k}_l = (0, 0, k_l)$ as a row vector and $\mathbf{r} = (x, y, z)$ as a column vector. Thus, applying the inverse rotation matrix R^{-1} to vector $\mathbf{r}$ is the same as applying the rotation matrix R to vector $\mathbf{k}_l$. As a result, we have that the rotated monochromatic plane-wave propagates in the direction $\hat{u}_{\mathbf{k}} = (\sin\theta_{\mathbf{k}}\cos\phi_{\mathbf{k}}, \sin\theta_{\mathbf{k}}\sin\phi_{\mathbf{k}}, \cos\theta_{\mathbf{k}})$. From this expression, it is clear that $(\theta_{\mathbf{k}}, \phi_{\mathbf{k}})$ represent the spherical polar angles in reciprocal space. Finally, as previously stated, the rotation also applies to the vectorial part of the electromagnetic field, i.e. to the polarization vector $\hat{u}^{\lambda} = (1, \lambda i, 0)/\sqrt{2}$. It can be checked that applying the rotation matrix in Eq. (3.17) to $\hat{u}^{\lambda}$ one recovers the expression for the polarization vector with well-defined helicity $\hat{e}^{\lambda}(\mathbf{k})$ given in Eq. (2.27).

Altogether, we have arrived to the final expression of the basis vectors of the massless and discrete-spin UIRs of the Poincaré group. The expression of the basis vector elements in the position representation is:

$$\Psi^{\lambda}_{\mathbf{k}}(\mathbf{r}, t) = |\mathbf{k}|\hat{e}^{\lambda}(\mathbf{k})e^{i\mathbf{k}\cdot\mathbf{r} - i\omega_k t}, \tag{3.18}$$

where $\mathbf{k} = k\hat{u}_{\mathbf{k}}$ and $k = \omega_{\mathbf{k}} = e^{-\xi}k_l$. For convenience, we have dropped the primes in the expression of the space and time coordinates. Note that considering the domains $\theta_{\mathbf{k}} \in (0, \pi)$ and $\phi_{\mathbf{k}} \in (0, 2\pi)$ and $\xi \in (-\infty, \infty)$, one actually spans all the possible points in reciprocal space. Thus, a general vector belonging to the invariant vector space associated with the massless and discrete-spin UIRs of the Poincaré group can most generally be written as a linear superposition of the states given in Eq. (3.18). We are finally left with the following fundamental relation:

$$\mathbf{\Psi}^{\lambda}(\mathbf{r}, t) = \frac{1}{(2\pi)^{3/2}} \int_{-\infty}^{+\infty} \frac{d\mathbf{k}}{|\mathbf{k}|} f^{\lambda}(\mathbf{k}) \mathbf{\Psi}^{\lambda}_{\mathbf{k}}(\mathbf{r}, t). \tag{3.19}$$

The expression above indicates that electromagnetic wave solutions expressed in terms of the RS vector in Eq. (2.32) are directly related with the basis vectors given by Eq. (3.18). Indeed, the $\mathbf{\Psi}^{\lambda}(\mathbf{r}, t)$ field can be constructed as a linear superposition of the basis vectors associated with the massless and discrete-spin UIRs of the Poincaré group. In this specific sense, it can be stated that the RS vector plays the role of the wave function in the electromagnetic theory [8, 18]. Finally, there is an argument that explains the presence of only positive frequencies in Eq. (3.19). It is that the sign of the frequency is also a Casimir invariant of the Poincaré group [24]. This justifies a posteriori our choice of positive frequencies in Eq. (2.32).

The discussion about the wave function of the photon in coordinate space has been long and intense through the years. A nice compilation can be found in Ref. [8]. It is not our aim to place ourselves in any specific position with respect to this discussion. We just choose the RS representation of electromagnetic wave solutions for the following practical reasons:

1. The RS vector is directly related with the symmetries of spacetime and, particularly, to the UIRs of the Poincaré group. This features makes it suitable for the study of light-matter interactions in the context of symmetries. In particular, as we show in the next Subsection, it facilitates the construction of electromagnetic wave solutions propagating in infinitely homogeneous media and the analysis of conserved quantities.

2. The RS vector is a mathematical object which is directly related with electric and magnetic fields. This makes it applicable to many different problems in which electromagnetic wave solutions are explicitly given in terms of electric, **D** or **E**, and magnetic, **B** or **H**, fields. We will use this approach in Chapter 4, where the RS vector will be shown to be a useful object in the framework of linear scattering theory.

3. As we will show in Chapter 5, the RS vector is also useful in the analysis of electromagnetic waves propagating through inhomogeneous media. The terms accounting for the conservation and mixing of electromagnetic helicity components natu-

rally emerge when writing Maxwell's equations in terms of the RS vector.

4. The description of the helicity components in terms of the RS vector is also possible within the framework of second quantization. This will employed in Chapter 6 to describe the scattering of multi photon states with cylindrically symmetric samples.

3.2 HELICITY AND EUCLIDEAN SYMMETRIES

In the previous Section, we have analyzed how electromagnetic wave solutions expressed in terms of the RS vector are related with the Poincaré group. As we have shown, the discussion is valid for waves propagating in vacuum. In this Section, we study the propagation of electromagnetic waves in infinitely homogeneous media. The direct and straightforward way of approaching this problem is probably considering solutions to the wave equation in Eq. (2.20) but, now considering the material parameters for a different medium. Here, however, we choose a different path which, in our view, further underlines the role of helicity within the electromagnetic theory. The analysis is adapted from Contribution VII.

Even though the derivation in the previous Subsection is elegant in its form, it is not applicable to any particular realistic problem. When dealing with optical problems, at least one of the symmetries of relativity is broken. This is just because, in common situations, electromagnetic waves interact with samples which, of course, are less symmetrical than vacuum itself. In particular, all problems of interest consider the presence of some medium different from vacuum. So, at this stage, we may ask ourselves: does just the presence of a medium reduce the symmetries in an optical problem? This is probably the first question we should answer before moving forward. As a starting point, we will consider the simplest underlying medium, i.e. one which is non-chiral, linear, static, homogeneous, isotropic and infinite in extension. In this context, non-chiral implies that the constitutive relations do not mix electric and magnetic types of fields; linear means that constitutive relations relate proportionally $\mathbf{D}/\mathbf{B}$ and $\mathbf{E}/\mathbf{H}$; the term static indicates that constitutive relations do not change with time; homogeneous refers to the fact that the constitutive relations are the same all over space; finally, isotropic indicates that constitutive relations are determined by scalar functions. Such a medium, which will in short be denoted as *homogeneous*, is characterized for having a constant scalar electric permittivity, ε, and a constant scalar magnetic permeability, μ.

3.2.1 *Electromagnetic waves in homogeneous media*

Let us discuss whether this kind of medium is left invariant under the whole Poincaré group of transformations. First, the fact that such a medium is static makes it invariant under translations in time. Then, homogeneity implies that the medium is invariant under continuous

translations, i.e. the response of the medium does not change from one point to another in space. In addition, isotropy ensures that every direction in the medium is equivalent and, thus, that it is also invariant under rotations. Finally, we are left with Lorentz transformations. We need to check whether a medium characterized by a constant electric permittivity, ε, and constant magnetic permeability, μ, is left invariant when observing it from a frame of reference moving at speed $-\mathbf{v}$. This situation is, of course, equivalent to being in a frame of reference in which the medium moves at speed $\mathbf{v}$. In other words, to answer this question, we should check whether the motion of a dielectric affects its constitutive relations. This problem was addressed by Minkowski in 1908 [40, 41], but it can be also checked in more recent books such as the series by Landau and Lifshitz (see Section 76 in Ref. [42]). The result is that a homogeneous medium generally becomes bianisotropic when it moves at certain speed $\mathbf{v}$. Thus, we can conclude that such a medium is not invariant under Lorentz transformations.

The fact that a homogeneous medium is not invariant under Lorentz transformations indicates that it is not invariant under the whole Poincaré group. In group theoretical terms, we say that the symmetry group associated with the system is a subgroup of the Poincaré group in which Lorentz transformations are not included. Such a particular way of addressing physical problems is commonly denoted as the *symmetry breaking principle* and it is extensively employed in the context of condensed matter and photonic crystals. The principle can be compactly stated in the following terms [35, 43–48]: *consider a physical system which is described by a given group G and an external influence reduces the symmetry from the original G to a subgroup $G_i \subset G$. Then, the subgroup G_i can be used to study the properties of the new modified system. In particular, the generators and Casimir operators of the subgroup will provide conserved quantities and the UIRs will determine the new wave functions or, at least, some of their properties*. In our case, the physical system of departure are electromagnetic waves and G is the Poincaré group. Thus, following the symmetry breaking principle, to study the properties of electromagnetic waves propagating in homogeneous media, we should analyze the subgroup G_i which does not include Lorentz transformations. Following the notation of Ref. [48], the group generated by the set $\{P_0, P_i, J_i\}$ will be denoted as $P_{3,1}$. Note that the subgroup of time translations T, generated by $\{P_0\}$, commutes with the Euclidean group in three dimensions $E(3)$, generated by $\{P_i, J_i\}$ (see Table 2). As a result, we say that $P_{3,1}$ is isomorphic to the direct product of two of its subgroups, i.e. $P_{3,1} = E(3) \times T$ [49].

On the other hand, $P_{3,1}$ has three Casimir operators, i.e. the generator of time translations, $\hat{P}_0$, a magnitude proportional to helicity, $\hat{\mathbf{J}} \cdot \hat{\mathbf{P}}$, and the square of linear momentum, $\hat{\mathbf{P}}^2 = \hat{\mathbf{P}} \cdot \hat{\mathbf{P}}$ [48]. This implies that every basis vector associated with the UIRs of $P_{3,1}$ must be an

eigenstate of these three operators. By denoting as $\mathbf{\Phi}^{\lambda}_{\mathbf{k}}(\mathbf{r},t)$ a generic vector belonging to the invariant vector space, we have that:

$$\hat{P}_0 \ \mathbf{\Phi}^{\lambda}_{\mathbf{k}}(\mathbf{r},t) = \omega \mathbf{\Phi}^{\lambda}_{\mathbf{k}}(\mathbf{r},t) \tag{3.20}$$

$$k^{-1}\hat{\mathbf{J}}\cdot\hat{\mathbf{P}} \ \mathbf{\Phi}^{\lambda}_{\mathbf{k}}(\mathbf{r},t) = \lambda \mathbf{\Phi}^{\lambda}_{\mathbf{k}}(\mathbf{r},t) \tag{3.21}$$

$$\hat{\mathbf{P}}^2 \ \mathbf{\Phi}^{\lambda}_{\mathbf{k}}(\mathbf{r},t) = k^2 \mathbf{\Phi}^{\lambda}_{\mathbf{k}}(\mathbf{r},t). \tag{3.22}$$

In principle, the possible spectra of the Casimir eigenvalues is the following: the values of ω and k are unrestricted, whereas helicity can only take certain values $\lambda = 0, \pm 1, \pm 2...$ and so on [19]. Like in the case of the Poincaré group, different choices of these parameters lead to the description of different physical systems. For instance, we may choose the zero helicity representations ($\lambda = 0$) and consider the dispersion relation $\omega = k^2/2M + V$, where M and V are real constants. In this case, we are lead to a non-relativistic description of a spinless particle of mass M propagating in an environment of constant potential V. Indeed, making use of the correspondence rule dictated by Eq. (2.49) and Eq. (2.50), it can be check that in this case Eq. (3.20) and Eq. (3.22) represent the time-independent Schrödinger's equations in a homogeneous environment (for a detailed discussion see Section 18 in Ref. [49]).

However, the description of electromagnetic waves cannot be associated to the zero helicity representations, but to the case $\lambda = \pm 1$. Moreover, to recover the electromagnetic equations of motion, we have to consider the dispersion relation of waves propagating in an homogeneous environment, i.e. $\omega = kn$, where $n = \sqrt{\epsilon\mu}$ is the refractive index of the medium. Employing again the correspondence rule given by Eqs. (2.49)-(2.51), it can be checked that Eqs. (3.20)-(3.22) lead now to the dynamic equations of monochromatic electromagnetic waves propagating in homogeneous media. Indeed, Eq. (3.20) represents the monochromaticity of the fields; Eq. (3.21) represents all four monochromatic Maxwell's equations as expressed in Eq. (2.34) and Eq. (2.35); and, finally, Eq. (3.22) represents Helmholtz's equation as expressed in Eq. (2.36). This is coherent with the previous results obtained for vacuum, where the Casimir invariants were also related with the equations of motion. From the derivation above it is also clear that the role of helicity is central in the description of electromagnetic waves propagating in homogeneous media. Indeed, helicity can be written as a product of two Casimirs of the group and, therefore, $\hat{\Lambda} = k^{-1}\hat{\mathbf{J}}\cdot\hat{\mathbf{P}}$ can also be regarded as an invariant of $P_{3,1}$. This is due to the fact that products of Casimir operators also commute with all the generators of a continuous group.

3.2.2 *Photon wave function in homogeneous media*

At this point, and following the prescription of the symmetry breaking principle, we should be able to obtain some information about the wave functions by analyzing the invariant vector spaces of the UIRs. As we mentioned before, $P_{3,1}$ can be split as the direct product of two of its subgroups which are the Euclidean group in three dimensions,

$E(3)$, and the one parameter subgroup of time-translations, T. As a result, the UIRs of $P_{3,1}$ are constructed as the product of the UIRs of $E(3)$ and the UIRs of T (see pages 60 and 61 in Ref. [49]). A simpler way of understanding this is by noting that the basis vectors $\mathbf{\Phi}^{\lambda}_{\mathbf{k}}(\mathbf{r},t)$ are necessarily constructed as the product of a spatial function and a temporal function. Indeed, Eq. (3.20) determines the temporal dependence of the basis vectors, whereas Eqs. (3.21)-(3.22) determine their spatial form. Thus, the basis vectors of the UIRs of $P_{3,1}$ associated with electromagnetic waves are constructed in the following way:

$$\mathbf{\Phi}^{\lambda}_{\mathbf{k}}(\mathbf{r},t) = \boldsymbol{\phi}^{\lambda}_{\mathbf{k}}(\mathbf{r})e^{-i\omega t}, \tag{3.23}$$

where $\boldsymbol{\phi}^{\lambda}_{\mathbf{k}}(\mathbf{r})$ is a basis vector associated with the UIRs of the $E(3)$ group.

Thus, to construct the UIRs of $P_{3,1}$ we need to check how the UIRs of $E(3)$ are obtained. As indicated by Wu-Ki Tung's Theorem 9.13 [19], whenever $k \neq 0$, the basis vectors can also be constructed by operating over a given standard vector. Such a vector is chosen to be an eigenstate of the $\hat{\mathbf{P}}$ operator. In addition, as the standard vector belongs to the invariant space, it has to be also an eigenstate of the two Casimir invariants of $E(3)$, i.e. $\hat{\mathbf{J}}\cdot\hat{\mathbf{P}}$ and $\hat{\mathbf{P}}^2$. All these constraints imply that the standard vector is a circularly polarized plane-wave. Fixing the direction of propagation in the OZ axis, we are finally left with the following explicit form of the standard vector:

$$\boldsymbol{\phi}^{\lambda}_{\mathbf{k}_0}(\mathbf{r}) \equiv \hat{u}^{\lambda}e^{ikz}, \tag{3.24}$$

where $\hat{u}^{\lambda} = (1,\lambda i,0)/\sqrt{2}$ is a normalized circular polarization vector, with $\lambda = \pm 1$, and $\mathbf{k}_0 = k\hat{z}$, where $k = \omega n \neq 0$. With the definition above and using the expressions of the operators given by Eq. (2.50) and Eq. (2.51), it can be checked that the following relations hold:

$$\hat{P}_z\ \boldsymbol{\phi}^{\lambda}_{\mathbf{k}_0}(\mathbf{r}) = k\boldsymbol{\phi}^{\lambda}_{\mathbf{k}_0}(\mathbf{r}) \tag{3.25}$$

$$k^{-1}\hat{\mathbf{J}}\cdot\hat{\mathbf{P}}\ \boldsymbol{\phi}^{\lambda}_{\mathbf{k}_0}(\mathbf{r}) = \lambda\boldsymbol{\phi}^{\lambda}_{\mathbf{k}_0}(\mathbf{r}) \tag{3.26}$$

$$\hat{\mathbf{P}}^2\ \boldsymbol{\phi}^{\lambda}_{\mathbf{k}_0}(\mathbf{r}) = k^2\boldsymbol{\phi}^{\lambda}_{\mathbf{k}_0}(\mathbf{r}). \tag{3.27}$$

Now, the basis vectors of the invariant space associated with the UIRs of the $E(3)$ group are constructed by operating over the state given in Eq. (3.24). Indeed, the construction of a generic basis vector, $\boldsymbol{\phi}^{\lambda}_{\mathbf{k}}(\mathbf{r})$, is carried out by applying a rotation over the standard vector (see Eq. 9.7-8 and Eq. 7.1-12 in Ref. [19]):

$$\boldsymbol{\phi}^{\lambda}_{\mathbf{k}}(\mathbf{r}) \equiv \left[\hat{R}_z(\phi_{\mathbf{k}})\hat{R}_y(\theta_{\mathbf{k}})\right]\boldsymbol{\phi}^{\lambda}_{\mathbf{k}_0}(\mathbf{r}). \tag{3.28}$$

Interestingly, the rotation matrices acting over the standard vector $\boldsymbol{\phi}^{\lambda}_{\mathbf{k}_0}(\mathbf{r})$ are exactly the ones which previously acted over the standard vector $\mathbf{\Psi}^{\lambda}_{\mathbf{k}_l}(\mathbf{r},t)$ of the Poincaré group. This implies that the basis vectors of the UIRs of $P_{3,1}$ are also related with the polarization vector $\hat{e}^{\lambda}(\mathbf{k})$ specified by Eq. (2.27). More explicitly, we have that the expression of the $E(3)$ basis vectors is:

$$\boldsymbol{\phi}^{\lambda}_{\mathbf{k}}(\mathbf{r}) = \hat{e}^{\lambda}(\mathbf{k})e^{i\mathbf{k}\cdot\mathbf{r}}. \tag{3.29}$$

In this line, any vector belonging to the invariant vector space associated with the UIRs of $E(3)$ can be written as a superposition of the states given by Eq. (3.29). As $|\mathbf{k}| = k$ is fixed by Eq. (3.22), such a superposition may only consider different propagating directions in reciprocal space.

As a result, any vector belonging to the invariant space of the $P_{3,1}$ UIRs that are associated with electromagnetic wave solutions, i.e. with $k \neq 0$, may be written as:

$$\mathbf{\Phi}^{\lambda}(\mathbf{r}, t) = \int d\Omega_{\mathbf{k}}\; g^{\lambda}(\theta_{\mathbf{k}}, \phi_{\mathbf{k}})\mathbf{\phi}^{\lambda}_{\mathbf{k}}(\mathbf{r}, t), \tag{3.30}$$

where $d\Omega_{\mathbf{k}} = \sin\theta_{\mathbf{k}} d\theta_{\mathbf{k}} d\phi_{\mathbf{k}}$ and $g^{\lambda}(\theta_{\mathbf{k}}, \phi_{\mathbf{k}})$ is an arbitrary complex function. Note that we would have obtained the same result just by considering in Eq. (2.32) an amplitude $f^{\lambda}(\mathbf{k}) = (2\pi)^{3/2}|\mathbf{k}|^{-2}\delta(|\mathbf{k}| - \omega n)g^{\lambda}(\theta_{\mathbf{k}}, \phi_{\mathbf{k}})$, i.e. by considering monochromatic plane-waves with a fixed frequency ω in the Fourier decomposition of the RS vector. In other words, the state given by Eq. (3.30) is nothing but an abstract form of the monochromatic RS vector. This is in agreement with the fact that no Lorentz transformation is applied in Eq. (3.28), in contrast with the expression given by Eq. (3.12). As we have previously shown, the presence of $\hat{L}_z(\xi)$ modifies the frequency of the electromagnetic waves through the relation specified by Eq. (3.16). In the case of $P_{3,1}$, the basis vectors are constructed just by applying rotations to the standard vector and, thus, all the plane-waves in the superposition share the same frequency. This is related with the fact that $\hat{P}_0$ is a Casimir invariant of $P_{3,1}$, but not of the Poincaré group.

Summing up, we have shown that the description of electromagnetic waves in homogeneous media is also possible through the theory of group representations. Following the symmetry breaking principle, we have shown that such a description must be based on the $P_{3,1}$ subgroup of the Poincaré group which does not include Lorentz transformations. In particular, we have shown that the Casimir operators $\hat{P}_0$, $\hat{\Lambda}$ and $\hat{\mathbf{P}}^2$ can be associated with the equations of motion of monochromatic electromagnetic waves. Moreover, we have also reached to the conclusion that the basis vectors of the UIRs of $P_{3,1}$ are related with the monochromatic RS vector. Thus, we may expect the monochromatic RS vector to be a useful tool in the study of the propagation of electromagnetic waves through matter. In the next Subsection we show that, by properly fixing the complex function $g^{\lambda}(\theta_{\mathbf{k}}, \phi_{\mathbf{k}})$ in Eq. (3.30), we can construct different monochromatic electromagnetic wave solutions [15, 50]. We will also show that the monochromatic RS vector plays a fundamental role in classical (Chapters 4 and 5) and quantum (Chapter 6) electromagnetic scattering theory.

3.3 MONOCHROMATIC ELECTROMAGNETIC WAVE SOLUTIONS

In the previous Section we have shown how helicity is intimately related with space-time symmetries. In particular, we have shown that it emerges as a Casimir invariant of both Poincaré and $P_{3,1}$ groups.

In addition, we have found that different forms of the RS vector expressed in Eq. (2.17) and Eq. (2.33) are also associated with the UIRs of such symmetry groups. In what follows, we show how the results of the previous discussion may also be useful for the construction of particular electromagnetic wave solutions. As we will mainly deal with the propagation of electromagnetic waves in material environments, we focus on the vector field given by Eq. (3.30). As we show next, different choices of the complex amplitude $g^{\lambda}(\theta_{\mathbf{k}}, \phi_{\mathbf{k}})$ lead to different electromagnetic wave solutions. In particular, we discuss the construction of solutions which are eigenstates of maximal sets of commuting operators of $P_{3,1}$. As $\hat{P}_0^2$ and $\hat{\mathbf{P}}^2$ are proportional for electromagnetic wave solutions, we just consider $\hat{\mathbf{P}}^2$ in the following discussion.

3.3.1 *Plane-waves*

Let us first consider the set of commuting operators: $\{\hat{\Lambda}, \hat{\mathbf{P}}^2, \hat{P}_x, \hat{P}_y\}$. The construction of monochromatic plane-wave solutions which are eigenstates of the aforementioned operators is reached by choosing the amplitude function:

$$g^{\lambda}(\theta_{\mathbf{k}}, \phi_{\mathbf{k}}) = (\sin\tilde{\theta})^{-1}\delta(\theta_{\mathbf{k}} - \tilde{\theta})\delta(\phi_{\mathbf{k}} - \tilde{\phi}), \tag{3.31}$$

where δ here represents the Dirac delta function. This form of the amplitude results in an electromagnetic wave solution of the form:

$$\mathbf{\Phi}^{\lambda}_{\mathbf{k}}(\mathbf{r}) = \hat{e}^{\lambda}(\tilde{\theta}, \tilde{\phi})e^{i\mathbf{k}\cdot\mathbf{r}}, \tag{3.32}$$

where the polarization vector is specified by Eq. (2.27). Due to the general properties of the state given by Eq. (3.30), it is not necessary to show that the solution specified by Eq. (3.32) is an eigenstate of $\{\hat{\Lambda}, \hat{\mathbf{P}}^2\}$ with eigenvalues $\{\lambda, k^2\}$. However, it can also be checked that it is also an eigenstate of the linear momentum components:

$$\hat{P}_x\ \mathbf{\Phi}^{\lambda}_{\mathbf{k}}(\mathbf{r}) = k\sin\tilde{\theta}\cos\tilde{\phi}\ \mathbf{\Phi}^{\lambda}_{\mathbf{k}}(\mathbf{r}) \tag{3.33}$$

$$\hat{P}_y\ \mathbf{\Phi}^{\lambda}_{\mathbf{k}}(\mathbf{r}) = k\sin\tilde{\theta}\sin\tilde{\phi}\ \mathbf{\Phi}^{\lambda}_{\mathbf{k}}(\mathbf{r}) \tag{3.34}$$

$$\hat{P}_z\ \mathbf{\Phi}^{\lambda}_{\mathbf{k}}(\mathbf{r}) = k\cos\tilde{\theta}\ \mathbf{\Phi}^{\lambda}_{\mathbf{k}}(\mathbf{r}). \tag{3.35}$$

Note that the eigenvalue of the $\hat{P}_z$ operator can be computed in terms of the operator $\hat{\mathbf{P}}^2 - \hat{P}_x^2 - \hat{P}_y^2$.

3.3.2 *Bessel beams*

Bessel beam wave solutions are eigenstates of the set $\{\hat{\Lambda}, \hat{\mathbf{P}}^2, \hat{P}_z, \hat{J}_z\}$ and are constructed by choosing the amplitude function [15]:

$$g^{\lambda}(\theta_{\mathbf{k}}, \phi_{\mathbf{k}}) = (\sin\tilde{\theta})^{-1}\delta(\theta_{\mathbf{k}} - \tilde{\theta})e^{im\phi_k}, \tag{3.36}$$

By substituting the amplitude given above in Eq. (3.30), one obtains the following abstract form of Bessel beams:

$$\mathbf{\Phi}^{\lambda}_{k_z m}(\mathbf{r}) = \int_0^{2\pi} d\phi_{\mathbf{k}}\ e^{im\phi_k}\left[\hat{R}_z(\phi_{\mathbf{k}})\hat{R}_y(\tilde{\theta})\right]\hat{u}^{\lambda}e^{ikz} \tag{3.37}$$

It can be noted that the complex exponential amplitude makes the solution be an eigenstate of $\hat{J}_z$ operator. Indeed, operating with the rotation operator $\hat{R}_z$, one gets:

$$\hat{R}_z(\alpha)\ \mathbf{\Phi}^{\lambda}_{k_z m}(\mathbf{r}) = \int_0^{2\pi} d\phi_{\mathbf{k}}\ e^{im\phi_{\mathbf{k}}} \left[\hat{R}_z(\phi_{\mathbf{k}}+\alpha)\hat{R}_y(\tilde{\theta})\right] \hat{u}^{\lambda} e^{ikz}. \quad (3.38)$$

And, by making the change of variable $\phi' = \phi_{\mathbf{k}} + \alpha$, it can be checked that [51]:

$$\hat{R}_z(\alpha)\ \mathbf{\Phi}^{\lambda}_{k_z m}(\mathbf{r}) = e^{-im\alpha}\mathbf{\Phi}^{\lambda}_{k_z m}(\mathbf{r}). \quad (3.39)$$

Moreover, the presence of the delta function in Eq. (3.36), makes the electromagnetic wave solution be an eigenstate of $\hat{P}_z$ operator with eigenvalue $k_z = k\cos\tilde{\theta}$.

Now, to obtain the coordinate space representation of the Bessel beam solution, we should carry out the integration indicated by Eq. (3.37). To that end, we should expand the plane-wave exponential term in cylindrical waves (see Section 6.10 in Ref. [52]):

$$e^{i\mathbf{k}\cdot\mathbf{r}} = \sum_{n=-\infty}^{\infty} i^n J_n(k_t\rho)e^{in(\phi-\phi_{\mathbf{k}})}e^{ik_z z}. \quad (3.40)$$

In the expression above, $\{\rho,\phi,z\}$ refer to the real space cylindrical coordinates, $k_t^2 = k^2 - k_z^2$ and $J_n(x)$ is the Bessel function of the first kind of order n. The result is conveniently expressed in terms of the eigenvector of the $\hat{S}_z$ operator given by Eq. (2.37): $\hat{l} = (\hat{x}+i\hat{y})/\sqrt{2}$, $\hat{r} = (\hat{x}-i\hat{y})/\sqrt{2}$ and $\hat{z}$. It is important to note that the components of a generic vector field in this basis are obtained from the Cartesian components in the following way: $V_l = (V_x - iV_y)/\sqrt{2}$, $V_r = (V_x + iV_y)/\sqrt{2}$ and V_z. Taking all this into account, the integral specified by Eq. (3.37) results in:

$$\begin{aligned}
\Phi^{\lambda}_l(\rho,\phi,z) &= -(i^m\pi)e^{ik_z z}\left[i\left(\lambda+\frac{k_z}{k}\right)J_{m-1}(k_t\rho)e^{i(m-1)\phi}\right]\\
\Phi^{\lambda}_r(\rho,\phi,z) &= -(i^m\pi)e^{ik_z z}\left[i\left(\lambda-\frac{k_z}{k}\right)J_{m+1}(k_t\rho)e^{i(m+1)\phi}\right]\\
\Phi^{\lambda}_z(\rho,\phi,z) &= -(i^m\pi)e^{ik_z z}\left[\sqrt{2}\left(\frac{k_t}{k}\right)J_m(k_t\rho)e^{im\phi}\right]. \quad (3.41)
\end{aligned}$$

From the expressions above, it can be explicitly computed that the wave solutions are eigenstates of the total angular momentum operator $\hat{J}_z = \hat{L}_z + \hat{S}_z$ operator, where $\hat{L}_z = -i\partial_\phi$. Indeed, Bessel beam wave solutions fulfill:

$$\hat{P}_z\ \mathbf{\Phi}^{\lambda}_{k_z m}(\mathbf{r}) = k\cos\tilde{\theta}\ \mathbf{\Phi}^{\lambda}_{k_z m}(\mathbf{r}) \quad (3.42)$$

$$\hat{J}_z\ \mathbf{\Phi}^{\lambda}_{k_z m}(\mathbf{r}) = m\ \mathbf{\Phi}^{\lambda}_{k_z m}(\mathbf{r}). \quad (3.43)$$

3.3.3 *Multipolar beams*

Multipolar beams are constructed as eigenstates of the set $\{\hat{\Lambda}, \hat{\mathbf{P}}^2, \hat{\mathbf{J}}^2, \hat{J}_z\}$ of commuting operators. And, they can be constructed by choosing the following amplitude function (see Eq. 9.8-6 in Ref. [19]):

$$g^{\lambda}(\theta_{\mathbf{k}},\phi_{\mathbf{k}}) = \left[D^{j}_{m\lambda}(\phi_{\mathbf{k}},\theta_{\mathbf{k}},0)\right]^*, \quad (3.44)$$

where $D^{j}_{m'm}(\alpha,\beta,\gamma)$ represents Wigner's rotation matrix. The use of the amplitude above leads to the construction of vector fields with total angular momentum eigenvalue $j(j+1)$ and z component of total angular momentum eigenvalue m.

It is also possible to build a coordinate space representation of multipolar beams by expanding the plane-wave term in scalar spherical harmonics, $Y_{jm}(\theta,\phi)$. Such an expansion can be found, for instance, in Section 8.7 of Ref. [19]. Making use of the relation of scalar spherical harmonics with Wigner's matrices and by carrying out the corresponding integrals, one finally retrieves an explicit expression of the multipolar beams [53]. However, at this point, our approach will deviate from such a way. We choose to make use of the specific notation introduced in Jackson's book [12]. We do this to facilitate the following discussions of Chapter 4, where this nomenclature is going to be extensively employed. Indeed, Jackson defines the following vector spherical harmonics to expand the electromagnetic field radiated by a generic localized source (see Eq. 9.119 in Ref. [12]):

$$\mathbf{X}(\theta,\phi) = \frac{1}{\sqrt{j(j+1)}}\hat{\mathbf{L}}Y_{jm}(\theta,\phi), \tag{3.45}$$

where $\hat{\mathbf{L}}$ represents the orbital angular momentum operator previously defined in Eq. (2.51).

Even if the expression above may seem a bit obscure, it clarifies if we compute the components of the vector spherical harmonics in the $\{\hat{l},\hat{r},\hat{z}\}$ basis. In this basis, we are lead with the following explicit expressions for the components of the vector spherical harmonics:

$$X_l(\theta,\phi) = \sqrt{\frac{(j+m)(j-m+1)}{2j(j+1)}}Y_{j,m-1}(\theta,\phi) \tag{3.46}$$

$$X_r(\theta,\phi) = \sqrt{\frac{(j-m)(j+m+1)}{2j(j+1)}}Y_{j,m+1}(\theta,\phi) \tag{3.47}$$

$$X_z(\theta,\phi) = \frac{m}{\sqrt{j(j+1)}}Y_{jm}(\theta,\phi). \tag{3.48}$$

Due to the properties of the scalar spherical harmonics (see Eq. 3.53 in Ref. [12]) it is direct to check that vector spherical harmonics given by Eq. (3.45) are eigenstates of the $\hat{J}_z$ operator. In addition, the presence of the specific coefficients in Eqs. (3.46)-(3.48), makes the $\mathbf{X}(\theta,\phi)$ vector functions also be eigenstates of the $\hat{\mathbf{J}}^2$ operator. This property can be understood by identifying such numerical factors as the Clebsch-Gordan coefficients associated with the coupling of orbital and spin angular momenta in vector fields [54].

On the other hand, the functions given by Eq. (3.45) are not, by themselves, solutions to Helmholtz's equation, i.e. eigenstates of the $\hat{\mathbf{P}}^2$ operator. They have to be multiplied by an specific radial function $f_j(r)$ which fulfills the following differential equation:

$$\frac{d^2f_j(r)}{dr^2} + \frac{2}{r}\frac{df_j(r)}{dr}\left[k^2 - \frac{j(j+1)}{r^2}\right]f_j(r) = 0, \tag{3.49}$$

where k^2 is the eigenvalue of the $\hat{\mathbf{P}}^2$ operator. Spherical Bessel functions constitute a complete set of solutions to the differential equation given by Eq. (3.49). In the next Chapter, depending on whether we describe incident or scattered electromagnetic fields, we will employ different linear combinations of such functions. However, for the time being, let us just stick with the general case and assume that a solution to Helmholtz's equation can be written as:

$$\mathbf{M}_{jm}(\mathbf{r}) \equiv f_j(r)\mathbf{X}(\theta,\phi). \tag{3.50}$$

Due to the arguments given above, we have that such a vector field is an eigenstate of the set $\{\hat{\mathbf{P}}^2, \hat{\mathbf{J}}^2, \hat{J}_z\}$.

However, it can be shown that the vector function given in Eq. (3.50) is not an eigenstate of the helicity operator for monochromatic fields, i.e $\hat{\Lambda} = k^{-1}\nabla\times$. This can be explicitly checked by computing the curl of $\mathbf{M}_{jm}(\mathbf{r})$. Taking this into account, we can define a different vector field exactly as

$$\mathbf{N}_{jm}(\mathbf{r}) \equiv \frac{1}{k}\nabla \times \mathbf{M}_{jm}(\mathbf{r}). \tag{3.51}$$

The pair of solutions $\mathbf{M}_{jm}(\mathbf{r})$ and $\mathbf{N}_{jm}(\mathbf{r})$ are usually denoted in the literature as Hansen multipoles. And, as the helicity operator commutes with all the operators we are dealing with, $\mathbf{N}_{jm}(\mathbf{r})$ is also an eigenvector of the set $\{\hat{\mathbf{P}}^2, \hat{\mathbf{J}}^2, \hat{J}_z\}$ and with the same eigenvalues as $\mathbf{M}_{jm}(\mathbf{r})$. Moreover, it can also be checked that Hansen multipoles are divergenceless [12, 54], which implies that for these fields the following operator relation holds: $\hat{\Lambda}^2 = \frac{1}{k^2}\hat{\mathbf{P}}^2 = \hat{\mathbb{I}}$, where $\hat{\mathbb{I}}$ is the identity operator. In other words, the square of the helicity operator for monochromatic and divergenceless vector fields acts as the identity. This particular feature permits us define multipolar beams with well-defined helicity by taking the following linear combinations:

$$\mathbf{\Phi}^{\lambda}_{jm}(\mathbf{r}) = \frac{1}{\sqrt{2}}\left[\mathbf{N}_{jm}(\mathbf{r}) + \lambda\mathbf{M}_{jm}(\mathbf{r})\right]. \tag{3.52}$$

3.4 SUMMARY

In Section 3.1, we have studied the theory of unitary representations of the Poincaré group and we have seen that helicity emerges as a Casimir operator for the massless and discrete-spin representations. In addition, we have shown that Maxwell's equations and the wave equation in vacuum can be derived from group theoretical principles. Furthermore, we have constructed the invariant space associated with the UIRs of the Poincaré group and we have shown that it is directly related with the RS vector, $\mathcal{F}(\mathbf{r}, t)$. Then, in Section 3.2, we have focused on the propagation of electromagnetic waves through material media, identifying the subgroup $P_{3,1}$ as the appropriate symmetry group for our study. We have seen that helicity is also a Casimir operator of this group and that time-independent Maxwell's equations and Helmholtz's equation emerge from similar group theoretical arguments. For completeness, we have constructed the invariant space

associated with the UIRs of $P_{3,1}$ and we have shown that it is associated with the monochromatic RS vector, $\mathbf{F}(\mathbf{r}, \omega)$. Finally, in Section 3.3, we have applied general symmetry arguments discussed in the previous Section to the construction of specific monochromatic electromagnetic wave solutions.

4

RIEMANN-SILBERSTEIN VECTOR IN SCATTERING THEORY

In this Chapter, we study the application of the Riemann-Silberstein vector to linear electromagnetic scattering theory. First, we introduce the general framework of scattering theory and define basic concepts such as the scattered energy, scattered helicity or extincted power for an arbitrary sample. Then, we delve into the study of dual spherical dielectric systems and show that their existence is highly restricted when dealing with lossy dielectric materials. We also study the limitations of building antidual samples from natural materials. Finally, we show that there exist general relations between integrated magnitudes and local densities for cylindrically symmetric samples.

Some analytical expressions of Section 4.1 have been adapted from Contributions III and IV. Derivations within Section 4.2 are based on Contributions II, III, IV and V. Finally, Section 4.3 is adapted from the results reported in Contribution VI.

4.1 CLASSICAL ELECTROMAGNETIC SCATTERING THEORY

Classical electromagnetic scattering theory is a relevant physical framework in which we can put in practice some of the mathematical concepts we have discussed in Chapter 3. In this thesis, we will refer as *scatterer* to a finite object whose size and shape are determined by sharp boundaries. Excluding the boundary itself, the two regions of space involved in the problem are considered to be homogeneous. In addition to this, as we will only consider linear media with time-independent constitutive relations, the frequency of electromagnetic waves is preserved through the scattering process. Consequently, all the fields in the problem are monochromatic, i.e. they have a fixed time dependence of the type $e^{-i\omega t}$. These general features already suggest that $P_{3,1}$ symmetry group may play a relevant role in linear electromagnetic scattering theory.

Within linear electromagnetic scattering theory, solutions are constructed in the following particular way: first, one proposes a solution to the Helmholtz's equation inside and outside the scatterers, with free coefficients; then, with the aid of boundary conditions, those free coefficients are fixed. The same procedure is applied to build solutions of electromagnetic waves propagating through arbitrary piecewise homogeneous media. The technique, of course, it is not new. For instance, the solution for the scattering of a homogeneous sphere illuminated by a plane electromagnetic wave was found by Gustav Mie in 1908 [21, 55]. However, our previous analysis permits us to identify electromagnetic waves with space-time symmetries and, thus, solutions will be asked to fulfill Eqs. (3.20)-(3.22) in each region. This differs from the conventional approach in the fact that we may express the wave solutions in terms of the monochromatic RS vector and not as a function of the usual electric and magnetic fields. As we will see, this particular approach has certain important advantages. In words of J. A. Stratton (see Section 12, Chapter I in Ref. [52]): *The procedure has no apparent physical meaning but frequently facilitates analysis*.

In contrast to Stratton's thoughts, we have just shown that the monochromatic RS vector does have a clear physical interpretation. In the upcoming, we show how it facilitates analysis within linear electromagnetic scattering theory.

4.1.1 *General framework*

The general situation considered in linear electromagnetic scattering problems is depicted in Fig. 4.1. There, a given incident electromagnetic wave scatters off a sample which, in turn, emits a scattered electromagnetic field. The black arrows represent the directionality of the fields, the green color represents the frequency (which is conserved) and the red/blue rotating arrows represent the polarization vector associated with each spatial Fourier component of both incident and scattered waves. Moreover, we also consider that a certain number of detectors are placed at a fixed distance $|\mathbf{R}|$ with respect to the center of

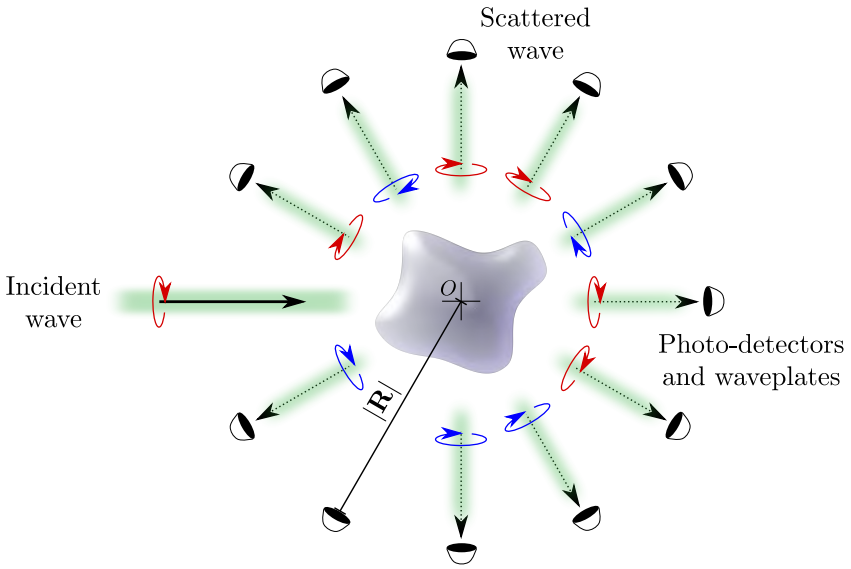

Figure 4.1: Generic scattering set up. An incident electromagnetic wave illuminates a samples which, in turn, emits a scattered wave. Detectors are placed in all directions at a fixed distance, $|\mathbf{R}|$, from the origin which is large with respect to the wavelength of the fields ($k|\mathbf{R}| \gg 1$).

the sample. Most commonly, this distance is large with respect to the wavelength of the fields, $k|\mathbf{R}| \gg 1$ and, thus, results within scattering theory are usually employed to replicate experimental measurements carried out far from the samples. Just to be precise, by *detector* we generally mean a set of photo-detectors and wave plates that may serve for the analysis of the properties of electromagnetic waves. If the detectors are small enough, for instance if their area fulfills $A \ll |\mathbf{R}|^2$, the field measured by each detector can be associated with a single spatial Fourier component.

Regarding the incident field, one may well choose any type of illumination as long as it is a solution of Helmholtz's equation. Of particular interest are those which have a preferable propagation direction such as plane-waves or Bessel beams, as they represent more closely experimental situations in which a source of light, such as a laser, illuminates a sample. The most general incident propagating electromagnetic field can be conveniently expressed in the following form [12]:

$$\mathbf{E}_i(\mathbf{r}) = \sum_{jm} C^e_{jm}\mathbf{N}^j_{jm}(\mathbf{r}) + C^m_{jm}\mathbf{M}^j_{jm}(\mathbf{r}) \tag{4.1}$$

$$iZ\mathbf{H}_i(\mathbf{r}) = \sum_{jm} C^e_{jm}\mathbf{M}^j_{jm}(\mathbf{r}) + C^m_{jm}\mathbf{N}^j_{jm}(\mathbf{r}), \tag{4.2}$$

where Z is the impedance of the surrounding medium; also, C^e_{jm} and C^m_{jm} are the electric and magnetic expansion coefficients for the incident field and the summations include the terms $j = 1, 2, 3, \ldots$ and $m = -j, -j+1, \ldots, j-1, j$. Hansen multipoles have been chosen to be of the form $\mathbf{M}^j_{jm}(\mathbf{r}) = j_j(kr)\mathbf{X}(\theta,\phi)$ and $\mathbf{N}^j_{jm}(\mathbf{r}) = k^{-1}\nabla \times \mathbf{M}^j_{jm}(\mathbf{r})$, where the radial part is determined by the spherical Bessel functions

of the first kind, $j_j(kr)$. The reason to employ spherical Bessel functions of the first kind has to do with the behaviour of the incident field in the origin, O, where the sample is placed. Most generally, to represent feasible physical situations, the incident field cannot diverge at the position of the sample and, thus, spherical Bessel functions of the second kind, $y_j(kr)$, should be avoided in this case. Summing up, by fixing different expansion coefficients in Eq. (4.1), one may represent different types of incident illuminations.

A relevant type of illumination that will be extensively employed in this thesis is one which has a well-defined helicity, λ. In terms of the monochromatic RS vector, this implies that the illumination has a vanishing amplitude for the $-\lambda$ component or, in other words, $\mathbf{F}^{-\lambda}(\mathbf{r}) = 0$. The easiest way of translating this constraint into the electric and magnetic expansion coefficients is just by explicitly computing the linear superpositions of Eq. (4.1) and Eq. (4.2):

$$\begin{aligned}\mathbf{F}_i^{-\lambda}(\mathbf{r}) &= \sqrt{\frac{\varepsilon}{2}}\left[\mathbf{E}_i(\mathbf{r}) - \lambda i Z \mathbf{H}_i(\mathbf{r})\right] \\ &= \sqrt{\varepsilon}\sum_{jm}\left(C^e_{jm} - \lambda C^m_{jm}\right)\left[\frac{\mathbf{N}^j_{jm}(\mathbf{r}) - \lambda \mathbf{M}^j_{jm}(\mathbf{r})}{\sqrt{2}}\right]. \end{aligned} \tag{4.3}$$

where ε is the electric permittivity of the surrounding medium. Thus, to fulfill the condition $\mathbf{F}_{-\lambda}(\mathbf{r}) = 0$ at every point of space, the only possibility is that $C^e_{jm} = \lambda C^m_{jm}$. An important example of this type of illumination is a circularly polarized plane-wave propagating in the OZ direction. This type of field has already been introduced in Eq. (3.24) and it is usually represented by the electric field: $\mathbf{E}_i(\mathbf{r}) = \hat{u}^\lambda e^{ikz}$, with $\hat{u}^\lambda = (1, \lambda i, 0)/\sqrt{2}$. Making use of the properties of the vector spherical harmonic components in Eqs. (3.46)-(3.48), it can be shown that for this kind of illumination $C^e_{jm} = \lambda C^m_{jm} = i^j\sqrt{2\pi(2j+1)}\delta_{m,\lambda}$ (see Section 3, Chapter 10 in Ref. [12]).

Regarding the scattered field, an expansion similar to the one given by Eqs. (4.1)-(4.2) may be done. However, in this case, as the field is not evaluated at the origin, both $j_j(kr)$ and $y_j(kr)$ may be used to represent scattered waves. Due to their appropriate behaviour at large distances, the spherical Hankel function of the first kind, $h^{(1)}_j(kr) = j_j(kr) + i y_j(kr)$, is most commonly employed for this task. As a result, the electromagnetic field scattered by a completely generic linear sample may be expanded as follows:

$$\mathbf{E}_s(\mathbf{r}) = \sum_{jm} \alpha_{jm}\mathbf{N}^h_{jm}(\mathbf{r}) + \beta_{jm}\mathbf{M}^h_{jm}(\mathbf{r}) \tag{4.4}$$

$$iZ\mathbf{H}_s(\mathbf{r}) = \frac{1}{k}\nabla \times \mathbf{E}_s(\mathbf{r}), \tag{4.5}$$

where α_{jm} and β_{jm} are the electric and magnetic expansion coefficients for the scattered field and the summations also include the terms $j = 1, 2, 3, \ldots$ and $m = -j, -j+1, \ldots, j-1, j$. Hansen multipoles are now written in terms of the spherical Hankel function of the first kind, i.e. $\mathbf{M}^h_{jm}(\mathbf{r}) = h^{(1)}_j(kr)\mathbf{X}(\theta, \phi)$ and $\mathbf{N}^h_{jm}(\mathbf{r}) = k^{-1}\nabla \times \mathbf{M}^h_{jm}(\mathbf{r})$. In general, the scattered fields of a generic scatterer contains both helicity components. Thus, in principle, we should consider the positive

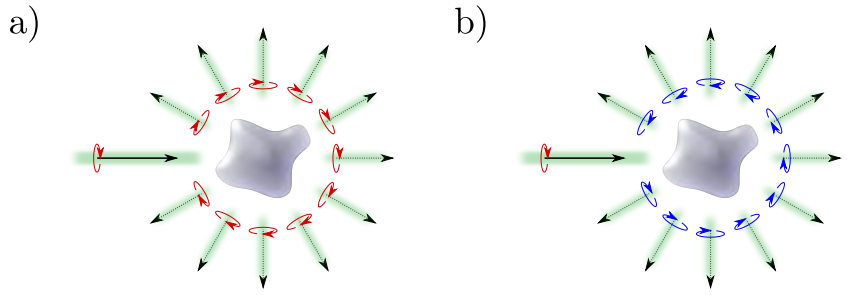

Figure 4.2: a) Sketch of a dual scatterer, i.e. one which preserves the helicity of an incident electromagnetic wave. b) Sketch of an antidual scatterer, i.e. one which completely flips the helicity of an incident electromagnetic wave.

and negative helicities of the scattered electromagnetic field. With the aid of the RS vector, these can be computed as:

$$\begin{aligned}\mathbf{F}_s^{\tilde{\lambda}}(\mathbf{r}) &= \sqrt{\frac{\varepsilon}{2}}\left[\mathbf{E}_s(\mathbf{r}) + \tilde{\lambda} i Z \mathbf{H}_s(\mathbf{r})\right] \\ &= \sqrt{\varepsilon}\sum_{jm}\left(\alpha_{jm} + \tilde{\lambda}\beta_{jm}\right)\left[\frac{\mathbf{N}_{jm}^h(\mathbf{r}) + \tilde{\lambda}\mathbf{M}_{jm}^h(\mathbf{r})}{\sqrt{2}}\right]\end{aligned} \tag{4.6}$$

where the symbol $\tilde{\lambda} = \pm 1$ is employed to differentiate the scattered helicity components from the incident helicity components.

Finally and for completeness, we may also compute the scattered electromagnetic field for an arbitrary scatterer illuminated by a beam with a well-defined helicity λ. For that aim, it is convenient to define the ratios between the expansion coefficients, i.e. $a_{jm} \equiv \alpha_{jm}/C_{jm}^e$ and $b_{jm} \equiv \beta_{jm}/C_{jm}^m$. In the particular case of spherical scatterers, $-a_{jm}$ and $-b_{jm}$ correspond with the Mie coefficients [56]. Imposing the constraint $C_{jm}^e = \lambda C_{jm}^m$ over the incident illumination, we are left with the following suggestive form of the scattered field helicity components:

$$\mathbf{F}_s^{\tilde{\lambda}}(\mathbf{r}) = \sqrt{\varepsilon}\sum_{jm} C_{jm}^e\left(a_{jm} + \lambda\tilde{\lambda}b_{jm}\right)\left[\frac{\mathbf{N}_{jm}^h(\mathbf{r}) + \tilde{\lambda}\mathbf{M}_{jm}^h(\mathbf{r})}{\sqrt{2}}\right]. \tag{4.7}$$

Given the expression above, note that we can split the scattered field into its helicity conserved ($\tilde{\lambda} = \lambda$) and helicity flipped ($\tilde{\lambda} = -\lambda$) components. Taking this into account, we can define two very specific types of scatterers, i.e. dual and antidual scatterers. Dual scatterers are those which conserve the helicity of the incident field and, thus, only emit in the same helicity component (see Fig. 4.2a). On the other hand, antidual scatterers are those which completely flip the helicity of the incident field and, consequently, only emit in the opposite helicity component (see Fig. 4.2b). From the expression of the scattered field in Eq. (4.7), it can be seen that dual scatterers are obtained under the condition $a_{jm} = b_{jm}$, whereas antidual scatterers emerge whenever $a_{jm} = -b_{jm}$.

4.1.2 *Energy conservation law*

Since we are considering that all the fields have a time-dependence $e^{-i\omega t}$, we should employ the monochromatic version of Poynting's theorem to derive the energy conservation law. Moreover, the scattering problems we are interested in do not contain any free charges, which implies that the theorem results in the following simplified relation (see Section 9, Chapter 6 in Ref. [12]):

$$-\oint_S dS\ \mathbf{S}(\mathbf{r})\cdot\hat{n} = 2\omega\int_V d\mathbf{r}\ \mathrm{Im}\left[u_m(\mathbf{r}) - u_e(\mathbf{r})\right], \tag{4.8}$$

where $\mathbf{S}(\mathbf{r}) = \frac{1}{2}\mathrm{Re}\left[\mathbf{E}(\mathbf{r})\times\mathbf{H}^*(\mathbf{r})\right]$ is the time-averaged Poynting vector, $u_e(\mathbf{r}) = \frac{1}{4}\left[\mathbf{E}(\mathbf{r})\cdot\mathbf{D}^*(\mathbf{r})\right]$ the electric energy density and $u_m(\mathbf{r}) = \frac{1}{4}\left[\mathbf{B}(\mathbf{r})\cdot\mathbf{H}^*(\mathbf{r})\right]$ the magnetic energy density. The result given by Eq. (4.8) indicates that, in the absence of free charges, the flux of the Poynting vector over a closed surface S, with normal vector $\hat{n}$, is related with the imaginary parts of the local energy densities in the volume V enclosed by the surface.

The usual way of employing Poynting's theorem in linear electromagnetic scattering theory is by evaluating the integral given in the left hand side of Eq. (4.8) over a closed surface S that contains the scatterer (see Fig. 4.3). In this line, note that if the scatterer is embedded in a lossless surrounding medium, the integral in the right hand side of Eq. (4.8) is reduced to the volume of the particle, V_p. Furthermore, for scatterers with fixed electric permittivity, ε_p, and magnetic permeability, μ_p, we arrive to the following expression of the flux of the Poynting vector:

$$-\oint_S dS\ \mathbf{S}(\mathbf{r})\cdot\hat{n} = \frac{\omega}{2}\mathrm{Im}[\varepsilon_p]\int_{V_p} d\mathbf{r}\ |\mathbf{E}(\mathbf{r})|^2 + \frac{\omega}{2}\mathrm{Im}[\mu_p]\int_{V_p} d\mathbf{r}\ |\mathbf{H}(\mathbf{r})|^2. \tag{4.9}$$

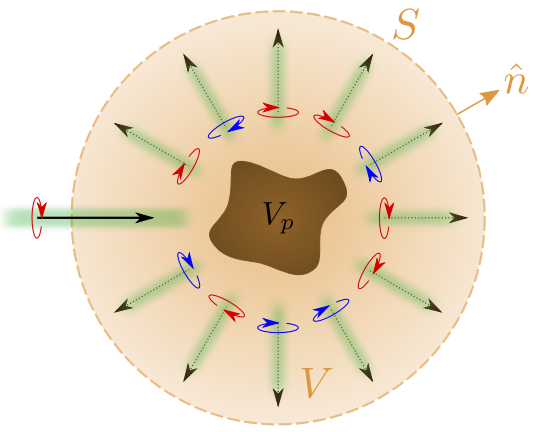

Figure 4.3: Integration surfaces and volumes for a linear scatterer embedded in a lossless medium. S is a closed surface that contains the particle and $\hat{n}$ is its normal vector. V is the volume enclosed by surface S and V_p is the volume of the scatterer.

From the result in Eq. (4.9) we can infer that the flux of the time-averaged Poynting vector over a surface S that contains the scatterer is directly related with the absorption in the particle. Indeed, if the particle is lossless, i.e. $\mathrm{Im}[\varepsilon_p] = \mathrm{Im}[\mu_p] = 0$, then, the flux of the time-averaged Poynting vector vanishes.

Consequently, it is natural to evaluate the power absorbed by a linear scatterer as (see Section 4, Chapter 3 in Ref. [14]):

$$W_a = -\oint_S dS\ \mathbf{S}(\mathbf{r}) \cdot \hat{n}. \tag{4.10}$$

This implies that, for any linear scatterer, we may compute the absorbed power in terms of the Poynting vector evaluated over a closed surface outside the scatterer. As the fields outside are computed as the superposition of the incident and scattered electromagnetic fields, i.e. $\mathbf{E}(\mathbf{r}) = \mathbf{E}_i(\mathbf{r}) + \mathbf{E}_s(\mathbf{r})$ and $\mathbf{H}(\mathbf{r}) = \mathbf{H}_i(\mathbf{r}) + \mathbf{H}_s(\mathbf{r})$, we may expand the time-averaged Poynting vector outside the scatterer as follows:

$$\mathbf{S}(\mathbf{r}) = \mathbf{S}_i(\mathbf{r}) + \mathbf{S}_s(\mathbf{r}) + \mathbf{S}_{ext}(\mathbf{r}), \tag{4.11}$$

where the terms in the right hand side are

$$\mathbf{S}_i(\mathbf{r}) = \frac{1}{2}\mathrm{Re}\left[\mathbf{E}_i(\mathbf{r}) \times \mathbf{H}_i^*(\mathbf{r})\right] \tag{4.12}$$

$$\mathbf{S}_s(\mathbf{r}) = \frac{1}{2}\mathrm{Re}\left[\mathbf{E}_s(\mathbf{r}) \times \mathbf{H}_s^*(\mathbf{r})\right] \tag{4.13}$$

$$\mathbf{S}_{ext}(\mathbf{r}) = \frac{1}{2}\mathrm{Re}\left[\mathbf{E}_i(\mathbf{r}) \times \mathbf{H}_s^*(\mathbf{r}) + \mathbf{E}_s(\mathbf{r}) \times \mathbf{H}_i^*(\mathbf{r})\right]. \tag{4.14}$$

However, we should note that $\mathbf{S}_i(\mathbf{r})$ is constructed from a solution of Maxwell's equations in the absence of the scatterer. Thus, from Eq. (4.9) it can be seen that, if the surrounding medium is considered to be lossless, the flux of this component across surface S vanishes, i.e. $\oint_S dS\ \mathbf{S}_i(\mathbf{r}) \cdot \hat{n} = 0$.

As a result, we are left with the following general statement of the energy conservation law in linear electromagnetic scattering theory:

$$W_{ext} = W_a + W_s, \tag{4.15}$$

where W_{ext} and W_s are usually denoted as the extincted and scattered powers, respectively, and are computed as:

$$W_{ext} = -\oint_S dS\ \mathbf{S}_{ext}(\mathbf{r}) \cdot \hat{n} \tag{4.16}$$

$$W_s = \oint_S dS\ \mathbf{S}_s(\mathbf{r}) \cdot \hat{n}. \tag{4.17}$$

The energy conservation law encoded in Eq. (4.15) can be understood in different ways, but let us briefly state the interesting interpretation proposed by Bohren and Huffman [14]. Indeed, due to the analytical form of Eq. (4.14), the extincted power can be understood as the power removed by the scattered field from the incident field by interference. In this line, Eq. (4.15) would just represent the fact that all

such power is then converted into absorption in the particle and scattering in all directions. This interpretation is actually strengthened when expressing $\mathbf{S}_{ext}(\mathbf{r})$ in terms of the monochromatic RS vector:

$$\mathbf{S}_{ext}(\mathbf{r}) = -\frac{1}{2n}\mathrm{Im}\left[\mathbf{F}_i^+(\mathbf{r}) \times (\mathbf{F}_s^+(\mathbf{r}))^* - \mathbf{F}_s^-(\mathbf{r}) \times (\mathbf{F}_i^-(\mathbf{r}))^*\right], \quad (4.18)$$

where n is the refractive index of the surrounding medium and we have employed the definition of the monochromatic RS vector given by Eq. (2.33). When writing the extinction in terms of the RS vector, it is clear that it only considers the power transfer between the same helicity components. The absence of cross helicity terms in Eq. (4.18) reinforces Bohren and Huffman's idea of extinction emerging as an interference between the incident and the scattered electromagnetic fields.

Regarding the scattered power specified by Eq. (4.17), it is interpreted as the total power emitted by the particle in all directions. Moreover, W_s is experimentally associated with the power measured by the detectors depicted in Fig. 4.1. Thus, it is most commonly evaluated far from the scatterer. Taking the appropriate limits of the Hansen multipoles far from the sample [57], it can be checked that, in this region, the scattered electric and magnetic fields fulfill $Z\mathbf{H}_s(\mathbf{r}) = \hat{\mathbf{r}} \times \mathbf{E}_s(\mathbf{r})$, where $\hat{\mathbf{r}}$ is the unitary vector in the radial direction. As a result, far from the sample, we can generally rewrite the scattered power in terms of the vector: $\mathbf{S}_s(\mathbf{r}) = n^{-1}u_s(\mathbf{r})\hat{\mathbf{r}}$, where $u_s(\mathbf{r})$ is the sum of the electric and magnetic energy densities associated with the scattered electromagnetic field. In other words, far from any linear sample, $\mathbf{S}_s(\mathbf{r})$ always points in the radial direction and its modulus is proportional to the energy density. Without any loss of generality, the local energy density can be expressed in terms of the RS vector defined in Eq. (4.6), leading to the following form of the scattered power:

$$W_s = \frac{1}{4n}|\mathbf{R}|^2 \int d\Omega \ \left[|\mathbf{F}_s^+(|\mathbf{R}|,\theta,\phi)|^2 + |\mathbf{F}_s^-(|\mathbf{R}|,\theta,\phi)|^2\right], \quad (4.19)$$

where the integrating surface S has been considered a sphere of radius $|\mathbf{R}|$, such that $k|\mathbf{R}| \gg 1$. Moreover, $d\Omega = \sin\theta d\theta d\phi$ and the integration domains are $\theta \in (0,\pi)$ and $\phi \in (0,2\pi)$.

As, far from the sample, the field is composed of plane-waves propagating in the radial direction, we can interpret the expression given by Eq. (4.19) in terms of the Stokes parameters in the circular polarization basis [12]. Indeed, W_s can be associated with the measurement of the local Stokes parameter $I = |\mathbf{F}_s^+(|\mathbf{R}|,\theta,\phi)|^2 + |\mathbf{F}_s^-(|\mathbf{R}|,\theta,\phi)|^2$ (sometimes it is also denoted as s_0) in the detectors placed at a fixed distance $|\mathbf{R}|$, as depicted in Fig. 4.1. In this line, Eq. (4.19) indicates that such measurements must be carried out in detectors covering all the possible scattering angles. W_s is finally obtained by integrating all the measurements of parameter I at each angle (θ,ϕ) [58].

4.1.3 *Scattered helicity and helicity expectation value*

In line with what we have just discussed, there is another magnitude which may also be computed in terms of the RS vector. Indeed, in Eq. (4.19) we have computed the scattered power as the sum of the power associated with positive and negative helicity components of the electromagnetic field. With the same detection system, we may also compute the difference in power between the positive and negative helicity components. This leads to the definition of the scattered helicity:

$$\Lambda_s = \frac{1}{4n\omega}|\mathbf{R}|^2 \int d\Omega \ \left[|\mathbf{F}_s^+(|\mathbf{R}|,\theta,\phi)|^2 - |\mathbf{F}_s^-(|\mathbf{R}|,\theta,\phi)|^2\right]. \tag{4.20}$$

Exactly as we have associated a Stokes parameter with the expression of the scattered power, we can similarly associate the local Stokes parameter $V = |\mathbf{F}_s^+(|\mathbf{R}|,\theta,\phi)|^2 - |\mathbf{F}_s^-(|\mathbf{R}|,\theta,\phi)|^2$ (sometimes it is also denoted as s_3) to the measurement of the scattered helicity. In this line, the expression given by Eq. (4.20) indicates that the scattered helicity, Λ_s, is obtained by summing up all the measurements of the Stokes parameter V at each scattering angle (θ,ϕ) at a distance $|\mathbf{R}|$ far from the optical sample.

A magnitude of interest is built when considering the unit-less ratio of the scattered helicity and the scattered power. This is what we call the normalized helicity or the helicity expectation value and it is defined as:

$$\langle\Lambda\rangle = \frac{\omega\Lambda_s}{W_s} = \frac{\int d\Omega \ \left[|\mathbf{F}_s^+(|\mathbf{R}|,\theta,\phi)|^2 - |\mathbf{F}_s^-(|\mathbf{R}|,\theta,\phi)|^2\right]}{\int d\Omega \ \left[|\mathbf{F}_s^+(|\mathbf{R}|,\theta,\phi)|^2 + |\mathbf{F}_s^-(|\mathbf{R}|,\theta,\phi)|^2\right]}. \tag{4.21}$$

Again, note that this is a physical magnitude which can be quantified through the measurement of I and V Stokes parameters. Furthermore, it is a bounded observable, i.e. $\langle\Lambda\rangle \in (-1,1)$ and, if the incident beam has a well-defined helicity, its extreme values correspond to a dual and an antidual scatterer. Employing the expression of the RS vector given by Eq. (4.6), we obtain the following general form of the helicity expectation value in terms of the expansion coefficients:

$$\langle\Lambda\rangle = \frac{\sum_{jm}\left(|\alpha_{jm}+\beta_{jm}|^2 - |\alpha_{jm}-\beta_{jm}|^2\right)}{\sum_{jm}\left(|\alpha_{jm}+\beta_{jm}|^2 + |\alpha_{jm}-\beta_{jm}|^2\right)} \tag{4.22}$$

where we have employed the orthogonality relations of the Hansen multipoles [12, 57]. Furthermore, if we fix the incident illumination to a beam with-well defined helicity ($C_{jm}^e = \lambda C_{jm}^m$) and rearrange the terms given by Eq. (4.22), we are left with the following form:

$$\langle\Lambda\rangle = 2\frac{\sum_{jm}|C_{jm}^e|^2 \ \mathrm{Re}(a_{jm}^* b_{jm})}{\sum_{jm}|C_{jm}^e|^2\left(|a_{jm}|^2 + |b_{jm}|^2\right)}. \tag{4.23}$$

In this last expression, the signs have been chosen such that $\langle\Lambda\rangle = +1$ implies a dual scatterer and $\langle\Lambda\rangle = -1$ implies an antidual scatterer. The expression given by Eq. (4.23) (or similar versions) is widely employed in scattering theory as it helps identify important features of the scattered fields.

At this point, let us discuss a particular example and show how to employ the monochromatic RS vector in the study of scattering problems which already have a solution in terms of the usual electric and magnetic fields. Our derivation will be based on a problem with analytical solution, but please note that exactly the same procedure may also be considered for problems with numerical solutions. In particular, we will construct an analytic expression of the helicity expectation value, $\langle \Lambda \rangle$, for isotropic spherical scatterers whose response may depend on the helicity of the incident illumination. In short, we call this kind of samples *chiral* and they are characterized for having the constitutive relations specified by Eqs. (2.11)-(2.12). The solution to such a scattering problem is given in Section 3, Chapter 8 of Ref. [14] in terms of the scattered electric and magnetic fields.

To begin with, it is important to note that the incident field chosen for the solution given in Ref. [14] is a linearly-polarized plane-wave. As we are interested in building a magnitude, $\langle \Lambda \rangle$, which determines whether a sample preserves or not the helicity of the incident beam, we should consider the illumination to be circularly-polarized instead. An incident linearly-polarized plane-wave can be split as a superposition of left-polarized ($m = 1$) and right-polarized ($m = -1$) plane-waves. In addition, a cylindrical sample preserves the eigenvalue of the z component of the total angular momentum, m. Thus, to compute the scattered field associated with an incident circularly-polarized field with helicity λ, we just need to consider the components of the scattered field given in Ref. [14] that have a fixed value of the total angular momentum, $m = \lambda$ [54, 59]:

$$\mathbf{E}_s(\mathbf{r}) = -\lambda \sum_j K_j \left\{ \left[\frac{a_j + b_j}{\sqrt{2}} - \lambda i \sqrt{2} c_j \right] \mathbf{\Phi}^{\lambda}_{j\lambda}(\mathbf{r}) + \left[\frac{a_j - b_j}{\sqrt{2}} \right] \mathbf{\Phi}^{-\lambda}_{j\lambda}(\mathbf{r}) \right\}, \tag{4.24}$$

where a_j, b_j and c_j are the Mie coefficients for chiral spheres [60] and $K_j = i^j \sqrt{2\pi(2j+1)}$ is the expansion coefficient for an incident circularly-polarized plane-wave. Note that the magnetic field is computed as $iZ\mathbf{H}_s(\mathbf{r}) = k^{-1} \nabla \times \mathbf{E}_s(\mathbf{r})$ and the multipolar fields with well-defined helicity are built as $\mathbf{\Phi}^{\lambda}_{jm}(\mathbf{r}) = 2^{-1/2}[\mathbf{N}^h_{jm}(\mathbf{r}) + \lambda \mathbf{M}^h_{jm}(\mathbf{r})]$.

With the solution given by Eq. (4.24) we can construct the RS vector associated with the scattered field of a chiral sphere. In particular, we get the following form of the helicity components of the scattered field:

$$\mathbf{F}^{\tilde{\lambda}}_s(\mathbf{r}) = -\sqrt{\frac{\varepsilon}{2}} \sum_j K_j \left\{ (\lambda + \tilde{\lambda}) \left[\frac{a_j + b_j}{\sqrt{2}} - \lambda i \sqrt{2} c_j \right] \mathbf{\Phi}^{\lambda}_{j\lambda}(\mathbf{r}) + (\lambda - \tilde{\lambda}) \left[\frac{a_j - b_j}{\sqrt{2}} \right] \mathbf{\Phi}^{-\lambda}_{j\lambda}(\mathbf{r}) \right\}, \tag{4.25}$$

where, again, $\tilde{\lambda}$ represents the helicity components of the scattered field. By considering the helicity conserved ($\tilde{\lambda} = \lambda$) and helicity flipped

($\tilde{\lambda} = -\lambda$) of the scattered field, we are finally left with the following expression of the helicity expectation value:

$$\langle \Lambda \rangle = 2 \frac{\sum_j (2j+1) \left\{ \mathrm{Re}(a_j^* b_j) + |c_j|^2 + \lambda \mathrm{Im}[(a_j + b_j)^* c_j] \right\}}{\sum_j (2j+1) \left\{ |a_j|^2 + |b_j|^2 + 2|c_j|^2 + 2\lambda \mathrm{Im}[(a_j + b_j)^* c_j] \right\}}. \quad (4.26)$$

Let us highlight the generality of the expression given above. In its full form, as we have just mentioned before, it represents the helicity expectation value for isotropic chiral spheres under circularly-polarized plane-wave illumination. However, note that imposing $c_j = 0$ in the solution given by Eq. (4.24) the scattered field of both conventional spheres and core-shells is recovered (see Section 3, Chapter 4 and Section 1, Chapter 8 in Ref. [14]). Thus, the expression of $\langle \Lambda \rangle$ given in Eq. (4.26) applies to, at least, three different types of systems: conventional spheres, core-shells and chiral spheres.

A few physical conclusions may be extracted from the expressions given by Eqs. (4.25)-(4.26). First, note that the scattered fields for a generic chiral sphere depend on λ, i.e. the helicity of the incoming electromagnetic field. This is the reason why this parameter is also present in the expression of the helicity expectation value in Eq. (4.26). Second, note that regardless of the sphere being chiral or not, the duality condition is $a_j = b_j$. Under this condition the helicity expectation value given by Eq. (4.26) yields $\langle \Lambda \rangle = 1$. Third, from the expression of the monochromatic RS vector in Eq. (4.25) we may also note that the antiduality condition must be $2\lambda i c_j = a_j + b_j$, as it is the condition that vanishes the components of the scattered field with same helicity. In this line, note that under this other condition the helicity expectation value in Eq. (4.26) yields $\langle \Lambda \rangle = -1$. In the case of non-chiral spherical particles ($c_j = 0$), the antiduality condition reduces to $a_j = -b_j$. This last condition only applies for conventional spheres and core-shells.

4.2 DUALITY, ANTIDUALITY AND ENERGY CONSERVATION

In the previous Section, we have shown that the interpretation of certain physical magnitudes is simplified when employing the monochromatic RS vector. We have introduced the notion of dual and antidual scatterers as those which preserve or completely flip the helicity of the incident field (see Fig. 4.2). Also, we have shown that the RS vector sheds light on the expressions of relevant quantities such as the extincted and scattered powers or the helicity expectation value. In particular, we have seen that the mapping between these theoretical magnitudes and experimentally measurable Stokes parameters is quite direct with the aid of the monochromatic RS vector. Finally, as a practical example, we have derived an expression of the helicity expectation value which applies to different systems.

In this Section, we employ the tools developed in Section 4.1 to discuss the relation between dual and antidual scatterers with the conservation of energy. As we have just discussed, many relevant physical magnitudes defined within linear electromagnetic scattering

theory can be related to the monochromatic RS vector. Thus, in principle, when studying particular types of scatterers, such magnitudes may be correlated in some way. In particular, we will show that the presence of losses and gain in the constituent materials modulates the possibility of building dual and antidual scatterers. We will first discuss the case of conventional spheres as a general symptom of the aforementioned phenomena. Then, we will show that the correlations between dual scatterers and losses in dielectric media are also present in other systems such as core-shells and chiral spheres. Finally, we will demonstrate that gain is a necessary condition to build antidual scatterers of any size and form.

4.2.1 *Conventional spheres as a general trend*

Let us begin by the fundamental result reported in Contribution II. The main result of that work is to demonstrate analytically that losses preclude the existence of spherical dual scatterers made of dielectric materials. On the one hand, by dielectric materials, we refer to those which do not have a magnetic response, i.e. $\mu = 1$. On the other hand, by lossy particles we refer to those which fulfill $\mathrm{Re}(n_p) > 0$ and $\mathrm{Im}(n_p) > 0$, implying that $\mathrm{Im}(\varepsilon_p) = \mathrm{Im}(n_p^2) > 0$. As we usually fix the sign of the frequency to be positive, the conditions above imply that the absorbed power given by Eq. (4.10) is positive, i.e. $W_a > 0$, for a lossy dielectric scatterer. In this setting, we showed that helicity preservation, $\langle \Lambda \rangle = 1$, is not reachable for lossy dielectric scatterers.

The proof is valid for conventional spheres, which implies $c_j = 0$. Thus, the expression of the helicity expectation value applicable to this particular type of scatterers is:

$$\langle \Lambda \rangle = 2 \frac{\sum_j (2j+1) \mathrm{Re}(a_j^* b_j)}{\sum_j (2j+1) \left(|a_j|^2 + |b_j|^2 \right)}, \tag{4.27}$$

where a_j and b_j are the usual electric and magnetic Mie coefficients. As it can be checked, for this type of particles, the only possibility of getting a dual scatterer is by fulfilling $a_j = b_j$. This means that for a dual conventional sphere, the electric and magnetic scattering coefficients must be equal both in amplitude and phase [61]. However, as it is shown in Contribution II, the condition above cannot be met for lossy dielectric spheres due to fundamental properties of the Riccati-Bessel functions and its derivatives. In Fig. 4.4 we show the helicity expectation value for a Germanium-like sphere ($\mathrm{Re}(n_p) = 4$) embedded in vacuum as a function of the imaginary part of the refractive index, $\mathrm{Im}(n_p)$, and the size parameter, x. The size parameter, $x = ka$, is the product of the modulus of the wave vector in the surrounding medium, k, and the radius of the sphere, a. Note that in the range $x < 1$, the sphere is smaller than the illuminating wavelength. In Fig. 4.4 we show a particular example where the emergence of dual dielectric scatterers ($\langle \Lambda \rangle = 1$) is constrained to the condition $\mathrm{Im}(n_p) = 0$. Note that, as losses or gain are introduced in the system, the helicity expectation value decreases.

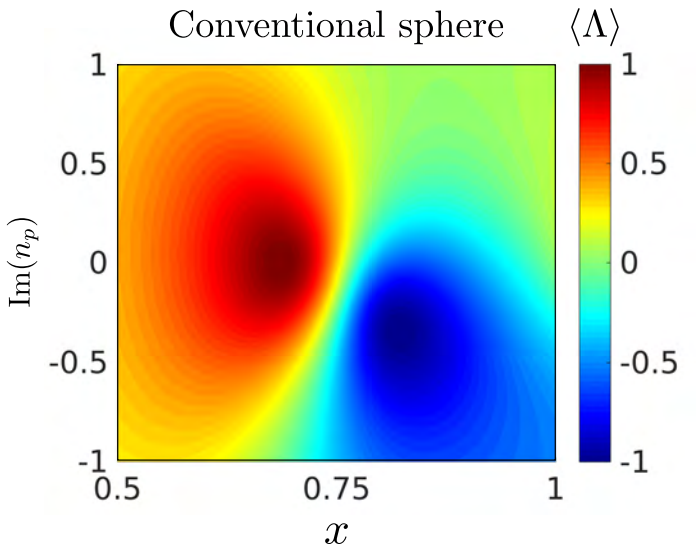

Figure 4.4: Helicity expectation value for a conventional dielectric sphere in terms of the imaginary part of the refractive index, $\mathrm{Im}(n_p)$, and the size parameter, x. The real part of the refractive index is fixed to $\mathrm{Re}(n_p) = 4$, which implies that the response is of a Germanium-like material. The fact that $x < 1$ implies that the sphere is small and, thus, its response is exclusively determined by the dipolar Mie coefficients a_1 and b_1. Figure adapted from Contribution II.

On the other hand, Fig. 4.4 also indicates that the emergence of antidual spherical scatterers ($\langle\Lambda\rangle = -1$) requires from optical gain, i.e. $\mathrm{Im}(n_p) < 0$. This result is also general for spherical antidual scatterers and it is based on symmetry arguments. Indeed, it can be shown that an antidual cylindrically symmetric scatterer illuminated by a plane wave propagating along the symmetry axis must have zero forward scattering amplitude [62]. The argument is as follows: because of cylindrical symmetry the scatterer must conserve the total angular momentum of the incident plane wave and, thus, the forward scattered component must have the same circular polarization than the incident field. On the other hand, as the scatterer is antidual, the forward scattered field must have the opposite circular polarization than the incident field. As both conditions cannot be met at the same time, the forward scattered field must vanish. This is also true for systems with discrete rotational symmetries [63].

However, systems which have zero forward scattering when illuminated by a plane-wave have problems regarding energy conservation. The reason lies on the specific form that the extincted power adopts under this type of excitation [64]. Indeed, the power extincted by a sample under plane-wave illumination can be computed as [14, 65]:

$$W_{ext} = \frac{2\pi}{Zk^2}\,\mathrm{Re}\left[\mathbf{A}_i^* \cdot \mathbf{A}_s(\mathbf{r})\right]\Big|_{x=y=0,z=|\mathbf{R}|}, \tag{4.28}$$

where $\mathbf{A}_i = \mathbf{E}_i(\mathbf{r})e^{-ikz}$ represents the vector amplitude of an incident plane-wave propagating in the OZ axis, $\mathbf{A}_s(\mathbf{r}) = -ikr\mathbf{E}_s(\mathbf{r})e^{-ikr}$ is the vector amplitude of the scattered field and we have used the fact that

the irradiance of a plane-wave is $|\mathbf{A}_i|^2/2Z$. Finally, the expression is evaluated at a point $(x = 0, y = 0, z = |\mathbf{R}|)$ far from the scatterer. The expression given by Eq. (4.28) is usually denoted as the *optical theorem*. From the optical theorem it is direct to check that having a zero forward scattering amplitude, $|\mathbf{A}_s(\mathbf{r})| = 0$ at $(x = y = 0, z = |\mathbf{R}|)$, implies a null extincted power, i.e. $W_{ext} = 0$. As a result, it can be concluded that antidual spheres under plane-wave illumination, necessarily produce a null extincted power [64]. In other words, all the scattered power is obtained from the optical gain of the material, i.e. $W_s = -W_a$ (see Eq. (4.15)). This means that either the absorbed power is negative, which implies that $\mathrm{Im}(n_p) < 0$, or the scattered power must vanish. Therefore, we can conclude that gain is a necessary condition to build spherical antidual scatterers under plane-wave illumination.

4.2.2 *Dual dielectric scatterers and optical losses*

As we have just seen, losses preclude the existence of dual dielectric spheres. However, the previous proof only applies to conventional spheres and, in principle, we cannot tell anything about the behaviour of other types of lossy scatterers. To shed light on this point, we may employ the general form of the helicity expectation value expressed in Eq. (4.26) and identify the behaviour of lossy core-shells and chiral spheres. This is the approach we follow in Contribution III.

In this line, we first provide the maps of the helicity expectation value, $\langle\Lambda\rangle$, for lossless core-shells and chiral spheres (see Fig. 4.5). The absence of losses is imposed by constraining the imaginary parts of the different refractive indices. In particular, we have considered that $\mathrm{Im}(n_1) = 0$ and $\mathrm{Im}(n_2) = 0$, where n_1 and n_2 are the refractive indices of the core and the shell, respectively. Also, we have considered that $\mathrm{Im}(n_p) = 0$ where $n_p = n_0 - \lambda\chi$ is the refractive index of a chiral sphere. Here, $\lambda = \pm 1$ refers to the helicity eigenvalue of the incident field and χ determines the degree of chirality of the scatterer. Regions in which the particles behave as dual ($\langle\Lambda\rangle = 1$) are found both in Fig. 4.5a and Fig. 4.5b. Also, we identify certain regions in which the particles efficiently flip the helicity of the incident wave, but never reaching the antidual condition $\langle\Lambda\rangle = -1$. This, of course, is due to the fact that the systems have no optical gain and, thus, as we have previously shown, a complete flip in the helicity of the scattered field is precluded by the optical theorem.

In Fig. 4.6 we show how helicity preservation is lost when introducing losses into the system. For that aim, we have reproduced the maps in Fig. 4.5 but for non-zero values of the imaginary part of the refractive index. Then, for each value of $\mathrm{Im}(n)$, we have picked the maximum value of the helicity expectation value map, $\max(\langle\Lambda\rangle)$. If helicity cannot be preserved in lossy core-shells and chiral spheres, then, whenever $\mathrm{Im}(n) > 0$, the maps should not contain any dual region, i.e. the helicity expectation value should fulfill $\max(\langle\Lambda\rangle) < 1$. The results of these calculations are depicted in Fig. 4.6. In green,

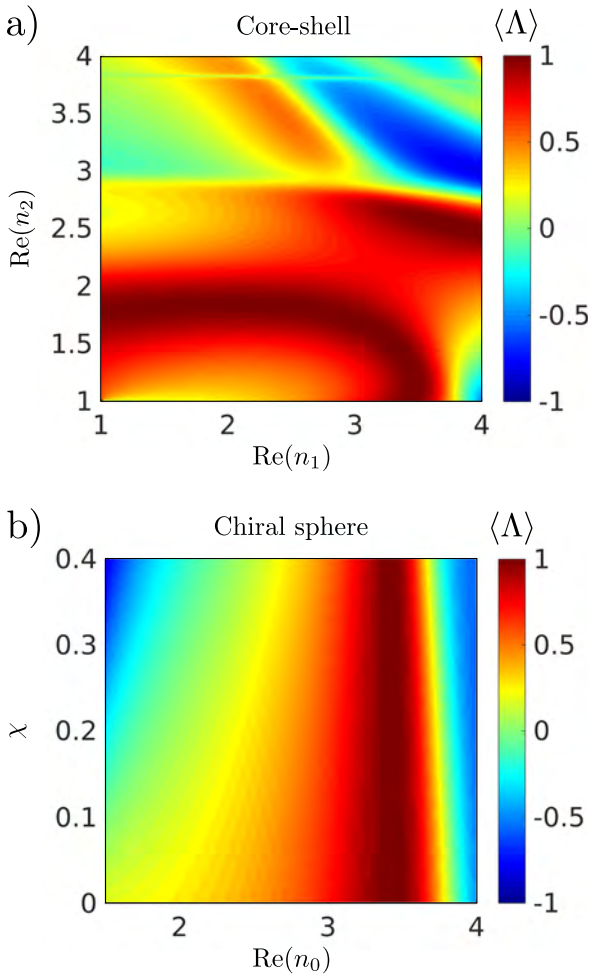

Figure 4.5: a) Helicity expectation value for a core-shell without losses. The refractive indices of the core and the shell are, respectively, n_1 and n_2. Size parameters of the core and the shell are $x = 0.8$ and $y = 1.5$, respectively. b) Helicity expectation value for a chiral sphere without losses. The refractive index of the chiral sphere is $n_p = n_0 - \lambda\chi$, and we have fixed the helicity eigenvalue of the incident wave to $\lambda = 1$. The size parameter in this case is $x = 0.8$. Figure adapted from Contribution III.

we show the case of losses being only present in the core, in other words, $\mathrm{Im}(n_1) > 0$ and $\mathrm{Im}(n_2) = 0$. In dashed red we plot the complementary situation in which the losses are considered in the shell instead, i.e. $\mathrm{Im}(n_2) > 0$ and $\mathrm{Im}(n_1) = 0$. Finally, in dashed yellow we depict the result obtained for a lossy chiral sphere in which losses have been introduced as $\mathrm{Im}(n_0) > 0$. Our results indicate that losses preclude the existence of dual dielectric scatterers beyond the conventional sphere case. Some situations seem more robust to the presence of losses, such as the case of a lossy core, however we always find that $\max(\langle\Lambda\rangle) < 1$ whenever $\mathrm{Im}(n) > 0$.

Based on the analytical proof for conventional spheres and the numerical results reported for core-shells and chiral spheres, we suspect that optical losses preclude the preservation of helicity in other dielectric scatterers. However, we have not succeeded in giving a general proof for this. At least we know that this phenomenon, if present in

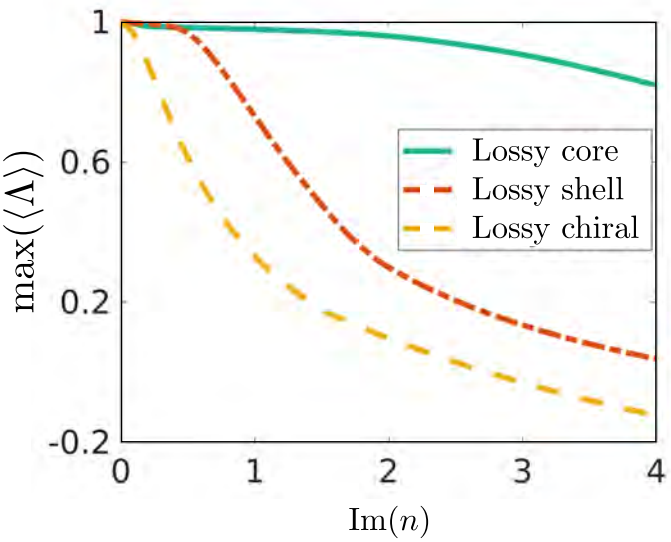

Figure 4.6: Maximum of the helicity expectation value, $\langle\Lambda\rangle$, for a core-shell and a chiral sphere with losses. We first consider the case when losses are only introduced in the refractive index of the core, $\mathrm{Im}(n_1) > 0$ (green). We also depict the result for losses being only present in the shell, $\mathrm{Im}(n_2) > 0$ (dashed red). Finally, we show the case in which a chiral sphere has losses, $\mathrm{Im}(n_0) > 0$ (dashed yellow). Figure adapted from Contribution III.

other systems, must be subjected to the presence of dielectric media. This is because lossy dual scatterers may indeed be built from lossy magnetic media [61]. There are a few ways in which we think that a further analysis of this phenomenon could be tackled. For instance, the expressions of the scattering expansion coefficients may be analyzed in terms of the sources of the field (see Section 10, Chapter 9 in Ref. [12]). In particular, it could be checked whether the constrains $\mu_p = 1$ and $\mathrm{Im}(\varepsilon_p) > 0$ have some fundamental consequences on such coefficients. In this line, the presence of both helicity components in the scattered might be a property of how lossy dielectric particles re-emit the energy that they absorb. Another interesting approach may be to study the effect of such constrains in the expression of the absorbed power given by Eq. (4.10).

4.2.3 *Antidual scatterers and optical gain*

As we have just shown, optical losses in dielectric materials seem to, quite generally, prevent the existence of dual scatterers. This is a property well understood for spheres and also numerically identified for core-shells and chiral spheres. In this Subsection, we analyze whether optical gain is also a necessary condition to build antidual scatterers of other sizes and forms. The first step towards the generality of this result can be carried out through the application of the optical theorem given by Eq. (4.28) to a non-spherical antidual particle. This approach is valid to study the extincted power under a circularly-polarized plane-wave illumination. In particular, the lack of geometrical symmetries in the scatterer does not impose any constrain on

the forward scattering amplitude which implies that, in general, we have that $|\mathbf{A}_s(\mathbf{r})| \neq 0$. This may seem to indicate that the extincted power does not vanish in the general case. However, this is not the case. The extincted power vanishes for a generic antidual scatterer, even if there is light scattered in the forward direction. As we show next, under plane-wave illumination, this occurs due to the orthogonality of the fields with opposite helicities. The derivation is adapted from Contribution IV.

If a sample is illuminated by a beam with well-defined helicity ($C^e_{jm} = \lambda C^m_{jm}$), such as a circularly-polarized plane-wave propagating in the OZ direction, and has an antidual behaviour ($a_{jm} = -b_{jm}$), the incident and scattered vector amplitudes acquire the following form:

$$\mathbf{A}_i = \frac{1}{\sqrt{2}}(\hat{x} + \lambda i \hat{y}) \tag{4.29}$$

$$\mathbf{A}_s(\mathbf{r}) = -ikr \sum_{jm} C^e_{jm} a_{jm} \left[\mathbf{N}^h_{jm}(\mathbf{r}) - \lambda \mathbf{M}^h_{jm}(\mathbf{r})\right] e^{-ikr}. \tag{4.30}$$

As the optical theorem, given by Eq. (4.28), requires the fields evaluated far from the scatterer, we have to consider the following limits of the Hansen multipoles [57] (see also Appendix of Contribution V):

$$\lim_{kr\to\infty} \mathbf{N}^h_{jm}(\mathbf{r}) = -\frac{e^{ikr}}{kr} \frac{(-i)^{j+1}}{\sqrt{j(j+1)}} \xi_{jm}(\theta, \phi) \tag{4.31}$$

$$\lim_{kr\to\infty} \mathbf{M}^h_{jm}(\mathbf{r}) = -\frac{e^{ikr}}{kr} \frac{(-i)^{j+1}}{\sqrt{j(j+1)}} i\eta_{jm}(\theta, \phi), \tag{4.32}$$

where we have defined the vector functions $\xi_{jm}(\theta, \phi) = r\nabla Y_{jm}(\theta, \phi)$ and $\eta_{jm}(\theta, \phi) = \hat{r} \times \xi_{jm}(\theta, \phi)$, with $Y_{jm}(\theta, \phi)$ the scalar spherical harmonics. Thus, far from the antidual particle, the scattered vector amplitude can be generally expressed as:

$$\lim_{kr\to\infty} \mathbf{A}_s(\mathbf{r}) = \sum_{jm} \frac{(-i)^j C^e_{jm} a_{jm}}{\sqrt{j(j+1)}} \left[\xi_{jm}(\theta, \phi) - \lambda i \eta_{jm}(\theta, \phi)\right]. \tag{4.33}$$

Note that, in the expression given by Eq. (4.33) the vectorial nature of the scattering vector amplitude is determined by a particular linear combination of $\xi_{jm}(\theta, \phi)$ and $\eta_{jm}(\theta, \phi)$ vectors. By analyzing the components of such a linear combination, it can be checked that it can be written in the following suggestive form:

$$\xi_{jm}(\theta, \phi) - \lambda i \eta_{jm}(\theta, \phi) = y_{jm}(\theta, \phi) \left[\hat{\theta} - \lambda i \hat{\phi}\right], \tag{4.34}$$

where $y_{jm}(\theta, \phi)$ is a scalar function of the spherical harmonics and its derivatives. Crucially, the optical theorem given by Eq. (4.28) should be evaluated at a point along the OZ axis, i.e. at a point at which $\hat{r} = \hat{z}$. In this situation, the angular unitary vectors $\hat{\theta}$ and $\hat{\phi}$ are indistinguishable from the Cartesian $\hat{x}$ and $\hat{y}$ unitary vectors. Most generally, the angular unitary vectors along the OZ axis can be expressed as an arbitrary rotation of the Cartesian unitary vectors, i.e. $\hat{\theta} = R_z(\gamma)\hat{x}$

and $\hat{\phi} = R_z(\gamma)\hat{y}$, with $\gamma \in (0, 2\pi)$. This implies that the scattering amplitude far from the sample along the OZ axis can be written as:

$$\mathbf{A}_s(\mathbf{r})\Big|_{x=y=0,z=|\mathbf{R}|} = \sum_{jm} \frac{(-i)^j C^e_{jm} a_{jm}}{\sqrt{j(j+1)}} y_{jm}(0,\gamma) e^{\lambda i \gamma} \left[\hat{x} - \lambda i \hat{y}\right], \quad (4.35)$$

where we have used the fact that the vector $\hat{x} - \lambda i\hat{y}$ is an eigenvector of the $R_z(\gamma)$ rotation matrix. Finally, considering Eq. (4.29) and (4.35), it is direct to check that $\mathbf{A}_i^* \cdot \mathbf{A}_s(\mathbf{r}) = 0$ along any point along the OZ axis far from the sample. Thus, for an antidual scatterer of any size and form, under plane-wave illumination the extincted power vanishes, i.e. $W_{ext} = 0$, due to the orthogonality of fields with opposite helicities.

However, the proof above is still restricted to scatterers under plane-wave illumination. As a result, the existence of antidual scatterers might still be subjected to a particular choice of the incident field. Let us now show that the result is even more general and applies to any type of incident illumination. For that aim, we should look at a previous form of the extincted power expressed in terms of the monochromatic RS vector, this is Eq. (4.16) and Eq. (4.18). Note that, in Section 4.1, to define a generic antidual scatterer, we have imposed that the incident electromagnetic field has a well-defined helicity λ. For this particular type of illumination, we have that:

$$\mathbf{S}_{ext}(\mathbf{r}) = -\frac{\lambda}{2n} \mathrm{Im}\left[\mathbf{F}_i^\lambda(\mathbf{r}) \times (\mathbf{F}_s^\lambda(\mathbf{r}))^*\right]. \quad (4.36)$$

This enlightening relation expresses that the only helicity component of the scattered field which contributes to the extinction is $\tilde{\lambda} = \lambda$. In other words, if the sample only radiates in the opposite helicity component, as do antidual scatterers, then, from Eq. (4.36), one has that $\mathbf{S}_{ext}(\mathbf{r}) = 0$. Therefore, the definition of an antidual scatterer implies, by construction, that $W_{ext} = 0$ and, thus, the presence of optical gain in the constituent materials is a necessary condition. The proof applies regardless of the size, form, material constituents, or, even, the spatial shape of the incident illumination, making the demonstration completely general within linear electromagnetic scattering theory. This general result is a paradigmatic example of the advantages of employing the RS vector. The use of the monochromatic RS vector clarifies concepts and helps simplify complex calculations within linear electromagnetic scattering theory.

Summing up, we have shown that duality, antiduality and energy conservation are closely correlated in linear electromagnetic scattering theory. We have first discussed the case of conventional spheres as a general trend of these phenomena. Then, we have shown that losses in dielectric materials also impede the existence of dual core-shells and chiral spheres. Altogether, these results indicate that the presence of losses in dielectric media preclude the construction of dual scatterers. Finally, we have shown in full generality that the construction of antidual scatterers leads to a zero extinction condition and, thus, requires from optical gain. We have first given a proof based on

the optical theorem, which applies to plane-wave illumination. However, based on the expression of the extincted power in terms of the monochromatic RS vector given in Eq. (4.18), we have shown that the result also holds under arbitrary illumination conditions.

4.3 SOME SPECIFIC RELATIONS FOR CYLINDRICAL PARTICLES

To conclude the Chapter, we would like to emphasize another aspect of linear electromagnetic scattering theory in which the monochromatic RS vector may also be useful. Up to now, we have been focused in the analysis of the helicity of the electromagnetic fields and, seemingly, the use of the RS vector may only be practical for this kind of studies. In this Section, we show that the possibilities of the monochromatic RS vector in linear electromagnetic scattering theory go far beyond the study of the polarization degree of freedom. Results are adapted from Contribution VI.

More specifically, we will delve into the study of cylindrical particles which have already been mentioned in the previous Sections. This kind of scatterers is characterized for conserving the eigenvalue of the z component of the total angular momentum, m. In other words, given an incident field which fulfills $\hat{J}_z \mathbf{E}_i(\mathbf{r}) = m\mathbf{E}_i(\mathbf{r})$, the scattered field produced by cylindrical particle necessarily fulfills $\hat{J}_z \mathbf{E}_s(\mathbf{r}) = m\mathbf{E}_s(\mathbf{r})$, where $\hat{J}_z$ is the z component of total angular momentum operator as defined in Chapter 3. This implies that the field scattered by a cylindrical sample which has been illuminated by a beam with a well-defined total angular momentum, m, does not contain terms $m' \neq m$ in the expansion given by Eq. (4.4). Moreover, if the fields emitted by the scatterer contain just a single multipole order, j, we can also get rid of the summation over this index in the expression given by Eq. (4.4). These two constrains are only feasible under particular circumstances where the response of the cylindrical particle is well-described by a single multipole order, j. However, as we show next, some fundamental relations obtained under these two particular constrains may be useful to characterize multipolar cylindrical samples.

4.3.1 *Integrated magnitudes and angular densities*

In Section 4.1, we have seen that relevant physical magnitudes of linear electromagnetic scattering theory, such as the scattered powered or the helicity expectation value, can be easily expressed in terms of the RS vector. In addition to this, we also mentioned that the mapping between the RS vector and the Stokes parameters in the circular basis is quite straightforward. This is just because, far from the sample, the monochromatic RS vector naturally splits the left- and right-polarized components in each of the scattering directions. And, it is exactly the absolute value of such components what is actually measured through the standard Stokes parameters I and V [12]. Taking

all this into account, we can express the Stokes parameters measured in each of the detectors depicted in Fig. 4.1 as:

$$I(|\mathbf{R}|,\theta,\phi) = |\mathbf{F}_s^+(|\mathbf{R}|,\theta,\phi)|^2 + |\mathbf{F}_s^-(|\mathbf{R}|,\theta,\phi)|^2 \tag{4.37}$$

$$V(|\mathbf{R}|,\theta,\phi) = |\mathbf{F}_s^+(|\mathbf{R}|,\theta,\phi)|^2 - |\mathbf{F}_s^-(|\mathbf{R}|,\theta,\phi)|^2. \tag{4.38}$$

Now let us explicitly evaluate the local expressions of the Stokes parameters for a cylindrical sample well-described by a single multipolar order j. Employing the expression of the scattered field in terms of the RS vector given by Eq. (4.6) and making use of the limits expressed in Eq. (4.31) and Eq. (4.32), we finally arrive to the following expression of the fields scattered by a sample with fixed j and m eigenvalues:

$$|\mathbf{F}_s^{\pm}(|\mathbf{R}|,\theta,\phi)|^2 = \frac{|A_{\pm}|^2\left[|\xi_{jm}(\theta,\phi)|^2 \mp \mathrm{Im}\left[\xi_{jm}^*(\theta,\phi)\cdot\eta_{jm}(\theta,\phi)\right]\right]}{(k|\mathbf{R}|)^2 j(j+1)}, \tag{4.39}$$

where we have defined $A_{\pm} = \sqrt{\varepsilon}(\alpha_{jm} \pm \beta_{jm})$ and, also, we have used that the vector functions defined in page 65 fulfill: $|\xi_{jm}(\theta,\phi)|^2 = |\eta_{jm}(\theta,\phi)|^2$. With the expression given by Eq. (4.39) we can compute the local densities of the Stokes parameters defined in Eq. (4.37) and Eq. (4.38). However, the total scattered power and helicity expectation value are related to the angular integrals of such magnitudes (see Eq. (4.19) and Eq. (4.20)):

$$I_s = (k|\mathbf{R}|)^2 \int d\Omega\; I(|\mathbf{R}|,\theta,\phi) \tag{4.40}$$

$$V_s = (k|\mathbf{R}|)^2 \int d\Omega\; V(|\mathbf{R}|,\theta,\phi). \tag{4.41}$$

It is direct to check that, in the case of a cylindrical sample well-described by a single multipolar order, j, such integrals result in [57]:

$$I_s = |A_+|^2 + |A_-|^2 \tag{4.42}$$

$$V_s = |A_+|^2 - |A_-|^2. \tag{4.43}$$

Moreover, considering the expressions above and by explicitly computing the Stokes parameters defined in Eq. (4.37) and (4.38) in terms of the RS vector of Eq. (4.39), we reach the following relation:

$$I(|\mathbf{R}|,\theta) = \frac{1}{(k|\mathbf{R}|)^2 j(j+1)}\left[f_{jm}(\theta)I_s - g_{jm}(\theta)V_s\right] \tag{4.44}$$

$$V(|\mathbf{R}|,\theta) = \frac{1}{(k|\mathbf{R}|)^2 j(j+1)}\left[-g_{jm}(\theta)I_s + f_{jm}(\theta)V_s\right], \tag{4.45}$$

where $f_{jm}(\theta) = |\xi_{jm}(\theta,\phi)|^2$, $g_{jm}(\theta) = \mathrm{Im}\left[\xi_{jm}^*(\theta,\phi)\cdot\eta_{jm}(\theta,\phi)\right]$ and the dependence on ϕ variable drops due to the cylindrical symmetry of the problem. Finally, inverting the expression we arrive to:

$$\begin{pmatrix} I_s \\ V_s \end{pmatrix} = \frac{(k|\mathbf{R}|)^2 j(j+1))}{f_{jm}^2(\theta) - g_{jm}^2(\theta)} \begin{pmatrix} f_{jm}(\theta) & g_{jm}(\theta) \\ g_{jm}(\theta) & f_{jm}(\theta) \end{pmatrix} \begin{pmatrix} I(|\mathbf{R}|,\theta) \\ V(|\mathbf{R}|,\theta) \end{pmatrix}. \tag{4.46}$$

The fundamental relation given by Eq. (4.46) indicates that for cylindrical samples illuminated with a beam with total angular momentum, m, and well-described by a single multipolar order, j, integrated magnitudes and angular densities are linearly related. In other words, for this type of scatterers, we can infer integrated magnitudes such as the scattered power or the helicity expectation value from local measurements of the Stokes parameters.

4.3.2 *Single Characterization Angle (SCA) method*

Let us briefly illustrate how can the relation given by Eq. (4.46) be employed to characterize cylindrical samples. In particular, we will discuss the Single Characterization Angle (SCA) technique which employs tightly-focused Laguerre-Gaussian (LG) beams to determine the different multipolar contributions of cylindrical particles. This kind of illumination is characterized for having a total angular momentum $m = \ell + \lambda$, where ℓ is the eigenvalue of the orbital angular momentum in the z direction [15].

When illuminating a cylindrical sample with a beam with total angular momentum, m, the multipolar contributions $j < |m|$ of the scattered field are cleared out. This is because, in the expansion of the scattered fields given by Eq. (4.4), the maximum value of the modulus of the total angular momentum is, $\max(|m|) = j$. This implies that, in cylindrical samples, a beam with angular momentum $m = 2$ cannot excite dipolar resonances ($j = 1$), a beam with angular momentum $m = 3$ cannot excite quadrupolar resonances ($j = 2$) and so on. In addition, the expansion coefficients of the incident LG beams can be tailored by focusing them with high numeric aperture systems such as a microscope objective. In particular, for tightly-focused LG beams, the expansion coefficients of order $j \sim m$ dominate, even if this may depend on specific parameters of the focusing system and the incident field [66]. As a result, tightly-focused LG beams are good candidates to excite single multipolar resonances in cylindrical samples, a condition which is necessary to employ the relation given in Eq. (4.46).

Most commonly, the measurement of integrated quantities such as the scattered power, W_s, requires the measurement and integration of the components of the scattered field in all directions. However, employing the expression in Eq. (4.46), important features of the scattering spectrum of cylindrical particles can be inferred from measurements at a single angle, θ. This is so because, through that expression, we have related the local value of the Stokes parameters, $I(|\mathbf{R}|, \theta)$ and $V(|\mathbf{R}|, \theta)$, with the integrated quantities, I_s and V_s. In this regard, note that the scattered power is proportional to I_s, whereas the scattered helicity defined is proportional to V_s. Importantly, the expression specified in Eq. (4.46) is valid for all scattering angles or, in other words, it does not rely on the measurements of the Stokes parameters at a specific location. This crucial feature permits us to distinguish the regimes at which the method ceases to be valid. We

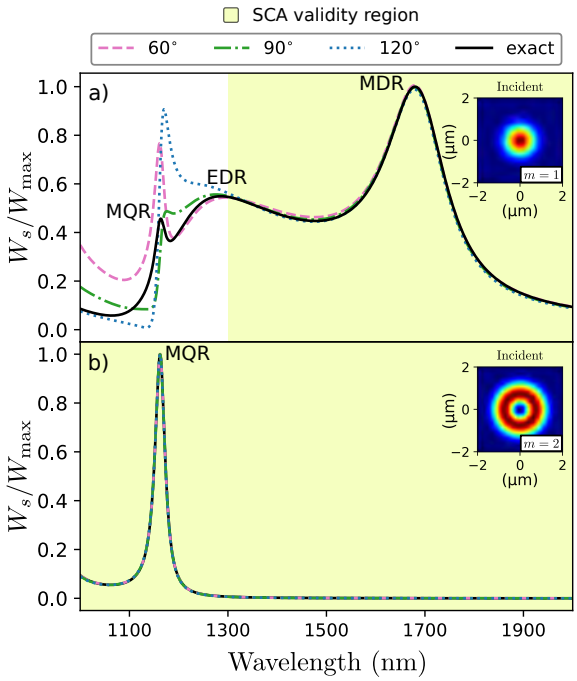

Figure 4.7: Normalized scattered power of a Silicon sphere of radius a = 230 nm in the infrared computed with the SCA method. In black the exact computation and in colors the values obtained from the evaluation of Stokes parameters at $\theta = 60°$ (dashed pink), $\theta = 90°$ (dashed green) and $\theta = 120°$ (dotted blue). EDR, MDR and MQR denote the electric dipolar, magnetic dipolar and magnetic quadrupolar resonances, respectively. a) Spectra obtained with a tightly-focused LG beam with $m = 1$ and $\lambda = 1$. b) Spectra obtained with a tightly-focused LG beam with $m = 2$ and $\lambda = 1$. Figure adapted from Contribution VI. Simulation performed by Iker Gómez-Viloria.

may evaluate the local Stokes parameters at a few different scattering angles, θ, but only rely on the measurements which lead to the same integrated magnitudes. This is the basis of the SCA technique.

An example is depicted in Fig. 4.7, where the SCA method is employed to characterize the optical resonances of a Silicon sphere of radius a = 230 nm in the infrared. In the long wavelength range, close to the so-called Rayleigh regime, dipolar resonances are expected. Thus, in that spectral region, we may employ a tighly-focused LG beam with $m = 1$ to characterize the response of the particle. This physical situation fixes $m = j = 1$ and, thus, it leads to a particular form of the matrix in Eq. (4.46), i.e. $f_{11}(\theta) = (3/8\pi)(1 + \cos^2\theta)$ and $g_{11}(\theta) = -(3/4\pi)\cos\theta$. In Fig. 4.7a we have computed the exact scattered power normalized to its maximum, W_{max}, (solid black) and the result obtained through SCA method by evaluating the Stokes parameters at angles $\theta = 60°$ (dashed pink), $\theta = 90°$ (dashed green) and $\theta = 120°$ (dotted blue). As we can infer, the scattered power is fully captured in the wavelength range $1300 - 2000$ nm, where the response of the particle can be described with electric and magnetic dipoles. However, due to the presence of the quadrupole, the scattering spectrum is ill-captured below 1300 nm because the response can

no longer be described with a single multipolar order j. Note that the disagreement in the measurements for different scattering angles at $\sim$ 1300 nm is helpful to identify the regime at which the sample ceases to be dipolar.

At this point, we may change the incident beam and excite the particle with a tightly-focused LG beam with $m = 2$ to fully capture the quadrupolar resonance. The result is depicted in Fig. 4.7b. Such a remarkable outcome stems from the fact that the illuminating beam cannot excite any dipolar ($j = 1$) resonances within the scatterer. As a result, the underlying dipolar resonances are cleared out, and the SCA technique can still be applied to characterize the particle below 1300 nm. Of course, when exciting a quadrupolar mode ($j = 2$) with a LG beam with total angular momentum $m = 2$, the matrix given by Eq. (4.46) has to be re-evaluated. In this case, the functions that have to be employed are $f_{22}(\theta) = (15/8\pi)\sin^2\theta(1+\cos^2\theta)$ and $g_{22}(\theta) = -(15/4\pi)\sin^2\theta\cos\theta$. Note that this procedure is recursive, i.e. a LG beam with $m = 3$ can be employed to characterize octupolar ($j = 3$) spectral regions and so on. Also, the numerical aperture employed in Fig. 4.7a and 4.7b is the same ($NA = 0.9$). This implies that SCA technique can be implemented within a single set up in which the angular momentum of the incident beam is switchable.

4.4 SUMMARY

In Section 4.1, we have first introduced the relevant physical magnitudes of linear electromagnetic scattering theory in terms of the monochromatic RS vector. In particular, we have defined dual and antidual scatterers as those which preserve or completely flip the helicity of an illuminating wave. Then, in Section 4.2, we have seen that the construction of dual and antidual scatterers is subjected to the energy properties of the constituent materials. We have shown that the presence of optical losses in dielectric materials impede the construction of dual samples and, also, that optical gain is a necessary condition to build antidual particles of any size and form. Finally, in Section 4.3, we have shown that the possibilities of the monochromatic RS vector in scattering theory go far beyond the analysis of the helicity features of the electromagnetic field. Indeed, we have shown that, for cylindrical particles well-described by a single multipolar order j, integrated and local values of the Stokes parameters are linearly related. This is the basis of the SCA technique which permits the characterization of cylindrical particles through local measurements of the Stokes parameters.

5

ELECTROMAGNETIC WAVES IN MAGNETIC MEDIA

In this Chapter, we study the form of Maxwell's equations in inhomogeneous magnetic media with the aid of the monochromatic RS vector. We examine the impedance and refractive index matching conditions based on the so-called *photon hamiltonian* and discuss the implications over Fresnel and Mie coefficients. Then, to get some additional physical insight into the matching conditions, we employ perturbation theory in 1D inhomogeneous systems. Finally, we discuss the conserved quantities associated with both matching conditions following the symmetry arguments developed in Chapter 3. Based on these developments, we propose a global explanation about the emergence of Kerker phenomena in piecewise homogeneous environments.

Derivations within Sections 5.1 and 5.2 are based on Contribution IV. Section 5.3 is based on results reported in Contribution VII.

5.1 MAXWELL'S EQUATIONS IN INHOMOGENEOUS MEDIA

In Chapter 4 we have discussed the application of the monochromatic RS vector to linear electromagnetic scattering theory. This implies that we have restricted the analysis of light-matter interactions to situations in which the angular frequency of the fields, ω, is fixed and the samples under consideration have sharp boundaries. In other words, we have been constrained to linear samples for which the constitutive relations are defined through step functions. In this Chapter, we relax this last assumption and consider that light may propagate through inhomogeneous environments for which the constitutive relations are scalar functions of the spatial coordinates. Moreover, we will not deal with chiral media, which implies that the constitutive relations for the electric and magnetic fields are going to be: $\mathbf{D}(\mathbf{r}) = \varepsilon(\mathbf{r})\mathbf{E}(\mathbf{r})$ and $\mathbf{B}(\mathbf{r}) = \mu(\mathbf{r})\mathbf{H}(\mathbf{r})$, where $\varepsilon(\mathbf{r})$ and $\mu(\mathbf{r})$ are the local electric permittivity and magnetic permeability, respectively.

In this Section, we first present the form of Maxwell's equations in inhomogeneous media in terms of the monochromatic RS vector. Our derivation is based on Maxwell's equations as specified by Eq. (2.46) and Eq. (2.47) of Chapter 2. We discuss the link of such form of Maxwell's equations with the so-called *photon hamiltonian* [8]. Also, we identify the impedance and refractive index matching conditions as naturally emerging from this particular way of expressing Maxwell's equations. Then, we analyze two physical situations in which both matching conditions play an important role, i.e. the scattering of a circularly polarized plane-wave by a plane magnetic surface and by a magnetic sphere. Indeed, we show that both impedance and index matching conditions have relevant consequences on the analytical form of Fresnel and Mie coefficients. Finally, we demonstrate that index-matched spheres flip the helicity of the incoming field as close as energy conservation law allows.

5.1.1 *The photon hamiltonian*

As previously mentioned, our starting point is Maxwell's equations in inhomogeneous media expressed in terms of the monochromatic RS vector (see Chapter 2 for a detailed derivation):

$$\omega\mathbf{F}^{+} = \frac{1}{\sqrt{n}}\nabla\times\left(\frac{\mathbf{F}^{+}}{\sqrt{n}}\right) + \frac{1}{n}\left(\nabla\ln\sqrt{Z}\right)\times\mathbf{F}^{-} \tag{5.1}$$

$$\omega\mathbf{F}^{-} = -\frac{1}{\sqrt{n}}\nabla\times\left(\frac{\mathbf{F}^{-}}{\sqrt{n}}\right) - \frac{1}{n}\left(\nabla\ln\sqrt{Z}\right)\times\mathbf{F}^{+} \tag{5.2}$$

$$\nabla\cdot\mathbf{F}^{+} = -\left(\nabla\ln\sqrt{n}\right)\cdot\mathbf{F}^{+} + \left(\nabla\ln\sqrt{Z}\right)\cdot\mathbf{F}^{-} \tag{5.3}$$

$$\nabla\cdot\mathbf{F}^{-} = -\left(\nabla\ln\sqrt{n}\right)\cdot\mathbf{F}^{-} + \left(\nabla\ln\sqrt{Z}\right)\cdot\mathbf{F}^{+}, \tag{5.4}$$

where, for convenience, we have omitted the dependence on the spatial variable, $\mathbf{r}$. Also, we have defined the local impedance $Z(\mathbf{r}) = \sqrt{\mu(\mathbf{r})/\varepsilon(\mathbf{r})}$ and local refractive index $n(\mathbf{r}) = \sqrt{\varepsilon(\mathbf{r})\mu(\mathbf{r})}$, with $c = 1$

(natural units). Please note that Eqs. (5.1)-(5.4) are completely equivalent to the time-independent Maxwell's equations in an isotropic and inhomogeneous magnetic medium. Indeed, such a particular form of Maxwell's equations is simply obtained through a change of basis where, instead of the usual electric and magnetic fields, the monochromatic RS vector is employed (see Section 2.2). Furthermore, it can be checked that, in this form, the equations only contain two different types of fields:

$$\mathbf{F}^{\pm}(\mathbf{r}) = \frac{1}{\sqrt{2}}\left[\frac{\mathbf{D}(\mathbf{r})}{\sqrt{\varepsilon(\mathbf{r})}} \pm i\frac{\mathbf{B}(\mathbf{r})}{\sqrt{\mu(\mathbf{r})}}\right]. \tag{5.5}$$

This is because in the derivation we have explicitly substituted the constitutive relations, $\mathbf{F}^{\pm}(\mathbf{r}) = n(\mathbf{r})\mathbf{G}^{\pm}(\mathbf{r})$.

The particular form of Maxwell's equations given by Eqs. (5.1)-(5.4) was first derived by Bialynicki-Birula in his seminal work "Photon wave function" published in 1996 [8]. There, the author sought a first quantized form of the dynamic equations for massless particles, in analogy to the formalism already developed for massive particles. In his view, such an analogy may lead to new methods to study the properties of electromagnetic waves and, thus, also photons [67]. In particular, he proposed that certain problems of electromagnetism may be addressed as quantum mechanical eigenvalue problems, in full analogy with the time-independent Schrödinger equation. In this line, he proposed an alternative way of interpreting Ampère-Faraday laws encoded in Eqs. (5.1)-(5.2). He indicated that such dynamical equations may also be expressed in the following form:

$$\begin{aligned}
&\hat{H}\begin{pmatrix}\mathbf{F}^{+}\\ \mathbf{F}^{-}\end{pmatrix} = \omega\begin{pmatrix}\mathbf{F}^{+}\\ \mathbf{F}^{-}\end{pmatrix}, \quad \text{with}\\
&\hat{H} = \begin{pmatrix}\frac{1}{\sqrt{n}}\nabla\times\left(\frac{\cdot}{\sqrt{n}}\right) & \frac{1}{n}\nabla\ln\sqrt{Z}\times\\ -\frac{1}{n}\nabla\ln\sqrt{Z}\times & -\frac{1}{\sqrt{n}}\nabla\times\left(\frac{\cdot}{\sqrt{n}}\right)\end{pmatrix}.
\end{aligned} \tag{5.6}$$

Here, the $\hat{H}$ operator represents the photon hamiltonian in inhomogeneous media. Importantly, note that, as in the conventional form of monochromatic Maxwell's equations (without charges and currents), Ampère-Faraday laws encoded in Eq. (5.6) represent themselves all four Maxwell's equations. This is just because Gauss' laws specified by Eq. (5.3)-(5.4) can be derived from Eqs. (5.1)-(5.2). As a result, we can conclude that the photon hamiltonian, $\hat{H}$, contains all the information about the dynamics of electromagnetic fields in isotropic and inhomogeneous media without charges and currents.

Interestingly, such a particular manner of expressing Maxwell's equations directly reminds us of a well-known physical problem in quantum mechanics: the dynamics of a two-level system. Indeed, if it were not for the vector nature of the fields and the operators constituting the photon hamiltonian, the concordance would be straightforward. Such an analogy is based on associating the helicity components of the electromagnetic field with two different levels whose

states are coupled by the environment. Curiously, when expressing Maxwell's equations in terms of the helicity components of the field, it is not $\varepsilon(\mathbf{r})$ or $\mu(\mathbf{r})$ which appear as crucial parameters, but their ratio, $Z(\mathbf{r})$, and their product, $n(\mathbf{r})$. In this line, we see that the role of such material parameters is divided into two different contributions. On the one hand, the spatial derivatives of the impedance contribute to the coupling of the two helicity components of the field. On the other hand, the spatial derivatives of the refractive index contribute exclusively to the diagonal terms. In particular, given the form of the operator in Eq. (5.6), we can identify two specific types of environments in which the electromagnetic field may have a particular behaviour: media for which the impedance is constant, $\nabla Z = 0$, or media for which the refractive index is constant, $\nabla n = 0$. We denote this two situations as the impedance matching and the refractive index matching conditions, respectively.

In general terms, the impedance matching condition, $\nabla Z = 0$, leads to a decoupling in the evolution of the two helicity components of the electromagnetic field. This can be deduced from the fact that the anti-diagonal terms of the photon hamiltonian, $\hat{H}$, vanish under this particular condition. Thus, if we fix the initial conditions such that only one of the two helicities is present (imposing, for instance, an illumination with well-defined helicity), the interaction with an impedance-matched medium only generates new field components of the same helicity. On the other hand, the refractive index matching condition, $\nabla n = 0$, seems to have a similar effect but over the diagonal terms of the photon hamiltonian. It is clear that this matching condition implies having an environment in which the helicity components are mixed. At first sight, however, one is not able to tell the difference with a common dielectric medium ($\mu = 1$ and, thus, $Z = 1/n$) in which the helicity components are also coupled. Indeed, the interpretation of the index matching condition is not so straightforward and it will take us a bit to understand it in detail. However, before going on with the analysis, let us give a few practical examples about what we have just discussed. Indeed, if the impedance and refractive index are such fundamental parameters, as they seem to be from the form of Maxwell's equations in Eq. (5.6), they must have some significant effects in problems with well-known solutions.

In what follows, we analyze the consequences of the impedance and refractive index matching conditions in two problems with analytical solutions, i.e. the scattering of a circularly-polarized plane-wave by a magnetic flat interface and by a magnetic sphere.

5.1.2 *Matching conditions in Fresnel coefficients*

The scattering of a plane-wave by a flat interface is a standard problem whose solution is given in terms of the so-called Fresnel coefficients. These coefficients relate the amplitude of the incident plane-wave with the amplitudes of the reflected and refracted plane-waves. In particular, the incident field is usually split in its $\hat{s}$ and $\hat{p}$ polariza-

tions, which represent, the perpendicular and parallel components with respect to the plane of incidence, respectively. Fresnel coefficients determine the amplitude of the reflected and transmitted waves in each of these components. More specifically, if the incident electric field is expressed as $\mathbf{E}_i(\mathbf{r}) = \left(E_i^s \hat{s} + E_i^p \hat{p}\right) e^{i\mathbf{k}_i \cdot \mathbf{r}}$, where $\mathbf{k}_i$ is the wave vector of the incident field, the amplitudes of the reflected, $\mathbf{E}_1(\mathbf{r})$, and transmitted, $\mathbf{E}_2(\mathbf{r})$, field components are determined as:

$$E_1^s = r^s E_i^s, \qquad E_1^p = r^p E_i^p \tag{5.7}$$

$$E_2^s = t^s E_i^s, \qquad E_2^p = t^p E_i^p. \tag{5.8}$$

In the expression above, the $r^{s/p}$ and $t^{s/p}$ coefficients represent the reflection and transmission Fresnel coefficients for $\hat{s}$ and $\hat{p}$ polarizations. In particular, if we choose a circularly-polarized incident field of helicity λ, i.e. we impose $E_i^p = \lambda i E_i^s$, the reflected and refracted fields, in terms of the monochromatic RS vector, are:

$$\mathbf{F}_1^{\tilde{\lambda}}(\mathbf{r}) = \sqrt{\varepsilon} E_i^s \left[r^s + \lambda\tilde{\lambda} r^p\right] \left(\frac{\hat{s} + \tilde{\lambda} i \hat{p}}{\sqrt{2}}\right) e^{i\mathbf{k}_1 \cdot \mathbf{r}} \tag{5.9}$$

$$\mathbf{F}_2^{\tilde{\lambda}}(\mathbf{r}) = \sqrt{\varepsilon} E_i^s \left[t^s + \lambda\tilde{\lambda} t^p\right] \left(\frac{\hat{s} + \tilde{\lambda} i \hat{p}}{\sqrt{2}}\right) e^{i\mathbf{k}_2 \cdot \mathbf{r}}, \tag{5.10}$$

where $\mathbf{k}_1$ and $\mathbf{k}_2$ are the wave vectors of the reflected and refracted waves, respectively. Also, note that $\hat{s} \times \hat{p} = \hat{k}$.

For magnetic media, Fresnel reflection and transmission coefficients acquire the following analytical form [65]:

$$r^s = \frac{k_{z_1} - msk_{z_2}}{k_{z_1} + msk_{z_2}}, \qquad r^p = \frac{sk_{z_1} - mk_{z_2}}{sk_{z_1} + mk_{z_2}} \tag{5.11}$$

$$t^s = \frac{2k_{z_1}}{k_{z_1} + msk_{z_2}}, \qquad t^p = \frac{2k_{z_1}}{sk_{z_1} + mk_{z_2}}, \tag{5.12}$$

where $s = Z_1/Z_2$ and $m = n_1/n_2$; here, Z_1 and n_1 are the impedance and refractive index in the medium of incidence; also, Z_2 and n_2 are the impedance and refractive index in the medium of transmittance; finally, k_{z_1} and k_{z_2} represent the z component of the wave vector in the medium of incidence and in the medium of transmittance, respectively. On the one hand, it is direct to check that, under the impedance matching condition ($s = 1$), the following relations are fulfilled:

$$r^s = r^p = \frac{k_{z_1} - mk_{z_2}}{k_{z_1} + mk_{z_2}} \tag{5.13}$$

$$t^s = t^p = \frac{2k_{z_1}}{k_{z_1} + mk_{z_2}}. \tag{5.14}$$

On the other hand, under the refractive index matching condition ($m = 1$, which also implies $k_{z_1} = k_{z_2}$), we get:

$$r^s = -r^p = \frac{1 - s}{1 + s} \tag{5.15}$$

$$t^s = t^p = \frac{2}{1 + s}. \tag{5.16}$$

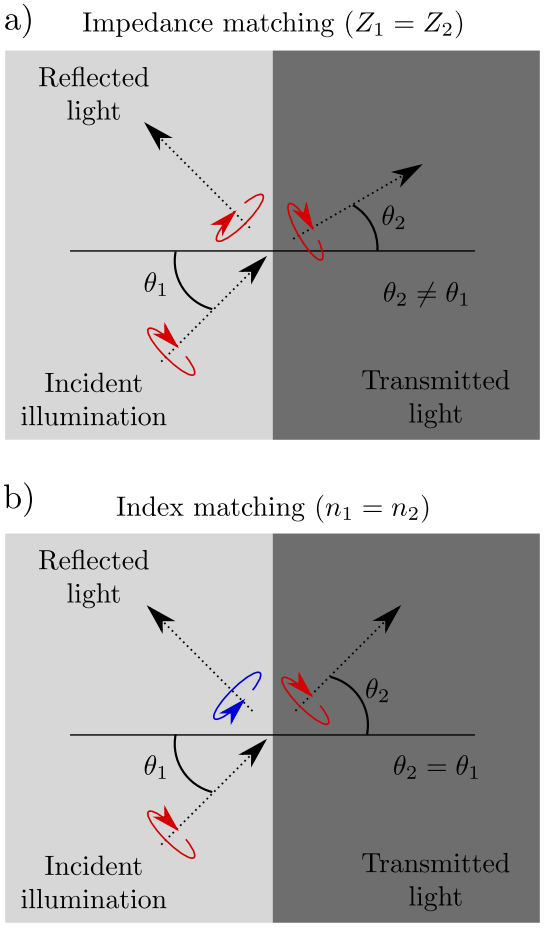

Figure 5.1: Matching conditions in Fresnel's scattering problem. a) Under the impedance matching condition incident, reflected and transmitted waves have the same helicity. b) Under the index matching condition incident and transmitted waves have the same helicity, whereas the reflected wave has the opposite helicity.

The effect of both matching conditions over the Fresnel reflection and transmission coefficients was first identified by Giles and Wild in 1982 [68]. Later, in 1990, a nice study was also provided by Lakhtakia in terms of circularly-polarized plane-waves [69], which is the basis of our analysis. The first result, as it can be checked from Eqs. (5.13)-(5.14), indicates that the reflection and transmission coefficients are equal under the impedance matching condition, $\nabla Z = 0$. Taking into account the expression of the fields given in Eqs. (5.9)-(5.10), this implies that both the transmitted and reflected waves have the same helicity as the incident field (see Fig. 5.1a). This in concurrence with the general features of the impedance matching condition we have just discussed. Indeed, this particular matching condition decouples the evolution of both helicity components in Eq. (5.6) and, thus, the interaction cannot generate field components of the opposite helicity. Secondly, the expressions in Eqs. (5.15)-(5.16) indicate that under the refractive index matching condition, $\nabla n = 0$, the transmitted wave has the same helicity as the incident field, whereas the reflected beam only has the opposite helicity component (see Fig. 5.1b). Moreover, under this matching condition, the reflection and transmission

coefficients are independent of the incidence angle and they are completely determined by the impedance contrast parameter, $s = Z_1/Z_2$. This results confirm that the refractive index matching condition has relevant consequences over Fresnel coefficients.

5.1.3 *Matching conditions in Mie coefficients*

The scattering of a plane-wave by a sphere is also a well-studied problem in electrodynamics whose solution is given in terms of the so-called Mie coefficients. The problem has been partially studied in Chapter 4, where the expression of the field scattered by a chiral sphere has been provided in Eq. (4.24). In this Subsection, we will exclusively deal with the solution for a conventional sphere whose complete solution is given in terms of both the scattered field, $\mathbf{E}_s(\mathbf{r})$, and the internal electric field, $\mathbf{E}_1(\mathbf{r})$. For an incident circularly-polarized plane-wave with helicity λ, the scattered and internal fields are:

$$\mathbf{E}_s(\mathbf{r}) = -\lambda \sum_j K_j \left[\left(\frac{a_j + b_j}{\sqrt{2}} \right) \mathbf{\Phi}^{\lambda}_{j\lambda} + \left(\frac{a_j - b_j}{\sqrt{2}} \right) \mathbf{\Phi}^{-\lambda}_{j\lambda} \right] \tag{5.17}$$

$$\mathbf{E}_1(\mathbf{r}) = \lambda \sum_j K_j \left[\left(\frac{d_j + c_j}{\sqrt{2}} \right) \bar{\mathbf{\Phi}}^{\lambda}_{j\lambda} + \left(\frac{d_j - c_j}{\sqrt{2}} \right) \bar{\mathbf{\Phi}}^{-\lambda}_{j\lambda} \right], \tag{5.18}$$

where $K_j = i^j \sqrt{2\pi(2j+1)}$; also, a_j and b_j are the electric and magnetic scattering Mie coefficients; on the other hand, d_j and c_j are the electric and magnetic internal Mie coefficients; finally, note that the radial function of the multipolar field which determines the scattered field, $\mathbf{\Phi}^{\lambda}_{jm}$, is the spherical Hankel function of the first kind, $h^{(1)}_j$, and the radial function of the multipolar field that determines the internal field, $\bar{\mathbf{\Phi}}^{\lambda}_{jm}$, is the spherical Bessel function of the first kind, j_j.

For a magnetic sphere, the scattering Mie coefficients are [14]:

$$a_j = \frac{\psi_j(mx)\psi_j'(x) - s\psi_j(x)\psi_j'(mx)}{\psi_j(mx)\xi_j'(x) - s\xi_j(x)\psi_j'(mx)} \tag{5.19}$$

$$b_j = \frac{s\psi_j(mx)\psi_j'(x) - \psi_j(x)\psi_j'(mx)}{s\psi_j(mx)\xi_j'(x) - \xi_j(x)\psi_j'(mx)}, \tag{5.20}$$

and, the internal Mie coefficients are:

$$d_j = ms\frac{\psi_j(x)\xi_j'(x) - \xi_j(x)\psi_j'(x)}{\psi_j(mx)\xi_j'(x) - s\xi_j(x)\psi_j'(mx)} \tag{5.21}$$

$$c_j = ms\frac{\psi_j(x)\xi_j'(x) - \xi_j(x)\psi_j'(x)}{s\psi_j(mx)\xi_j'(x) - \xi_j(x)\psi_j'(mx)}, \tag{5.22}$$

where $s = Z_1/Z_2$ and $m = n_1/n_2$ are the impedance and refractive index contrasts, with subscript 1 now referring to the sphere and subscript 2 to the surrounding medium; also, $x = ka$ is the size parameter, with k the wave vector in the surrounding medium and a the radius of the sphere; finally, $\psi_j(z) = zj_j(z)$ and $\xi_j(z) = zh^{(1)}_j(z)$ are the Ricatti-Bessel functions. On the one hand, it can be checked

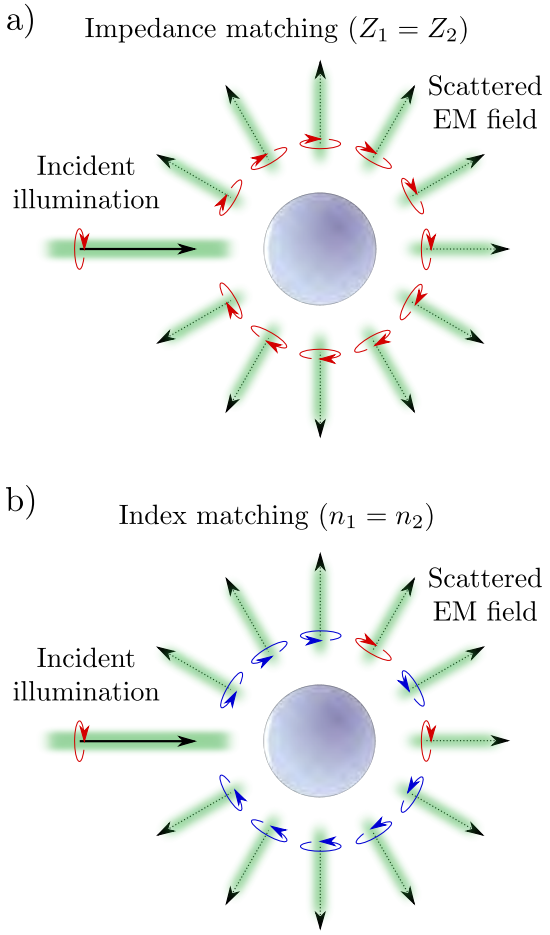

Figure 5.2: Matching conditions in Mie's scattering problem. a) Under the impedance matching condition incident and scattered waves have the same helicity. b) Under the index matching condition incident and scattered waves almost have the opposite helicity.

that, whenever the impedance matching condition is fulfilled ($s = 1$), the following relations hold:

$$a_j = b_j = \frac{\psi_j(mx)\psi_j'(x) - \psi_j(x)\psi_j'(mx)}{\psi_j(mx)\xi_j'(x) - \xi_j(x)\psi_j'(mx)}, \ \forall j \tag{5.23}$$

$$d_j = c_j = m\frac{\psi_j(x)\xi_j'(x) - \xi_j(x)\psi_j'(x)}{\psi_j(mx)\xi_j'(x) - \xi_j(x)\psi_j'(mx)}, \ \forall j. \tag{5.24}$$

On the other hand, it can also be checked that, under the refractive index matching condition ($m = 1$):

$$\frac{a_j}{b_j} = -\frac{d_j}{c_j} = -\frac{s\psi_j(x)\xi_j'(x) - \xi_j(x)\psi_j'(x)}{\psi_j(x)\xi_j'(x) - s\xi_j(x)\psi_j'(x)}, \ \forall j. \tag{5.25}$$

The effect of the matching conditions over the Mie coefficients was analyzed for the first time in the seminal paper by Kerker, Wang and Giles in 1983 [70]. Indeed, they were the first ones to report the relation of the scattering Mie coefficients under the impedance matching condition given in Eq. (5.23). However, to the best of our knowledge, the relations given by Eq. (5.24) and Eq. (5.25) have been reported for the first time in Contribution IV. On the one hand, under the

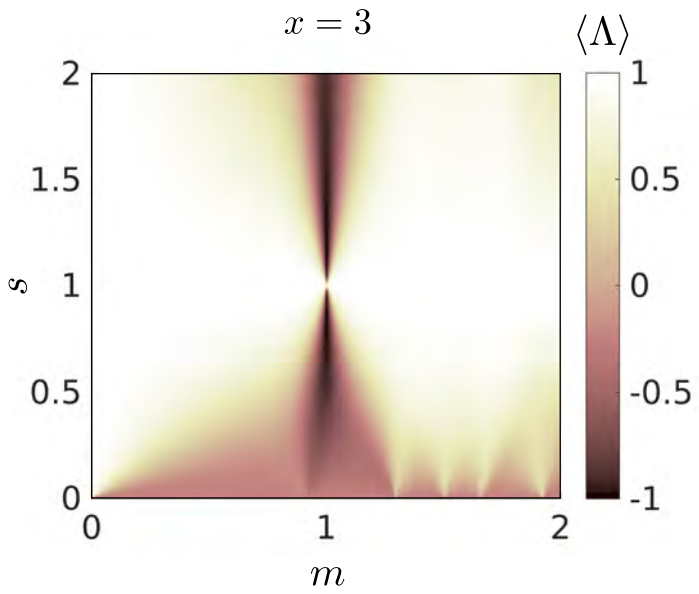

Figure 5.3: Helicity expectation value, $\langle\Lambda\rangle$, for a passive sphere of size parameter $x = 3$ illuminated by a circularly-polarized plane-wave. $\langle\Lambda\rangle$ is given as a function of the impedance contrast, $s = Z_1/Z_2$, and refractive index contrast, $m = n_1/n_2$. In particular, $\langle\Lambda\rangle = 1$ implies a dual scatterer and $\langle\Lambda\rangle = -1$ an antidual one. The impedance matching condition is fulfilled through the line $s = 1$ and refractive index matching condition through the line $m = 1$. Figure adapted from Contribution IV.

impedance matching condition, $\nabla Z = 0$, we see that the electric and magnetic coefficients are equal for both the scattered and the internal fields. Bearing in mind the expression of the fields in Eqs. (5.17)-(5.18), this implies that the scattered and internal fields only contain the same helicity component as the incident field (see Fig. 5.2a). This is in concurrence with the properties of the photon hamiltonian and what we have just discussed for Fresnel coefficients. On the other hand, under the refractive index matching condition, $\nabla n = 0$, we see that Mie coefficients are analytically related in a very specific way. In addition, from the relation in Eq. (5.25), it can be further checked that $\lim_{s\to 1} a_j/b_j = -1$ holds. In other words, for index-matched spheres in the limit of low impedance contrast, one analytically has that $a_j = -b_j$, which implies an antidual scatterer. However, please note that the relation is fulfilled in the very particular situation of having both $m = 1$ and $s = 1$, meaning that, in the limit, there is no scatterer at all. Without reaching such a limit, we may say that index matched spheres flip the helicity of the incoming field very efficiently (see Fig. 5.2b).

In Fig. 5.3 we summarize the effect of both impedance and refractive index matching conditions in magnetic spheres. We plot the helicity expectation value, $\langle\Lambda\rangle$, for a sphere of size parameter $x = 3$ in terms of the impedance contrast, s, and refractive index contrast, m. On the one hand, whenever the impedance of the sphere and the surrounding medium are matched, along the horizontal $s = 1$ line, the system behaves as dual, i.e. it preserves the helicity of the inci-

dent field ($\langle\Lambda\rangle = 1$). On the other hand, an outstanding behaviour is found when the index matching condition is fulfilled, through the line $m = 1$. Values of $\langle\Lambda\rangle \sim -1$ are obtained in the vicinities of such a line but never reaching the exact antiduality condition. Of course, this is because we are considering both s and m real parameters, which implies that the sphere has no optical gain and, thus, it cannot behave as an antidual scatterer. However, although passive antidual scatterers are precluded by the energy conservation law, we see that one can obtain a pretty similar behaviour for index-matched spheres. This is due to the analytical form of the Mie coefficients under the refractive index matching condition given in Eq. (5.25), which had previously been overlooked in the literature.

5.2 ANALOGY WITH A TWO-LEVEL SYSTEM

From the results in the previous Section, we can conclude that both matching conditions lead to very specific forms of Fresnel and Mie coefficients and, thus, imply very particular behaviours of the fields. Indeed, we have shown that the impedance matching condition completely uncouples the evolution of the two helicity components of the field. Also, we have seen that the refractive index matching condition leads to a singular type of helicity mixing. More specifically, in spherical scatterers, this matching condition enables the construction of samples which almost completely flip the helicity of the incident beam. However, while the study of the impedance matching condition is widespread [61, 62], the refractive index matching condition has been quite ignored in the literature.

In this Section, we characterize the refractive index matching condition making use of some standard tools employed in quantum mechanical eigenvalue problems. All the previous analysis points in the direction that the $\nabla n = 0$ condition allows for helicity flipping media as close as energy conservation allows. However, the exact mechanism for this helicity conversion still remains hidden. To shed light on this, we derive the form of Maxwell's equations for smooth inhomogeneous media and compute the energies of the propagating electromagnetic waves in terms of Z and n. We choose smoothly varying media because, as we will see, for this particular type of media the eigenvalue problem given in Eq. (5.6) can be solved in terms of time-independent perturbation theory. In this line, we first compute the exact solutions for the unperturbed system, i.e. an infinitely homogeneous medium. Then, we derive the form of the photon hamiltonian in smoothly varying 1D inhomogeneous media and we apply standard perturbation theory. Finally, we propose an interpretation of the impedance and refractive index matching conditions through a formal analogy with quantum two-level systems.

5.2.1 *Unperturbed solutions and perturbation term*

Standard perturbation theory may only be employed if the operator given by Eq. (5.6), can be expressed as a sum of two terms, i.e. $\hat{H} = \hat{H}_0 + \hat{V}$, where $\hat{H}_0$ is the hamiltonian of the unperturbed system and $\hat{V}$ is the perturbation term. In general, the method permits the construction of approximate solutions to the perturbed system based on already known exact solutions to the unperturbed problem. In our case, the unperturbed system is an infinitely homogeneous medium and, thus, $\hat{H}_0$ represents the photon hamiltonian in a medium with constant Z and n. Based on the exact solutions of $\hat{H}_0$, we will then compute the approximate solutions for a smoothly varying 1D inhomogeneous medium.

We consider that inhomogeneities are exclusively given in the OX direction, namely, that the impedance and refractive index are expressed as $Z(x) = Z_0 + d(x)$ and $n(x) = n_0 + e(x)$, respectively. Translation symmetry in the OY and OZ directions suggests that the solutions to this problem must be of the form:

$$\mathbf{\Phi}(\mathbf{r}) = \mathbf{\Phi}(x) e^{ik_y y + ik_z z}, \tag{5.26}$$

where $\mathbf{\Phi}(x) = [\mathbf{F}^+(x), \mathbf{F}^-(x)]^T$ is a six component vector field whose first (last) three Cartesian components constitute the positive (negative) helicity components of the field. Please note that, in this Section, the field $\mathbf{\Phi}(\mathbf{r})$ does not represent a multipolar beam. Moreover, as the OY and OZ directions are physically equivalent, the result cannot change depending on the direction of propagation in the YZ plane. Thus, for simplicity, we can fix the transverse linear momentum component to be, for instance, in the OY direction, i.e. we fix the axes such that $k_y = k_t$ and $k_z = 0$. Thus, for a 1D inhomogeneous medium, the unperturbed hamiltonian, i.e. time-independent Maxwell's equations in an infinitely homogeneous medium, can be expressed as:

$$\hat{H}_0 = \frac{1}{n_0} \begin{pmatrix} 0 & 0 & ik_t & 0 & 0 & 0 \\ 0 & 0 & -\partial_x & 0 & 0 & 0 \\ -ik_t & \partial_x & 0 & 0 & 0 & 0 \\ 0 & 0 & 0 & 0 & 0 & -ik_t \\ 0 & 0 & 0 & 0 & 0 & \partial_x \\ 0 & 0 & 0 & ik_t & -\partial_x & 0 \end{pmatrix} \tag{5.27}$$

The solution to the unperturbed system is obtained from the resolution of the system of differential equations $\hat{H}_0 \mathbf{\Phi}(x) = \omega \mathbf{\Phi}(x)$. The exact solution to such a system of equations is found by applying the usual techniques and it is most generally given in terms of four integration constants. Fixing such integration constants, we find four

different types of normalized solutions to the unperturbed hamiltonian:

$$\mathbf{\Phi}_1(x) = \sqrt{\frac{\omega}{2}}\left(\tfrac{ik_t}{\omega n_0}, -\tfrac{ik_x}{\omega n_0}, 1, 0, 0, 0\right)^T e^{ik_x x} \tag{5.28}$$

$$\mathbf{\Phi}_2(x) = \sqrt{\frac{\omega}{2}}\left(\tfrac{ik_t}{\omega n_0}, \tfrac{ik_x}{\omega n_0}, 1, 0, 0, 0\right)^T e^{-ik_x x} \tag{5.29}$$

$$\mathbf{\Phi}_3(x) = \sqrt{\frac{\omega}{2}}\left(0, 0, 0, \tfrac{ik_t}{\omega n_0}, -\tfrac{ik_x}{\omega n_0}, 1\right)^T e^{ik_x x} \tag{5.30}$$

$$\mathbf{\Phi}_4(x) = \sqrt{\frac{\omega}{2}}\left(0, 0, 0, \tfrac{ik_t}{\omega n_0}, \tfrac{ik_x}{\omega n_0}, 1\right)^T e^{-ik_x x}, \tag{5.31}$$

where we have defined $k_x^2 = \omega^2 n_0^2 - k_t^2$. As we see, the exact solutions to the unperturbed system are circularly-polarized plane-waves propagating along the positive and negative OX directions. Moreover, by construction, all of them fulfill $\hat{H}_0 \mathbf{\Phi}_k(x) = \omega \mathbf{\Phi}_k(x)$, which implies that they are degenerate.

Once we have computed the solutions to the unperturbed system, we should compute the perturbation term, $\hat{V}$. However, depending on whether we consider the perturbation in the direction of constant impedance or constant refractive index, the perturbation has a different analytical form. At first order, the perturbation potential in an arbitrary direction of the (Z, n) parameter space can be constructed as a linear combination of the perturbation potentials in each direction. Thus, we may discuss each of these cases independently. Let us first consider the case of a medium where the refractive index is constant and the impedance is only a function of one space coordinate. In this case, the photon hamiltonian directly splits into the sum of two operators and the perturbation term is:

$$\hat{V}_Z = \frac{1}{n_0}\begin{pmatrix} 0 & 0 & 0 & 0 & 0 & 0 \\ 0 & 0 & 0 & 0 & 0 & -\zeta(x) \\ 0 & 0 & 0 & 0 & \zeta(x) & 0 \\ 0 & 0 & 0 & 0 & 0 & 0 \\ 0 & 0 & \zeta(x) & 0 & 0 & 0 \\ 0 & -\zeta(x) & 0 & 0 & 0 & 0 \end{pmatrix}, \tag{5.32}$$

where $\zeta(x) = \partial_x \ln \sqrt{Z(x)}$ is a real function. For smoothly varying media we can consider that $Z(x) = Z_0 + d(x)$, with $d(x)/Z_0 << 1$, and, thus, the perturbation is determined by the function $\zeta(x) \sim (2Z_0)^{-1}\partial_x d(x)$.

In the complementary case where the impedance is constant and the refractive index is only a function of one space coordinate, the photon hamiltonian cannot be generally separated as the sum of two terms as $\hat{H} = \hat{H}_0 + \hat{V}$. For this particular system, the photon hamiltonian can be expressed:

$$\hat{H} = \frac{1}{n(x)}\left(n_0 \hat{H}_0 + \nu(x)\hat{N}\right), \tag{5.33}$$

where $\nu(x) = -\partial_x \ln \sqrt{n(x)}$ and $\hat{N}$ is the following matrix operator:

$$\hat{N} = \begin{pmatrix} 0 & 0 & 0 & 0 & 0 & 0 \\ 0 & 0 & -1 & 0 & 0 & 0 \\ 0 & 1 & 0 & 0 & 0 & 0 \\ 0 & 0 & 0 & 0 & 0 & 0 \\ 0 & 0 & 0 & 0 & 0 & 1 \\ 0 & 0 & 0 & 0 & -1 & 0 \end{pmatrix}. \tag{5.34}$$

However, if we now expand the inverse of the refractive index function, $n^{-1}(x) = [n_0 + e(x)]^{-1}$ in Taylor series, at first order we have that $n^{-1}(x) \sim n_0^{-1}[1 - e(x)/n_0]$. Also, if employ that $[n_0 - e(x)]\nu(x) \sim -\partial_x e(x)/2$, the operator in Eq. (5.33) splits and we are left with the following expression of the perturbation term:

$$\hat{V}_n = -\frac{1}{n_0^2} \begin{pmatrix} 0 & 0 & ik_t e(x) & 0 & 0 & 0 \\ 0 & 0 & -\delta_x & 0 & 0 & 0 \\ -ik_t e(x) & \delta_x & 0 & 0 & 0 & 0 \\ 0 & 0 & 0 & 0 & 0 & -ik_t e(x) \\ 0 & 0 & 0 & 0 & 0 & \delta_x \\ 0 & 0 & 0 & ik_t e(x) & -\delta_x & 0 \end{pmatrix}. \tag{5.35}$$

We have defined the differential operator $\delta_x = \sqrt{e(x)}\partial_x[\sqrt{e(x)}\ \cdot\ ]$, which acts as: $\delta_x e^{\pm ik_x x} = [E(x) \pm ik_x e(x)]e^{\pm ik_x x}$, over the one dimensional complex exponential, with $E(x) = \partial_x e(x)/2$.

5.2.2 *Approximate perturbed solutions*

With the exact solutions to the unperturbed system given in Eqs. (5.28)-(5.31) and the perturbation term $\hat{V} = \hat{V}_Z + \hat{V}_n$ specified by Eq. (5.32) and Eq. (5.35), we can already apply standard time-independent perturbation theory. At this point, we should take into account that the solutions to the unperturbed system are all degenerate, i.e. they share the same hamiltonian eigenvalue ω. This implies that, to find the approximate solutions to our problem, we must employ degenerate perturbation theory. Technical details of how to apply degenerate perturbation theory can be found in standard textbooks [71–73]. In the case of 4-fold degeneracy, the solution to the perturbed system is given in terms of a square 4×4 matrix, P, whose elements are computed as:

$$P_{ij} = \int_{-\infty}^{+\infty} dx\ \mathbf{\Phi}_i^*(x) \cdot \left[\hat{V}\ \mathbf{\Phi}_j(x)\right], \tag{5.36}$$

where $\mathbf{\Phi}_k(x)$ are the exact solutions to the unperturbed system given in Eqs. (5.28)-(5.31). Once the matrix P is computed, its eigenvectors are the approximate solutions to the perturbed system and its eigenvalues are associated with the frequency corrections. More specifically, the computation of the integrals specified by Eq. (5.36) results

in the matrix equation $P\mathbf{K} = \frac{\Delta\omega}{\omega}\mathbf{K}$, where $\mathbf{K} = (K_1, K_2, K_3, K_4)^\intercal$ are the coefficients of the perturbed solutions in the unperturbed state basis. In other words, any solution of the perturbed system can be expressed as $\mathbf{\Phi}^{(0)}(x) = \sum_i K_i \mathbf{\Phi}_i(x)$. And, $\Delta\omega$ represents the first order correction to the frequency such that the frequencies of the perturbed states are determined as $\omega^{(1)} = \omega + \Delta\omega$.

In our case, the perturbed solutions and energies are obtained from the following eigensystem:

$$\begin{pmatrix} \mathbb{D} & \mathbb{F} & \mathbb{C} & 0 \\ \mathbb{F}^* & \mathbb{D} & 0 & \mathbb{C}^* \\ \mathbb{C}^* & 0 & -\mathbb{D} & -\mathbb{F} \\ 0 & \mathbb{C} & -\mathbb{F}^* & -\mathbb{D} \end{pmatrix} \begin{pmatrix} K_1 \\ K_2 \\ K_3 \\ K_4 \end{pmatrix} = \frac{\Delta\omega}{\omega} \begin{pmatrix} K_1 \\ K_2 \\ K_3 \\ K_4 \end{pmatrix}. \tag{5.37}$$

In the expression above, it is important to note that K_1 and K_2 represent the amplitudes of positive helicity modes, whereas K_3 and K_4 represent the amplitudes of negative helicity modes. On the other hand, the matrix elements are:

$$\mathbb{C} = \frac{ik_x}{\omega n_0^2} \frac{1}{2Z_0} \int_{-\infty}^{\infty} dx\, \partial_x d(x) \tag{5.38}$$

$$\mathbb{D} = -\frac{\omega}{n_0} \int_{-\infty}^{\infty} dx\, e(x) \tag{5.39}$$

$$\mathbb{F} = -\frac{k_t^2}{\omega n_0^3} \int_{-\infty}^{\infty} dx\, e(x) e^{2ik_x x}. \tag{5.40}$$

To keep the matrix P hermitian and, thus, have real corrections to the frequency we have considered that $n(x)$ and $Z(x)$ are real functions and, also, that $\lim_{x\to\infty} e(x) = \lim_{x\to-\infty} e(x)$. Note that parameter $\mathbb{C}$ captures the effect of the inhomogeneities in the impedance, i.e. $\mathbb{C}$ vanishes whenever $\partial_x Z(x) = 0$. On the other hand, $\mathbb{D}$ and $\mathbb{F}$ capture the effect of the inhomogeneities in the refractive index, i.e. $\mathbb{D}$ and $\mathbb{F}$ are zero whenever $\partial_x n(x) = 0$. Finally, the expressions of the four energy corrections are $\Delta\omega = \pm\omega[\sqrt{\mathbb{D}^2 + \mathbb{C}^2} \pm |\mathbb{F}|]$.

Even if the matrix P specified in Eq. (5.37) contains all the information of the perturbed system, much more insight is obtained if we write it in a different basis. This is equivalent to choosing a different set of solutions of the unperturbed system instead of the one given in (5.28)-(5.31). As all four states are degenerate, we may choose any linear combination to express the matrix P. In particular, we may express it in the basis which diagonalizes its upper-left and bottom-right 2×2 blocks:

$$\begin{pmatrix} K_1 \\ K_2 \\ K_3 \\ K_4 \end{pmatrix} = \begin{pmatrix} \sqrt{\mathbb{F}} & -\sqrt{\mathbb{F}} & 0 & 0 \\ \sqrt{\mathbb{F}^*} & \sqrt{\mathbb{F}^*} & 0 & 0 \\ 0 & 0 & \sqrt{\mathbb{F}} & -\sqrt{\mathbb{F}} \\ 0 & 0 & \sqrt{\mathbb{F}^*} & \sqrt{\mathbb{F}^*} \end{pmatrix} \begin{pmatrix} K_1' \\ K_2' \\ K_3' \\ K_4' \end{pmatrix}. \tag{5.41}$$

In the new basis, K_1' and K_2' still represent positive helicity components and the negative helicity components are also associated with

K_3' and K_4'. By doing so we arrive to a very suggestive form of the equations. Indeed, in the primed basis, the eigensystem reads as:

$$\begin{pmatrix} \mathbb{D}+|\mathbb{F}| & \mathbb{C}^* & 0 & 0 \\ \mathbb{C} & -(\mathbb{D}-|\mathbb{F}|) & 0 & 0 \\ 0 & 0 & \mathbb{D}-|\mathbb{F}| & \mathbb{C}^* \\ 0 & 0 & \mathbb{C} & -(\mathbb{D}+|\mathbb{F}|) \end{pmatrix} \begin{pmatrix} K_1' \\ K_4' \\ K_2' \\ K_3' \end{pmatrix} = \frac{\Delta\omega}{\omega} \begin{pmatrix} K_1' \\ K_4' \\ K_2' \\ K_3' \end{pmatrix}. \tag{5.42}$$

Note that K_j' amplitudes are reordered in this last expression.

Given the matrix in Eq. (5.42), we can straightforwardly analyze the effect of both matching conditions in 1D inhomogeneous systems. First of all, it is clear that for an arbitrary perturbation in the (Z, n) parameter space, the whole system can be split into two independent subsystems: one concerning K_1' and K_4' and the other one K_2' and K_3'. Indeed, the matrix equation given by Eq. (5.42) can be understood as a simplified version of the general expression of the photon hamiltonian given by Eq. (5.6). The matrix components in Eq. (5.42) are now complex numbers, which takes the previous analogy with quantum two-level systems even closer. In particular, the case of impedance matching ($\mathbb{C} = 0$) implies, in this formalism, that the levels are decoupled and, thus, there is no mixing between the helicities. This can be inferred from the fact that, in this case, the anti-diagonal terms of both subsystems vanish. In addition to this, the form of the matrix in Eq. (5.42) makes the interpretation of the refractive index matching ($\mathbb{F} = \mathbb{D} = 0$) much more clear. As it can be checked, this matching condition makes the diagonal terms of each subsystem to be equal, while still keeping a non-zero coupling term. Such a situation is commonly denoted as *quantum resonance* in the language of two-level systems.

5.2.3 *Resonant helicity mixing and avoided crossing*

In the previous Subsection we have seen that perturbation theory facilitates an interpretation of the matching conditions through an analogy with quantum two-level systems. In particular, in this formalism, the impedance matching condition leads to the decoupling of the levels, whereas the refractive index matching condition leads to a situation analogous to quantum resonance. Let us now show an example and discuss this in detail.

In Fig. 5.4 we have numerically computed a particular case of a one-dimensional inhomogeneous system. We have considered that the inhomogeneities are determined by the functions $d(x) = \alpha/[1 + \exp(x/\ell)]$ and $e(x) = -\beta \exp(-x^2/\ell^2)$ (see Fig. 5.4a). The amplitude of the perturbation in the impedance is determined by the parameter α and in the refractive index by β. Note that whenever $\alpha = 0$ or $\beta = 0$ the impedance or refractive index matching condition is fulfilled, respectively. To meet the requirements imposed by perturbation theory we have chosen $\alpha = 0.01 \ll Z_0$ and $|\beta| \leqslant 0.01 \ll n_0$. In Fig. 5.4b we have computed the corrections to the frequency as a

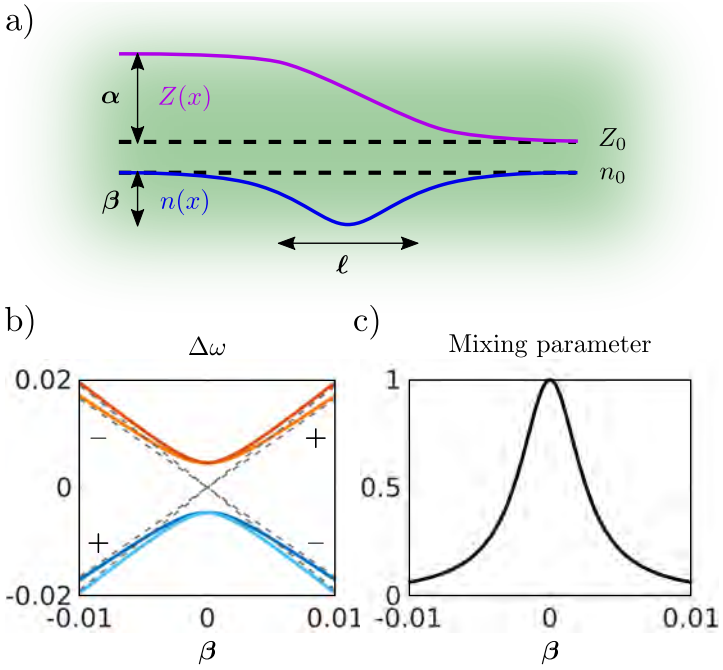

Figure 5.4: a) Sketch of an inhomogeneous medium with $Z(x) = Z_0 + d(x)$ and $n(x) = n_0 + e(x)$, with the functions $d(x) = \alpha/[1+\exp(x/\ell)]$ and $e(x) = -\beta \exp(-x^2/\ell^2)$. b) First order frequency corrections: $Z_0 = n_0 = 1$, $\omega = 1$, $k_t = 0.4$, $\ell = 1$ and $\alpha = 0.01$ (in colors). All units are normalized to an arbitrary frequency ω_0 and $c = 1$. The grey dashed lines are obtained with the same parameters but fixing $\alpha = 0$, which implies that $\mathbb{C} = 0$ in this case. c) Mixing parameter of the analogous two-level systems [72]: $4|W_{12}|^2/[4|W_{12}|^2 + (E_1 - E_2)^2]$. Here, $W_{12} = \mathbb{C}$, $E_1 = \mathbb{D} + |\mathbb{F}|$ and $E_2 = -(\mathbb{D} - |\mathbb{F}|)$. Whenever $\beta = 0$, the refractive index matching condition is fulfilled. Figure adapted from Contribution IV.

function of β (in colors). For comparison, in the same figure, we also display the frequency corrections for the case in which $\alpha = 0$ (grey dashed lines). Whenever $\alpha = 0$ we have that $\mathbb{C} = 0$ and, thus, the helicity components are decoupled in this case. In addition, from the form of the matrix in Eq. (5.42) it can be checked that the ascending (descending) diagonal grey lines in Fig. 5.4b correspond to solutions with well-defined positive (negative) helicity. Finally, in Fig. 5.4c, we have computed the mixing parameter of the two subsystems identified in Eq. (5.42) for the case $\alpha = 0.01$. Among others, this parameter has been employed to study the resonant mixing of neutrino flavours in matter [74, 75] and it is a signature of quantum resonance when it approaches unity [72].

The results are completely compatible with the phenomenon of the avoided level-crossing. Indeed, as we see from Fig. 5.4b levels cross in the absence of perturbation, i.e. whenever $\alpha = \beta = 0$. We certainly expect this from the fact that the unperturbed states given by Eq. (5.28)-(5.31) are all degenerate. Now, if we turn on a perturbation which does not couple the levels (we take $\beta \neq 0$ while keeping $\alpha = 0$), we see that frequency corrections are linear with respect to the perturbation parameter β (dashed grey lines). This behaviour is

analogous to how the perturbed energies depend on the initial energies on a decoupled two-level system [72]. In addition to this, the analogy also holds whenever we switch on the coupling term, i.e. whenever $\alpha \neq 0$. In this case, the crossing of levels at $\beta = 0$ is avoided (in colours). On the other hand, in this situation, the perturbed energies are analytically computed as $\omega^{(1)} = \omega \pm \omega|\mathbb{C}|$, which is the exact mathematical form that energies take in a resonant two-level system. Finally, whenever $\beta = 0$ and $\alpha \neq 0$, perturbed states can be written as linear superpositions of the unperturbed states with amplitudes of the same modulus, which is also a key characteristic of the systems undergoing quantum resonance [72].

Summing up, with this extensive discussion based on perturbation theory, we have been able to study the particularities of the impedance and refractive index matching conditions. The analysis has been particularly fruitful to characterize the dynamics of electromagnetic waves propagating through media in which the refractive index is matched. Our results indicate that this type of media induce a resonant helicity mixing on the electromagnetic waves that propagate through them. Strikingly and completely unexpectedly, we have identified that the refractive index matching condition leads to the phenomenon of avoided level-crossing. A great deal of phenomena in physics are related to the avoided crossing of energy levels, but this is the first time that such a connection is reported for the helicity components of electromagnetic fields.

5.3 CONSERVED QUANTITIES

The results of the previous Section confirm that both the impedance and refractive index matching conditions have profound physical consequences over Maxwell's equations, as initially suggested by the photon hamiltonian given by Eq. (5.6). However, there is an important aspect of these conditions which we have not discussed yet in detail: conserved quantities. An astute reader may have noticed that, at least, the impedance matching condition seems to imply the conservation of the electromagnetic helicity, $\hat{\Lambda}$. Indeed, this is correct. In what follows, we show that both matching conditions lead to the conservation of a physical magnitude.

The discussion of the conserved physical magnitudes is frequently considered in the framework of generators of continuous groups. In other words, conserved quantities have usually been associated with the restoration of a symmetry through Noether's theorem. However, from the discussion in Chapter 3, we know that conserved quantities are not only linked to the generators of continuous groups. For instance, the rest mass M or the spin S are preserved magnitudes in the context of relativistic massive particles, but they are not related to any particular generator of the Poincaré group. They are preserved because they are the eigenvalues of two Casimir operators of the group, i.e. $\hat{C}_1$ and $\hat{C}_2$. This implies that, the association between conserved magnitudes and symmetries is not perfectly bidirectional. Given a

symmetry of a problem it is quite straightforward to associate it with a conserved quantity, but not the other way around. That is, given a conserved physical magnitude, in principle, it may not be so direct to link it with a particular generator or Casimir invariant of a specific group. As a matter of fact, this is exactly what happened with the mass of the particles, which has longly been known to be a preserved magnitude in free space. However, its identification as a Casimir invariant of the Poincaré group was not put forward until the middle of the 20^{th} century.

In this Section, we first analyze the symmetries of piecewise homogeneous media, which are the environments in which we are going to discuss the emergence of conserved quantities. Then we identify helicity, $\hat{\Lambda}$, and square of linear momentum, $\hat{\mathbf{P}}^2$, as the magnitudes which are preserved under the impedance and refractive index matching conditions, respectively. As we show, the conservation of $\hat{\Lambda}$ and $\hat{\mathbf{P}}^2$ naturally relates to their condition of Casimir operators of $P_{3,1}$ subgroup. Finally, based on these considerations, we propose a general interpretation of the emergence of the Kerker effects. The results are adapted from Contribution VII.

5.3.1 *Symmetries of piecewise homogeneous media*

Before going on, let us center the discussion of the conserved quantities on a specific type of inhomogeneous medium, i.e. those which are piecewise homogeneous. By a piecewise homogeneous medium, we refer to an inhomogeneous medium which can be split in volumes, V_j, which are, themselves, homogeneous. This type of environments is characterized for having a local electric permittivity and magnetic permeability defined in terms of steplike functions, i.e. $\varepsilon(\mathbf{r}) = \varepsilon_j$ and $\mu(\mathbf{r}) = \mu_j$ for $\mathbf{r} \in V_j$. Consequently, in a piecewise medium, the impedance and the refractive index are defined as: $Z(\mathbf{r}) = \sqrt{\mu_j/\varepsilon_j}$ and $n(\mathbf{r}) = \sqrt{\varepsilon_j \mu_j}$ for $\mathbf{r} \in V_j$. Importantly, the domains V_j can be of arbitrary shape and size, which makes our discussion quite general. Also, note that solutions to Maxwell's equations in this type of media are constructed by finding a solution to the equations in each homogeneous domain and, then, applying boundary conditions. This implies that, exactly as we argued in Chapter 4, solutions may be asked to fulfill Eqs. (3.20)-(3.22) in each region V_j.

In static piecewise homogeneous media there is only one symmetry left, i.e. the one parameter subgroup of time translations, T. Thus, only a few things can be generally stated about the solutions in this type of media, i.e. that frequency, ω, is conserved and that the electromagnetic wave solutions are eigenstates of $\hat{P}_0$. For completeness, and following the discussion of Chapter 3, the UIRs of the time translations group can be labelled as (see Ref. [19], Chapter 6, Section 6):

$$\hat{P}_0 \boldsymbol{\psi}(\mathbf{r}, t) = \omega \boldsymbol{\psi}(\mathbf{r}, t), \tag{5.43}$$

where $\boldsymbol{\psi}(\mathbf{r}, t)$ represents any electromagnetic wave solution in a piecewise homogeneous medium. In practice, the condition above simply

implies that the time dependence of the solutions is fixed and it is given by a complex exponential. On the contrary, the spatial functional form of the solutions will strongly depend on the specific symmetries of the particular system one may consider. The generators and Casimir invariants of the subgroups of $E(3)$ associated with the different piecewise media are not the same and, thus, the bases of the invariant vector spaces will be required to be eigenfunctions of different operators [48]. As a result, conserved quantities strongly depend on the geometry of each particular problem.

In plain words, in piecewise homogeneous media, one only expects $\hat{P}_0$ to be generally conserved. And, then, depending on the particular geometry of each problem other conserved quantities may emerge. For instance, in Fresnel's scattering problem, apart from $\hat{P}_0$, we have that two components of the linear momentum, $\hat{P}_x$ and $\hat{P}_y$, are also preserved, due to the translational symmetries in the directions parallel to the interface. Also, $\hat{J}_z$ is preserved due to rotational symmetries in the direction orthogonal to the interface. On the other hand, in Mie's scattering problem, all three components of total angular momentum, $\hat{J}_i$, and the modulus squared, $\hat{\mathbf{J}}^2$, are conserved. The first three magnitudes are conserved due to their condition of generators, whereas the conservation of the last magnitude can be associated with its condition of Casimir invariant in rotationally symmetric problems. We conclude that, apart from $\hat{P}_0$, conserved quantities strongly depend on the particular geometries. This is the context in which the peculiarities of the impedance and refractive index matching conditions can be better understood.

5.3.2 *Helicity and square of linear momentum*

In piecewise homogeneous media, the matching conditions can be expressed in terms of the values of the electric permittivity and magnetic permeability in each of the regions. We say that the impedance matching condition, $\nabla Z = 0$, is fulfilled in a piecewise homogeneous medium when the ratio μ_j/ε_j is constant in all domains V_j. On the other hand, the refractive index matching condition, $\nabla n = 0$ is fulfilled whenever the product $\varepsilon_j \mu_j$ is constant in all domains V_j.

In this line, Fernandez-Corbaton and coworkers indicated that the impedance matching condition leads to the conservation of electromagnetic helicity [61]. It was shown that, whenever μ_j/ε_j is constant, Maxwell's equations in the whole piecewise medium remain invariant under electromagnetic duality transformations. As helicity had previously been identified as the generator of the duality transformation [76], it was then concluded that helicity had to be preserved in an impedance-matched piecewise homogeneous medium. However, there is also a dynamical way of understanding the conservation of helicity in impedance-matched media. Indeed, given the form of Maxwell's equations specified in Eqs. (5.1)-(5.2), it can be checked that the impedance matching condition makes the two helicity components of the electromagnetic field to be decoupled. This implies

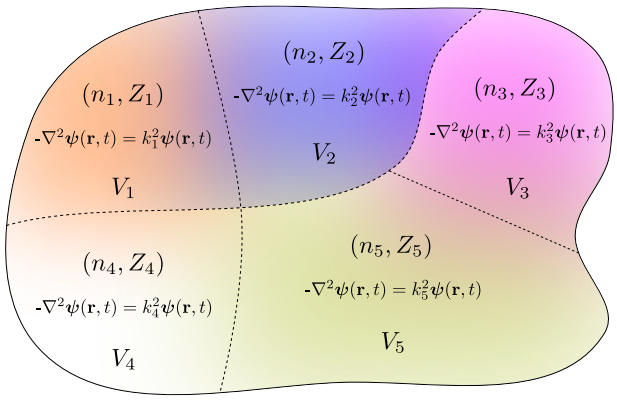

Figure 5.5: Sketch of a piecewise homogeneous medium. Electromagnetic wave solutions are obtained by solving Helmholtz's equation and applying boundary conditions in the interfaces.

that, if we fix the initial conditions at time $t = 0$ to contain a single helicity component, the solutions in an impedance-matched piecewise medium will have a single helicity component at times $t > 0$. In this line, any electromagnetic wave solution under the impedance matching condition, $\boldsymbol{\psi}_\lambda(\mathbf{r}, t)$, fulfills: $\hat{\Lambda}\boldsymbol{\psi}_\lambda(\mathbf{r}, t) = \lambda\boldsymbol{\psi}_\lambda(\mathbf{r}, t)$, with $\lambda = \pm 1$. As a result, in piecewise media, we can also infer the conservation of helicity from the fact that eigenstates of $\hat{\Lambda}$, acting as the Casimir operator given by Eq. (3.21), remain being eigenstates of $\hat{\Lambda}$.

In this sense, the helicity operator has a double role. On the one hand, it is the generator of dual transformations, but as seen in Eq. (3.21), it also acts as a Casimir operator. This could raise the question of whether Casimir operators are of some interest to study electromagnetic wave dynamics in piecewise homogeneous media. We will show now that, in the case of index-matched piecewise media, the conserved quantity is not associated with the generator of a continuous symmetry transformation, but with another Casimir operator: the square of linear momentum, $\hat{\mathbf{P}}^2$.

Under the refractive index matching condition, the conservation of a physical magnitude can be inferred from how electromagnetic wave solutions are built in piecewise media. Indeed, as it is shown in Fig. 5.5, solutions of electromagnetic waves propagating in this type of environments are constructed by solving Helmholtz's equation in each domain V_j and, then, applying boundary conditions. This implies that, in a generic piecewise homogeneous medium, electromagnetic wave solutions fulfill, $-\nabla^2\boldsymbol{\psi}(\mathbf{r}, t) = k_j^2\boldsymbol{\psi}(\mathbf{r}, t)$ for $\mathbf{r} \in V_j$, where $k_j = \omega n_j$. Note that, for a generic piecewise homogeneous medium, k_j changes depending on the region of space we may consider. Thus, the eigenvalue of $\hat{\mathbf{P}}^2 = -\nabla^2$ operator varies from one region V_j to another $V_{j'}$, as long as $n_j \neq n_{j'}$. However, whenever the refractive index matching condition is fulfilled ($n_j = n_{j'}$, $\forall j, j'$), the wavevector modulus is constant all over the medium and the square of linear momentum operator fulfills: $\hat{\mathbf{P}}^2\boldsymbol{\psi}_k(\mathbf{r}, t) = k^2\boldsymbol{\psi}_k(\mathbf{r}, t)$, where now k is fixed and $\boldsymbol{\psi}_k(\mathbf{r}, t)$ represents any electromagnetic wave solution in an index-matched piecewise medium. Note that this way of representing the conservation of the square of linear momentum is exactly the

same as in Eq. (3.22). The refractive index matching condition recovers that same relation, but in piecewise environments.

Following the previous discussion on helicity conservation, we may try to link the conservation of $\hat{\mathbf{P}}^2$ with the restoration of a symmetry. This, however, is not possible because the square of linear momentum is not a generator of any continuous symmetry transformation. Therefore, we are led to comprehend the conservation of $\hat{\mathbf{P}}^2$ from its condition of Casimir invariant. Indeed, Casimir operators of a group G may remain as conserved quantities in environments whose symmetry group is a subgroup $G_i \subset G$ [77]. This phenomenon is not a particularity of electromagnetic waves, it is known to occur also in the dynamics of massive particles. Let us put forward an example which very closely mimics the refractive index matching condition for electromagnetic waves. As we have shown in Section 3, the conservation of $\hat{\mathbf{P}}^2$ for non-relativistic massive particles can also be related to the symmetries of Euclidean space [49]. Thus, in principle, we may expect the square of linear momentum to be exclusively preserved when massive particles propagate in free space. This, however, is not true. There is a particular interaction potential (or environment), i.e. the hard sphere potential, for which $\hat{\mathbf{P}}^2$ is a conserved quantity. The same also holds for classical mechanics, where the kinetic energy, proportional to the square of the linear momentum, is known to be preserved provided that the interactions are elastic. To the best of our knowledge, the conservation of kinetic energy in elastic collisions has not been linked, through Noether's theorem, with the restoration of any continuous symmetry.

There are more cases in which a Casimir invariant of a group G is preserved in an environment whose symmetry group is a subgroup G_i. A well-known example is the conservation of mass, M, and spin, S. As we have shown in Section 3, the conservation of these magnitudes can be concluded from their condition of Casimir invariants of the Poincaré group. This, in principle, would imply that M and S are exclusively preserved for massive particles propagating in vacuum. We know, however, that these magnitudes are preserved in a great deal of problems for which the symmetry group is a subgroup of the Poincaré group. For instance, there are many situations in which the mass and spin of the particles are preserved in the framework of non-relativistic quantum scattering theory. Indeed, mass is quite generally assumed to be conserved in this context, whereas spin may not be conserved only in particular cases such as spin-orbit or nucleon-nucleon interactions [78]. All these examples point in the direction that the conservation of certain physical magnitudes cannot be related with the restoration of a continuous symmetry, but to their condition of Casimir invariants.

5.3.3 *Origin of the Kerker phenomena*

Finally, let us apply the previous analysis to a case of special significance, i.e. the emergence of the Kerker effects in magnetic spheres.

As we show, the origin of these unusual effects can be explained in terms of $\hat{P}_0$, $\hat{\Lambda}$ and $\hat{\mathbf{P}}^2$, i.e. the Casimir operators of $P_{3,1}$ subgroup.

In Fig. 5.6, we show the analysis of conserved quantities associated with the helicity map previously discussed in Section 5.1. Let us briefly remind that $\langle\Lambda\rangle$ represents the helicity expectation value, which is an observable that determines whether electromagnetic helicity of the incident wave is conserved, $\langle\Lambda\rangle = 1$, or completely flipped, $\langle\Lambda\rangle = -1$, upon scattering [59]. Along the vertical axis we tune the impedance contrast, s, which is the ratio between the impedances of the sphere and the surrounding medium. In the horizontal axis, we fix the refractive index contrast, m, which is the ratio between the refractive indices. Due to the static nature of the media involved, all the solutions represented in the figure are constructed as eigenstates of the generator of time-translations, $\hat{P}_0$. Then, under the duality condition, along the line $s = 1$, helicity is conserved and, thus, solutions are eigenstates of $\hat{\Lambda}$. In addition to this, under the resonant helicity mixing condition, whenever $m = 1$, the square of linear momentum is conserved and, as a result, the solutions are eigenstates of $\hat{\mathbf{P}}^2$ operator. The line $s = 1/m$ indicates the response of dielectric materials. Finally, note that in the singular point $[m, s] = [1, 1]$ of the colormap solutions are eigenstates of all three operators $\hat{P}_0$, $\hat{\Lambda}$ and $\hat{\mathbf{P}}^2$. This is

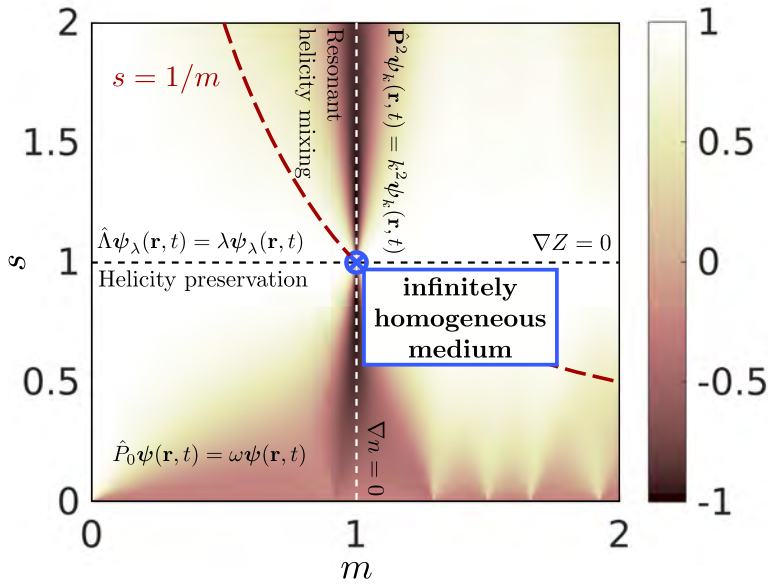

Figure 5.6: Emergence of the duality and resonant helicity mixing conditions in a magnetic sphere embedded in a homogeneous surrounding. The helicity expectation value, $\langle\Lambda\rangle$, quantifies the helicity of the scattered electromagnetic field. s is the impedance contrast and m the refractive index contrast. Frequency, ω, is preserved at every point due to the static nature of the piecewise system. Helicity, is preserved whenever the impedance is constant (horizontal dashed line). Square of linear momentum, is conserved whenever the refractive index is constant (vertical dashed line). The singular point $[m, s] = [1, 1]$ represents an infinitely homogeneous medium. Figure adapted from Contribution VII.

because the particular case $m = s = 1$, represents an infinitely homogeneous medium and, by means of Eqs. (3.20)-(3.22), monochromatic electromagnetic wave solutions are built as eigenstates of the three Casimir operators of $P_{3,1}$ group.

This phenomena can also be interpreted making use of the photon hamiltonian given by Eq. (5.6). Indeed, under both matching conditions, i.e. $\nabla Z = 0$ and $\nabla n = 0$, the environment ceases to be inhomogeneous and it becomes infinitely homogeneous. In this situation, the photon hamiltonian converges to the analytical form of Maxwell's equations as expressed in Eq. (3.21), i.e. electromagnetic wave solutions are constructed as eigenstates of $\hat{P}_0$, $\hat{\Lambda}$ and $\hat{\mathbf{P}}^2$ operators. This situation is equivalent to the dynamics represented by $[m, s] = [1, 1]$ point in Fig. 5.6. Then, it is clear that the photon hamiltonian indicates two preferential directions in which the homogeneity of space may be broken. These two preferential directions are associated with the impedance and index matching conditions. On the one hand, homogeneity of space may be broken while still keeping the impedance constant. In piecewise media, this leads to the conservation of both $\hat{P}_0$ and $\hat{\Lambda}$ and the situation is equivalent to the $s = 1$ line in Fig. 5.6. On the other hand, homogeneity of space may also be broken while keeping the refractive index constant. In piecewise media, this leads to the conservation of $\hat{P}_0$ and $\hat{\mathbf{P}}^2$ and the situation is equivalent to the $m = 1$ line in Fig. 5.6.

In our view, this analysis provides a harmonic interpretation of time-independent Maxwell's equations in inhomogeneous media as expressed in Eqs. (5.1)-(5.4). Such a particular form of Maxwell's equations is simply obtained through a change of basis. Indeed, instead of the usual electric, $\mathbf{E}(\mathbf{r})$, and magnetic, $\mathbf{H}(\mathbf{r})$, fields we rewrite the equations in terms of the monochromatic RS vector, $\mathbf{F}^{\lambda}(\mathbf{r})$, which has previously been shown to be linked with $P_{3,1}$ subgroup of the Poincaré group. As a result, we obtain a completely equivalent form of Maxwell's equations in which instead of the usual material parameters, derivatives of the local impedance and refractive index appear. Finally, as we have just discussed, we find that this new material parameters are closely related with the Casimir invariants of $P_{3,1}$. It really seems like the connection of Maxwell's equations with spacetime symmetries is clarified when expressing them in terms of the RS vector. In this line, the phenomena reported by Kerker, Wang and Giles in 1983 [70] can be interpreted as the materialization of this fundamental connection in a particular electromagnetic scattering problem.

5.4 SUMMARY

In Section 5.1, we have first introduced Maxwell's equations in inhomogeneous media in terms of the monochromatic RS vector. Based on this form of Maxwell's equations we have analyzed the impedance and refractive index matching conditions, showing that they have relevant consequences over both Fresnel and Mie coefficients. Then,

in Section 5.2, we have characterized the matching conditions with the aid of time-independent perturbation theory. We have concluded that they can be interpreted in close analogy with the dynamics of quantum two-level systems. In particular, we have understood the impedance matching as the condition which decouples the levels, whereas the index matching conditions leads to the phenomenon of avoided crossing. Finally, in Section 5.3, we have studied the conserved quantities associated with both matching conditions. We have concluded that helicity, $\hat{\Lambda}$, is conserved under the impedance matching condition and the square of linear momentum, $\hat{\mathbf{P}}^2$, is conserved under the refractive index matching condition. As a conclusion, we have linked the condition of Casimir invariants of these magnitudes with the emergence of the Kerker effects in magnetic spheres.

6

SYMMETRIES IN QUANTUM SCATTERING THEORY

In this Chapter, we introduce the second quantized form of the electromagnetic field. Based on this, we discuss the input-output description of quantum scattering theory and the construction of the scattering matrix. Then, we analyze the scattering of photon states by cylindrically symmetric samples. Due to the symmetry of the problem, we choose Bessel modes as input states and construct the post-selected scattering matrix associated with this type of structures. Finally, we show that there are certain input states which are preserved in the interaction with *all* cylindrical samples. This kind of states, denoted as symmetry-protected states, are found both in the form of single photon and multi photon states.

Derivations within Sections 6.2 and 6.3 have been adapted from Contribution I.

6.1 QUANTUM ELECTROMAGNETIC SCATTERING THEORY

In the previous Chapters we have studied the scattering and propagation of electromagnetic waves in different environments. We have analyzed some of the properties of light such as helicity, angular momentum, linear momentum and so on. In this line, we have shown that the use of the RS vector facilitates the study of many relevant physical phenomena and, in particular, those associated with the helicity of the electromagnetic field. So far, all the analysis has been developed within the framework of electromagnetic waves, i.e. considering that the field has a continuous energy spectrum. In this Chapter, we show that many of the previously discussed concepts can also be applied in the framework of quantum electrodynamics. We focus on the topic of scattering of photon states by linear optical samples, which can be regarded as the quantum version of the scattering theory discussed in Chapter 4.

In this Section, we formally introduce the second quantization of the electromagnetic field and its fundamental excitation: the photon. As we show, this formulation of electromagnetism allows to study the scattering of non-classical states of light by linear optical samples. For that aim, we first discuss a paradigmatic linear electromagnetic scattering problem: a beam splitter. We see that the quantization of the action of this optical device can be carried out within the input-output formalism, just by substituting the electric field amplitudes with the corresponding annihilation operators. Based on this, we quantize the action of a generic linear scatterer, leading to a quantum version of the scattering theory discussed in Chapter 4. Such a procedure naturally results in the construction of the scattering matrix which contains all the information of the dynamics of the system.

6.1.1 *Quantization of the electromagnetic field*

The quantization of the electromagnetic field is usually carried out by expressing the energy of the electromagnetic field in free space in canonical variables. We start by considering the field of a circularly-polarized monochromatic plane-wave propagating in free space:

$$\mathbf{E}(\mathbf{r}) = E_0 \hat{e}^{\lambda}(\tilde{\theta}, \tilde{\phi}) e^{i\mathbf{k}\cdot\mathbf{r}} \tag{6.1}$$

$$iZ\mathbf{H}(\mathbf{r}) = \frac{1}{k}\nabla \times \mathbf{E}(\mathbf{r}), \tag{6.2}$$

where E_0 is a complex amplitude, whereas $\hat{e}^{\lambda}(\tilde{\theta}, \tilde{\phi})$ is a circular polarization vector orthogonal to the wavevector, $\mathbf{k}$. Note that other types of monochromatic electromagnetic wave solutions can be expressed as superpositions of circularly polarized plane-waves propagating in different directions (see Eq. (3.30)). The total energy, U, of such a field in a volume V can be obtained by integrating the local energy density:

$$U = \frac{1}{4}\int_V d\mathbf{r}\left(|\mathbf{E}(\mathbf{r})|^2 + |Z\mathbf{H}(\mathbf{r})|^2\right) = \frac{1}{2}V|E_0|^2. \tag{6.3}$$

Now, let us define the following magnitudes in terms of the complex amplitude E_0 [79, 80]:

$$q = \omega^{-1}\sqrt{V}\,\mathrm{Re}\,(E_0) \tag{6.4}$$

$$p = \sqrt{V}\,\mathrm{Im}\,(E_0)\,, \tag{6.5}$$

Note that, inverting the relations above, the amplitude of the electric field can be expressed as:

$$E_0 = \frac{1}{\sqrt{V}}\,(\omega q + ip)\,. \tag{6.6}$$

Finally, with the aid of the q and p variables, we can express the total energy U in the following particular form:

$$U = \frac{1}{2}\left(p^2 + \omega^2 q^2\right). \tag{6.7}$$

The expression given by Eq. (6.7) can be recognized as the energy of a harmonic oscillator expressed in terms of canonical variables. Thus, the quantization of the electromagnetic field can be carried out following the rules of quantization of a harmonic oscillator. The usual procedure to quantize the dynamics of a harmonic oscillator is to associate the classical variables, q and p, with operators, $\hat{q}$ and $\hat{p}$, such that they fulfill: $[\hat{q}, \hat{p}] = i\hbar$.[1] In this line, within second quantization, the operator form of the classical observables is simply obtained by expressing them in terms of the $\hat{q}$ and $\hat{p}$ operators, instead of the classical q and p variables. For instance, the energy operator is:

$$\hat{U} = \frac{1}{2}\left(\hat{p}^2 + \omega^2 \hat{q}^2\right), \tag{6.8}$$

whereas the complex electric and magnetic field operators are:

$$\hat{\mathbf{E}}(\mathbf{r}) = \frac{1}{\sqrt{V}}\,(\omega\hat{q} + i\hat{p})\,\hat{e}^{\lambda}(\tilde{\theta}, \tilde{\phi})e^{i\mathbf{k}\cdot\mathbf{r}} \tag{6.9}$$

$$iZ\hat{\mathbf{H}}(\mathbf{r}) = \frac{\lambda}{\sqrt{V}}\,(\omega\hat{q} + i\hat{p})\,\hat{e}^{\lambda}(\tilde{\theta}, \tilde{\phi})e^{i\mathbf{k}\cdot\mathbf{r}}. \tag{6.10}$$

The expressions given by Eq. (6.9) and (6.10) represent the second quantized versions of the electric and magnetic fields given by Eq. (6.1) and Eq. (6.2).

For many purposes, it is convenient to deal with a different set of operators, i.e. the creation and annihilation operators, which are defined as:

$$\hat{a} = \frac{1}{\sqrt{2\hbar\omega}}\,(\omega\hat{q} + i\hat{p}) \tag{6.11}$$

$$\hat{a}^{\dagger} = \frac{1}{\sqrt{2\hbar\omega}}\,(\omega\hat{q} - i\hat{p})\,, \tag{6.12}$$

and fulfill the commutation relation $[\hat{a}, \hat{a}^{\dagger}] = 1$. In terms of these operators, the energy operator is expressed as:

$$\hat{U} = \hbar\omega\left(\hat{a}^{\dagger}\hat{a} + \frac{1}{2}\right), \tag{6.13}$$

1 Note that, in natural units, $\hbar = 1$, however, for historical reasons, we keep the dependence on Planck's constant explicit during this Subsection.

whereas the second quantized electric and magnetic fields adopt the form:

$$\hat{\mathbf{E}}(\mathbf{r}) = \hat{a}\left[\sqrt{\frac{2\hbar\omega}{V}}\hat{e}^{\lambda}(\tilde{\theta},\tilde{\phi})e^{i\mathbf{k}\cdot\mathbf{r}}\right] \tag{6.14}$$

$$iZ\hat{\mathbf{H}}(\mathbf{r}) = \hat{a}\left[\lambda\sqrt{\frac{2\hbar\omega}{V}}\hat{e}^{\lambda}(\tilde{\theta},\tilde{\phi})e^{i\mathbf{k}\cdot\mathbf{r}}\right]. \tag{6.15}$$

This implies that both the complex electric and magnetic field operators are proportional to the annihilation operator, $\hat{a}$. Taking a look at the classical expression of the fields in Eqs. (6.1)-(6.2), we see that the role of the complex amplitude E_0, in the second quantized electromagnetic theory, is played by the $\hat{a}$ operator. As we show in the next Subsection, this correspondence is useful to translate well-known results of classical optics into quantum optics.

Finally, let us briefly discuss the eigenstates and spectrum of the energy operator. From Eq. (6.13) it is clear that the energy eigenstates are also eigenstates of the $\hat{a}^{\dagger}\hat{a}$ operator. We usually refer to this operator as the number operator, $\hat{N}$, and its eigenvalues, N, conform a discrete set $N \in (0, 1, 2...)$. The $\hat{N}$ operator takes count of the number of excitations of the electromagnetic field, which are most commonly regarded as photons. If we denote by $|N\rangle$ the eigenstates of the number operator, we have the following relations:

$$\hat{N}|N\rangle = N|N\rangle \tag{6.16}$$

$$\hat{a}|N\rangle = \sqrt{N}|N-1\rangle \tag{6.17}$$

$$\hat{a}^{\dagger}|N\rangle = \sqrt{N+1}|N+1\rangle. \tag{6.18}$$

Thus, we see that the action of the $\hat{a}$ and $\hat{a}^{\dagger}$ operators is to destroy and create an excitation of the electromagnetic field, respectively. The state for which the number of excitations is zero, $|0\rangle$, is known as the vacuum state. To conclude, note that the quantization of the electromagnetic field could have been done choosing different values of the wave vector, $\mathbf{k}$, and helicity, λ. Thus, to be more precise in the notation, we may represent the annihilation and creation operators defined in Eqs. (6.11)-(6.12) as $\hat{a}_{\mathbf{k},\lambda}$ and $\hat{a}^{\dagger}_{\mathbf{k},\lambda}$. In this line, the operators associated with other types of waves, such as Bessel beams or multipolar modes, can simply be expressed as linear combinations of these operators with different weights (see Eq. (3.30) in Chapter 3).

6.1.2 *Beam splitters and input-output formalism*

The second quantized form of the electromagnetic field can be applied to a wide variety of different physical phenomena. However, in this Chapter, we are interested in quantum scattering problems, i.e. situations in which a photon impinges on a sample and then it is scattered into a particular direction. Moreover, we strictly constrain to situations in which the scattering is linear. As we have discussed in Chapter 4, this means that the frequency of both the incident and scattered fields is fixed, but note that this has further effects in the

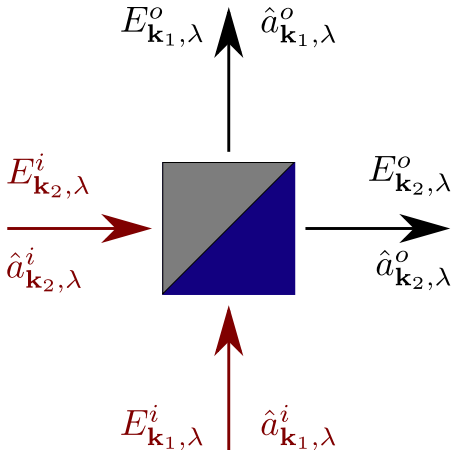

Figure 6.1: Sketch of a beam splitter, both in the classical and quantum pictures. $E^i_{\mathbf{k},\lambda}$ and $E^o_{\mathbf{k},\lambda}$ represent the electric field amplitudes in the input and output ports, respectively. In the quantum version of the beam splitter, the transformation is performed over the input, $\hat{a}^i_{\mathbf{k},\lambda}$, and output, $\hat{a}^o_{\mathbf{k},\lambda}$, annihilation operators.

quantum regime. Keeping the frequency of the fields fixed implies that the scattering occurs at the single photon level, i.e. if a single photon impinges on a sample, then, only a single photon may be scattered away. This can be understood from the energy conservation law and the operator in Eq. (6.13).

To fix ideas, let us discuss a system which can be regarded as the simplest non-trivial linear electromagnetic scattering problem: a beam splitter. This system will aid us to translate some of previously discussed classical results into the quantum regime. A sketch of the problem is depicted in Fig. 6.1. As it can be checked, a conventional beam splitter has two input ports and two output ports and, assuming that the device preserves the polarization state of light, the input and output ports represent exactly the same modes (monochromatic plane-waves propagating in a certain direction $\mathbf{k}_1$ or $\mathbf{k}_2$), but in different regions of the space. As a result, a beam splitter can be understood as a device which carries out a linear transformation over the input fields. Indeed, this can be explicitly checked from the classical solution to the problem [81]:

$$E^o_{\mathbf{k}_1,\lambda} = tE^i_{\mathbf{k}_1,\lambda} + rE^i_{\mathbf{k}_2,\lambda} \tag{6.19}$$

$$E^o_{\mathbf{k}_2,\lambda} = rE^i_{\mathbf{k}_1,\lambda} + tE^i_{\mathbf{k}_2,\lambda}, \tag{6.20}$$

where $E^i_{\mathbf{k},\lambda}$ represents the amplitude of the input electric field, $E^o_{\mathbf{k},\lambda}$ is the amplitude of the output electric field and $\{r, t\}$ are the complex reflection and transmission amplitude coefficients of the beam splitter.

The relations given by Eqs. (6.19)-(6.20) indicate that the amplitude of the electric field in the output ports is given as a linear superposition of the amplitudes in the input ports. Following the quantization procedure explained in the previous Subsection, this would indicate that the annihilation operators associated with such electric field amplitudes are related exactly in the same way. In other words, if we

would like to translate the classical results to the quantum regime, we would just need to consider the following transformation [82]:

$$\hat{a}^{o}_{\mathbf{k}_1,\lambda} = t\hat{a}^{i}_{\mathbf{k}_1,\lambda} + r\hat{a}^{i}_{\mathbf{k}_2,\lambda} \tag{6.21}$$

$$\hat{a}^{o}_{\mathbf{k}_2,\lambda} = r\hat{a}^{i}_{\mathbf{k}_1,\lambda} + t\hat{a}^{i}_{\mathbf{k}_2,\lambda}. \tag{6.22}$$

This indicates that a linear optical phenomena, such as the action of a beam splitter, can be translated to the quantum regime just as a linear transformation of the annihilation operators. As we have previously mentioned, this implies that the process occurs at the single photon level as the relations given by Eqs. (6.21)-(6.22) do not include quadratic terms of the annihilation operators. On the other hand, the input annihilation operators fulfill the commutation relations previously discussed, but, in principle, nothing ensures that the output annihilation operators also fulfill such commutation relations. It can be proved that the commutation relations of the output modes only hold provided that $|r|^2 + |t|^2 = 1$ and $rt^* + tr^* = 0$, which ensures the energy balance in the beam splitter [81].

In our view, the beam splitter problem clarifies the relation between classical and quantum fields, and permits us to elucidate the way in which other linear scattering problems may be quantized. Indeed, even if we have not discussed it in detail in Chapter 4, the relation between the scattered and incident field amplitudes is also linear in classical electromagnetic scattering theory [83, 84]. This implies that, for every linear scattering problem, we may build a relation analogous to that given by Eqs. (6.19)-(6.20), where the "input port" is now associated with the incident field and the "output port" with the scattered or total field. Following exactly the same procedure, we may substitute the electric field amplitudes of each mode by the corresponding annihilation operators. In this way, we may represent a generic quantum scattering problem just as a linear transformation that relates input and output annihilation operators.

6.1.3 *Scattering matrix*

In a linear electromagnetic scattering problem, the fields are not usually expressed in terms of plane-waves, but as a superposition of multipolar modes (see Eqs. (4.1) and (4.4) in Chapter 4). Moreover, due to the linearity of Maxwell's equations and boundary conditions, the relation between the incident (C^{e}_{jm} and C^{m}_{jm}) and scattered field (α_{jm} and β_{jm}) multipolar expansion coefficients can be expressed as [84]:

$$\alpha_{jm} = \sum_{JM} \left[\mathbb{T}^{ee}_{jmJM} C^{e}_{JM} + \mathbb{T}^{em}_{jmJM} C^{m}_{JM} \right] \tag{6.23}$$

$$\beta_{jm} = \sum_{JM} \left[\mathbb{T}^{me}_{jmJM} C^{e}_{JM} + \mathbb{T}^{mm}_{jmJM} C^{m}_{JM} \right], \tag{6.24}$$

where $\mathbb{T}^{ee}_{jmJM}$, $\mathbb{T}^{em}_{jmJM}$, $\mathbb{T}^{me}_{jmJM}$ and $\mathbb{T}^{mm}_{jmJM}$ are components of the so-called T matrix; also, the summations include the terms $J = 1, 2, 3, ...$ and $M = -J, -J+1, ..., J-1, J$.

Given the relations above, we could already consider the second quantized form of the scattered and incident electromagnetic field amplitudes. However, in line with the previous Chapters, we prefer to give a formulation of the quantum scattering problem based on the helicity components instead. This implies considering a linear combination of the incident and scattering expansion coefficients, as discussed in Chapter 4, which leads to the following quantum form of the scattering problem:

$$\hat{a}^{s}_{jm,+} = \sum_{JM} \left[\mathbb{T}^{++}_{jmJM} \hat{a}^{i}_{JM,+} + \mathbb{T}^{+-}_{jmJM} \hat{a}^{i}_{JM,-} \right] \tag{6.25}$$

$$\hat{a}^{s}_{jm,-} = \sum_{JM} \left[\mathbb{T}^{-+}_{jmJM} \hat{a}^{i}_{JM,+} + \mathbb{T}^{--}_{jmJM} \hat{a}^{i}_{JM,-} \right]. \tag{6.26}$$

Here, $\hat{a}^{s}_{jm,\lambda}$ and $\hat{a}^{i}_{jm,\lambda}$ (with $\lambda = \pm 1$) are the annihilation operators associated with the scattered and incident field amplitudes, respectively. The components of the T matrix in the helicity basis are [85]:

$$\begin{pmatrix} \mathbb{T}^{++}_{jmJM} & \mathbb{T}^{+-}_{jmJM} \\ \mathbb{T}^{-+}_{jmJM} & \mathbb{T}^{--}_{jmJM} \end{pmatrix} = \frac{1}{2} \begin{pmatrix} 1 & 1 \\ 1 & -1 \end{pmatrix} \begin{pmatrix} \mathbb{T}^{ee}_{jmJM} & \mathbb{T}^{em}_{jmJM} \\ \mathbb{T}^{me}_{jmJM} & \mathbb{T}^{mm}_{jmJM} \end{pmatrix} \begin{pmatrix} 1 & 1 \\ 1 & -1 \end{pmatrix}. \tag{6.27}$$

The relations expressed in Eq. (6.25) and Eq. (6.26) represent the quantum formulation of the linear electromagnetic scattering theory. The difference with the classical theory is that this formulation permits to analyze the scattering of non-classical states of light, such as multi photon states or entangled states.

Finally, the scattering matrix is computed taking into account that the total field also includes the incident field. This way we obtain a complete representation of the quantum scattering problem in an input-output form:

$$\hat{a}^{o}_{jm,+} = \sum_{JM} \left[\mathbb{S}^{++}_{jmJM} \hat{a}^{i}_{JM,+} + \mathbb{S}^{+-}_{jmJM} \hat{a}^{i}_{JM,-} \right] \tag{6.28}$$

$$\hat{a}^{o}_{jm,-} = \sum_{JM} \left[\mathbb{S}^{-+}_{jmJM} \hat{a}^{i}_{JM,+} + \mathbb{S}^{--}_{jmJM} \hat{a}^{i}_{JM,-} \right], \tag{6.29}$$

where $\hat{a}^{o}_{jm,\lambda}$ represent the annihilation operators associated with the output (or total) field amplitudes. In this line, the components of the scattering matrix are computed as $\mathbb{S}^{\tilde{\lambda}\lambda}_{jmJM} = \mathbb{T}^{\tilde{\lambda}\lambda}_{jmJM} + \delta^{J}_{j}\delta^{M}_{m}\delta^{\lambda}_{\tilde{\lambda}}$, where δ^{i}_{j} is the Kronecker delta and λ ($\tilde{\lambda}$) represents the helicity of the incident (scattered) field. The necessity of introducing the identity operator in the definition of the scattering matrix stems from the fact that, in the absence of a scatterer, the input and output modes must be the same. Moreover, the expressions given by Eqs. (6.28)-(6.29) indicate that a generic scatterer does not preserve neither the total angular momentum, nor the helicity of the incident states. However, as we show in the next Section, we may try to simplify such general input-output relations by studying particular physical situations in which some of these magnitudes may not be considered. This leads to more tractable scattering matrices from which new phenomena can be inferred.

6.2 QUANTUM SCATTERING WITH CYLINDRICAL PARTICLES

In the previous Section we have discussed a procedure to translate classical results of electromagnetism to the framework of second quantization. We have seen that the input-output formalism is particularly useful to describe linear optical phenomena, such as the action of a beam splitter. Based on this, we have introduced the second quantized form of a generic linear scattering problem. We have shown that such a problem can be studied, within the input-output formalism, considering that the annihilation operators are linearly related through the scattering matrix. This matrix contains all the information of the scatterer and, thus, it also contains the information about its symmetries. For instance, if a scatterer is dual, this implies that the scattering matrix does not couple different helicity components and, thus, $\mathbb{S}^{\tilde{\lambda}\lambda}_{jmJM} = \mathbb{S}^{\lambda}_{jmJM}\delta^{\lambda}_{\tilde{\lambda}}$. Also, if the sample is spherically symmetric, we have that both the square and the z component of total angular momentum are preserved, i.e. $\mathbb{S}^{\tilde{\lambda}\lambda}_{jmJM} = \mathbb{S}^{\tilde{\lambda}\lambda}_{jm}\delta^{J}_{j}\delta^{M}_{m}$.

In this Section, we focus on the study of scattering by cylindrically symmetric structures. In terms of the scattering matrix, this implies dealing with samples for which $\mathbb{S}^{\tilde{\lambda}\lambda}_{jmJM} = \mathbb{S}^{\tilde{\lambda}\lambda}_{jmJ}\delta^{M}_{m}$. The classical version of this scattering problem has already been addressed in Section 4.3 of Chapter 4. The difference with the previous approach is that we now consider the scattering of non-classical states of light. We first discuss the degrees of freedom that we are going to consider in our input-output description of quantum scattering. In this line, we introduce the concept of post-selection that allows to treat the scattering problem in a simplified manner. Then, we discuss the constrains that the mirror symmetry of the system imposes on the scattering matrix components. Finally, we show that such constrains are different depending on whether we consider single photon states with zero or non-zero total angular momentum, m. The results are adapted from Contribution I.

6.2.1 *Post-selected scattering matrix*

Let us first address the scattering problem by simplifying some of the degrees of freedom. In particular, in our treatment we consider that the square of the total angular momentum, j, is not going to play a relevant role. As we have previously mentioned, regarding the implementation of the SCA method in Chapter 4, this approach is fully justified in situations in which the cylindrical scatterer is well-described by a single multipolar order, but the approximation is not valid for a generic cylindrical scatterer. However, there are other situations in which the description of the scattering problem may still be reduced to just the z component of total angular momentum, m, and helicity, λ. Such a description is possible if, by experimental means, we are able to discard the rest of the labels describing the photon states. This procedure is usually denoted as post-selection.

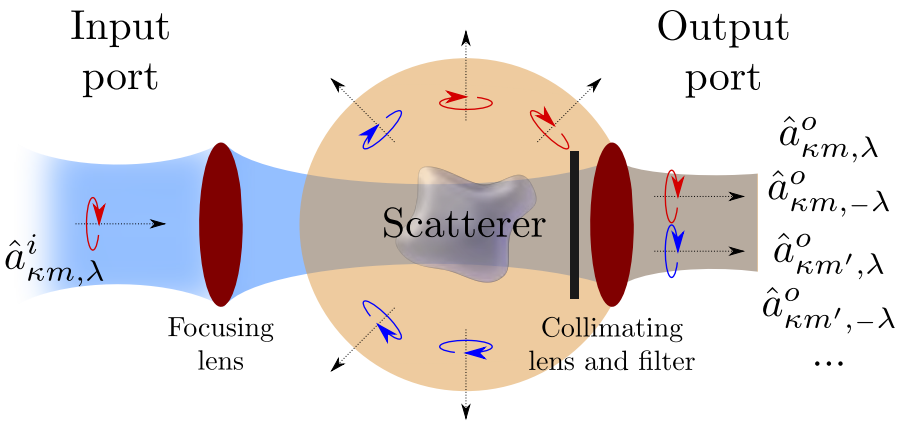

Figure 6.2: Sketch of the post-selection process. An incident state, $\hat{a}^{i}_{\kappa m,\lambda}$, is focused into a generic scatterer and, then, a portion of the total field is recovered through a collimating lens. Due to the characteristics of the set up, the states in the output port have the same linear momentum as the input states.

In our case, the procedure of post-selection can be better understood representing the scattering problem in terms of Bessel beams instead of multipolar solutions. In Fig. 6.2 we depict a typical experimental situation, frequently found in quantum scattering problems. There, an input state with well-defined z component of linear momentum, κ, z component of total angular momentum, m, and helicity, λ, is focused with a lens into a generic linear scatterer. Due to the interaction, the field is scattered in all directions and a portion of the total field is recovered by a second collimating lens. Finally, in Fig. 6.2, it can also be seen that we add a filter which allows us to select a particular linear momentum component from all those that form part of the scattered field. In this particular case, for simplicity, we choose the same component than the incident field. However, we could have chosen other mode filtering options and, in real experimental conditions, one should choose the most convenient one. Nevertheless, one can consider this filtering as an ideal one leading to post-selecting the photons with the adequate linear momentum component. This means that, due to the particular disposition of the optical elements, there are situations in which some labels of the photon states do not play a significant role. In the following discussion, we constrain ourselves to these specific situations.

Moreover, if the scatterer is rotationally symmetric with respect to the OZ axis, this implies that the z component of the total angular momentum is preserved. As a result, if a state with total angular momentum m impinges on a cylindrical scatterer, then, the output state must have the same eigenvalue of the $\hat{J}_z$ operator. In other words, for a cylindrical scatterer we have that the post-selected input-output relations are reduced to:

$$\hat{a}^{o}_{m,+} = \mathcal{S}^{++}_{m}\hat{a}^{i}_{m,+} + \mathcal{S}^{+-}_{m}\hat{a}^{i}_{m,-} \tag{6.30}$$

$$\hat{a}^{o}_{m,-} = \mathcal{S}^{-+}_{m}\hat{a}^{i}_{m,+} + \mathcal{S}^{--}_{m}\hat{a}^{i}_{m,-}, \tag{6.31}$$

where $\mathcal{S}_m^{\tilde{\lambda}\lambda}$ are the components of the post-selected scattering matrix of a cylindrical scatterer for modes with total angular momentum m. Note that the relations expressed in Eqs. (6.30)-(6.31) bear a resemblance with the transformation induced by a beam splitter. However, there are a few differences between the two systems. On the one hand, the post-selected scattering matrix components do not fulfill the requirements imposed by energy conservation. This is because, due to the nature of the scattering problem depicted in Fig. 6.2, there are field components which are not collected by the collimating lens and, thus, part of the incident energy does not reach the output port. Due to all this, and contrary to what happens in a unitary beam splitter, $\mathcal{S}_m^{\tilde{\lambda}\lambda}$ coefficients can virtually take any value. Later on we will see that, in some particular cases, the post-selected scattering matrix coefficients can be related due to symmetry considerations.

Finally, for future convenience, let us rewrite the relation given by Eqs. (6.30)-(6.31) in terms of the creation operators instead of the annihilation operators. Moreover, inverting the relation we obtain:

$$\hat{a}_{m,+}^{\dagger i} \to \eta \hat{a}_{m,+}^{\dagger o} + \zeta \hat{a}_{m,-}^{\dagger o} \tag{6.32}$$

$$\hat{a}_{m,-}^{\dagger i} \to \epsilon \hat{a}_{m,+}^{\dagger o} + \gamma \hat{a}_{m,-}^{\dagger o}, \tag{6.33}$$

where η, ζ, ϵ and γ coefficients are computed by complex conjugating and inverting the post-selected scattering matrix specified in Eqs. (6.30)-(6.31). The advantage of specifying a transformation over the creation operators resides in the fact that single photon states are constructed by applying these operators to the vacuum state, $|0\rangle$. Thus, physically, it is more convenient to express the transformation in terms of $\hat{a}^\dagger$ operators, instead of $\hat{a}$ operators. Moreover, inverting the input-output relation also helps in clarifying the effect of the scattering matrix over the states. Indeed, with the presence of the "$\to$" symbol, we want to stress that the action of the scatterer is to transform an input state into a superposition of output states. For a detailed discussion on the computation of such input-output relations in the case of a spherical scatterer check Refs. [80] and [86]. Also, details of the experimental implementation of such linear transformations can be found in Ref. [87].

6.2.2 *States with zero total angular momentum*

As a first example let us discuss the quantum scattering of states with null total angular momentum, $m = 0$. This particular problem has been theoretically addressed in Contributions I and XII.

A consequence of the cylindrical symmetry of the scatterers is that they are also mirror symmetric. In particular, let us consider the mirror symmetry with respect to any plane containing the OZ axis, like, for instance, the XZ plane. Following the usual conventions, we denote by $\hat{M}_y$ the operator which performs a mirror transformation with respect to the XZ plane. From the properties of classical electromagnetic fields it can be checked that the mirror operator, $\hat{M}_y$, acts

in the following way over states with null total angular momentum [87]:

$$\hat{M}_y \, \hat{a}^{\dagger}_{0,\lambda}|0\rangle = \hat{a}^{\dagger}_{0,-\lambda}|0\rangle. \tag{6.34}$$

The expression above implies that the states of null total angular momentum are mapped into themselves through the action of the mirror operator. Due to the symmetry of the problem, the post-selected scattering operator has to be invariant under mirror transformations, which imposes the constrain $\epsilon = \zeta$ and $\eta = \gamma$, i.e. that the diagonal and anti-diagonal terms are equal.

To avoid repeating the same symbols, let us express the transformation of a cylindrical scatterer for states with null total angular momentum, $m = 0$, in terms of different parameters, α and β. Please note that this parameters are different from the scattering coefficients expressed in Eqs. (6.23)-(6.24). As we have seen, mirror symmetry imposes that the transformation of states with null total angular momentum is:

$$\hat{a}^{\dagger i}_{0,+}|0\rangle \rightarrow \left(\alpha \hat{a}^{\dagger o}_{0,+} + \beta \hat{a}^{\dagger o}_{0,-}\right)|0\rangle \tag{6.35}$$

$$\hat{a}^{\dagger i}_{0,-}|0\rangle \rightarrow \left(\beta \hat{a}^{\dagger o}_{0,+} + \alpha \hat{a}^{\dagger o}_{0,-}\right)|0\rangle. \tag{6.36}$$

By inverting back the input-output relation, it can be checked that the relations given by Eqs. (6.35)-(6.36) exactly represent the transformation of a beam splitter. However, in this case, the system has losses, which implies that the output operators do not fulfill the canonical commutation relations [81]. There are a few ways to get around this issue. On the one hand, one may consider extra modes to account for all the losses of the system and, thus, recover the conservation of energy [88]. Another approach, which is the one we follow here, is just to accept that energy is not preserved in the scattering process and employ Eqs. (6.35)-(6.36) considering that α and β coefficients are arbitrary complex numbers. Note that by considering that the scattering coefficients α and β are arbitrary, the description applies to any post-selected cylindrical scattering problem, making our discussion general.

If we do not impose any constrain over α and β coefficients, the transformation given by Eqs. (6.35)-(6.36) describes the interaction of photon states with a generic cylindrical scatterer. In this line, note that the action of a post-selected cylindrical scatterer can be resumed into a single matrix:

$$\mathbf{S} = \begin{pmatrix} \alpha & \beta \\ \beta & \alpha \end{pmatrix}. \tag{6.37}$$

This matrix contains all the dynamical information of the evolution of states belonging to the space $\mathcal{H}_0 = \text{span}\{\hat{a}^{\dagger}_{0,+}|0\rangle, \hat{a}^{\dagger}_{0,-}|0\rangle\}$ within the input-output formalism. The matrix form of the transformation suggests that there may be certain single photon states that may remain invariant in the scattering process, i.e. those linear combinations

which diagonalize the **S** matrix. Indeed, such states are also eigenstates of the mirror operator and transform in the following way:

$$\frac{1}{\sqrt{2}}\left(\hat{a}^{\dagger i}_{0,+}+\tau\hat{a}^{\dagger i}_{0,-}\right)|0\rangle \rightarrow \frac{\alpha+\tau\beta}{\sqrt{2}}\left(\hat{a}^{\dagger o}_{0,+}+\tau\hat{a}^{\dagger o}_{0,-}\right)|0\rangle, \tag{6.38}$$

where $\tau=\pm 1$ is the eigenvalue of the mirror operator, $\hat{M}_y$. Crucially, note that the input states in Eq. (6.38) do not depend on α and β parameters, which implies that they are eigenstates of every cylindrical scatterer. This is what we call symmetry-protected states: photon states which, for symmetry considerations, remain invariant in the scattering with *all* the samples that belong to a specific symmetry group. In the case we are discussing here, the group is $C_{\infty v}$.

The reason why the states in Eq. (6.38) are protected in the interaction with all cylindrically symmetric scatterers is that, due to the symmetries of the scatterers, both m and τ labels are preserved in the interaction. This implies that states with different angular momentum and mirror eigenvalues are decoupled in the scattering process. The states expressed in Eq. (6.38) are simultaneous eigenvectors of $\hat{J}_z$ and $\hat{M}_y$ operators, with eigenvalues $m=0$ and $\tau=\pm 1$. As a result, they cannot be mixed with any other optical mode and they remain invariant through the scattering process. Here, with "invariant" we mean that, if a photon is found in the output port, then, it must be in the same state as in the input port. But, of course, it could also happen that the photon is lost due to optical absorption in the scatterer or due to the post-selection process. Thus, if we are precise with the wording, the states given by Eq. (6.38) are protected only if we can further post-select on having no losses. In practice, this implies keeping only the events in which the output state has the same number of photons as the input state.

6.2.3 *States with non-zero total angular momentum*

In the previous Subsection, we have studied the dynamics of single photon states with $m=0$. Now, we may analyze the scattering of states with non-zero total angular momentum, $m\neq 0$. This problem has been theoretically addressed in Contribution I considering that the evolution is fixed by the transformation specified in Eqs. (6.32)-(6.33).

The main difference with the previous case is that states with $m\neq 0$ do not transform into themselves under mirror transformations. This can also be checked from the properties of clasical electromagnetic fields:

$$\hat{M}_y\,\hat{a}^{\dagger}_{m,\lambda}|0\rangle=\hat{a}^{\dagger}_{-m,-\lambda}|0\rangle. \tag{6.39}$$

Therefore, if we want to consider mirror eigenstates in our scattering problem, we have to consider also states with total angular momentum $-m$. By setting our space of states to

$$\mathcal{H}_m=\text{span}\left\{\hat{a}^{\dagger}_{m,+}|0\rangle,\hat{a}^{\dagger}_{m,-}|0\rangle,\hat{a}^{\dagger}_{-m,+}|0\rangle,\hat{a}^{\dagger}_{-m,-}|0\rangle\right\}, \tag{6.40}$$

we see that the evolution of the system is now fixed by the following transformation:

$$\hat{a}^{\dagger i}_{m,+} \to \left(\eta \hat{a}^{\dagger o}_{m,+} + \zeta \hat{a}^{\dagger o}_{m,-}\right)|0\rangle \tag{6.41}$$

$$\hat{a}^{\dagger i}_{m,-} \to \left(\epsilon \hat{a}^{\dagger o}_{m,+} + \gamma \hat{a}^{\dagger o}_{m,-}\right)|0\rangle \tag{6.42}$$

$$\hat{a}^{\dagger i}_{-m,+} \to \left(\gamma \hat{a}^{\dagger o}_{-m,+} + \epsilon \hat{a}^{\dagger o}_{-m,-}\right)|0\rangle \tag{6.43}$$

$$\hat{a}^{\dagger i}_{-m,-} \to \left(\zeta \hat{a}^{\dagger o}_{-m,+} + \eta \hat{a}^{\dagger o}_{-m,-}\right)|0\rangle, \tag{6.44}$$

where we have already considered the constrains that mirror symmetry imposes over the scattering coefficients. Apart from the explicit relations imposed by mirror symmetry, we allow η, ζ, ϵ and γ coefficients adopt arbitrary complex values. As before, this implies that the expressions specified in Eqs. (6.41)-(6.44) describe the scattering of states with total angular momentum $m \neq 0$ with any post-selected cylindrical sample.

In analogy with the case of zero total angular momentum, we see that the evolution of the system is now determined by the properties of the matrix

$$\mathbf{S} = \begin{pmatrix} \eta & \zeta & 0 & 0 \\ \epsilon & \gamma & 0 & 0 \\ 0 & 0 & \gamma & \epsilon \\ 0 & 0 & \zeta & \eta \end{pmatrix}. \tag{6.45}$$

As we have doubled the dimensions of our space, the evolution now resembles the action of two decoupled beam splitters. One of them operates over the states with positive angular momentum, m, whereas the other one operates over the states with negative angular momentum, $-m$. In this analogy, the transmission and reflection coefficients of the two beam splitters are related, but the diagonal and anti-diagonal coefficients of each of them are different. This differs from the case of states with null total angular momentum, where the diagonal and anti-diagonal coefficients were set to be the same by symmetry considerations. As a result, the transformation of states with m and $-m$ angular momentum can be associated with the action of two non-symmetric lossy beam splitters [82, 89, 90].

At this point, we could try to diagonalize the $\mathbf{S}$ matrix and obtain the set of states which remain invariant through the scattering process. This, of course, can be done, but the result is not very useful, as all the eigenstates of $\mathbf{S}$ depend on the η, ζ, ϵ and γ coefficients. This means, that in the single photon case there are no states with total angular momentum $m \neq 0$ which remain invariant for *all* cylindrically symmetric scatterers. There are just particular states that remain invariant for particular cylindrically symmetric scatterers. This implies that there are no single photon symmetry protected states with $m \neq 0$. As we show in the following Section, symmetry protection for states with non-zero total angular momentum emerges in the multi photon regime and due to phenomenon of quantum interference.

6.3 SYMMETRY-PROTECTION OF MULTI PHOTON STATES

Once we have settled the description of the scattering of single photon states by cylindrical particles, we can take advantage of the second quantization formalism and study the dynamics of multi photon states. The prescriptions to consider such multi particle transformations are relatively simple. First, we build a multi photon input state, we then apply the transformation to each of the creation operators and, finally, we compute the output state assuming that $[\hat{a}^{\dagger o}_{m,\lambda}, \hat{a}^{\dagger o}_{m',\lambda'}] = 0$ for every value of the total angular momentum and helicity. Thus, we implicitly assume that, even if we have not explicitly constructed it, there exists a larger set of output modes for which the scattering process can be expressed as a quasiunitary operator. This is a sufficient condition to recover the canonical commutation relations for the output modes [88].

Bearing this in mind, in this Section we discuss the construction of multi photon symmetry-protected states. First, we discuss the two photon case for states with both $m = 0$ and $m \neq 0$ total angular momenta. On the one hand, we show that the emergence of symmetry protection in the case of states with $m = 0$ is a natural extension of the single particle dynamics. For the case of $m \neq 0$, we show that symmetry protection emerges as a consequence of quantum interference, when considering two photon states. This is in stark contrast with the single particle regime, where we have shown that no symmetry-protected states can be built with $m \neq 0$. Then, we extend the notion of symmetry protection to an arbitrary number of photons, N. We show that multi photon symmetry-protected states can be expressed as products of the states already discussed for the single and two photon case. Finally, we discuss possible applications of symmetry-protected states in the construction of decoherence free subspaces. The results are adapted from Contribution I.

6.3.1 *Two photon symmetry-protected states*

Two photon symmetry-protected states with $m = 0$ can be built based on what we have already discussed in the single particle regime. Indeed, in this specific case, we may choose a different way of expanding the space $\mathcal{H}_0$ in terms of single photon protected states specified in Eq. (6.38):

$$\mathcal{H}_0 = \text{span}\left\{\hat{a}^{\dagger}_{0,s}|0\rangle, \hat{a}^{\dagger}_{0,a}|0\rangle\right\}, \tag{6.46}$$

where subscripts "s" and "a" stand for symmetric and antisymmetric, repectively. This subscripts indicate whether the eigenvalue of the mirror operator, $\hat{M}_y$, is $\tau = 1$ (symmetric) or $\tau = -1$ (antisymmetric). The expansion of $\mathcal{H}_0$ space in terms of the mirror symmetric and antisymmetric states can be just seen as a change of basis, where we choose to express the states in terms of their mirror eigenvalue, τ, instead of their helicity, λ.

With this choice, we may now build the space of two photon states with $m = 0$, which can be expressed as:

$$\mathcal{H}_0^{N=2} = \text{span}\left\{(\hat{a}_{0,s}^\dagger)^2|0\rangle, \hat{a}_{0,s}^\dagger \hat{a}_{0,a}^\dagger|0\rangle, (\hat{a}_{0,a}^\dagger)^2|0\rangle\right\}. \tag{6.47}$$

As the commutation relations impose that $\hat{a}_{0,s}^\dagger \hat{a}_{0,a}^\dagger|0\rangle = \hat{a}_{0,a}^\dagger \hat{a}_{0,s}^\dagger|0\rangle$, the space specified in Eq. (6.47) is three dimensional. This is closely related with the fact that photons are bosons and, as a result, multi particle wave functions are required to be symmetric under the particle exchange operation. It is direct to check that the three basis vectors defined above remain invariant when scattering off a cylindrically symmetric sample. Indeed, employing the transformation in Eqs. (6.35)-(6.36), we get:

$$\left(\hat{a}_{0,s}^{\dagger i}\right)^2|0\rangle \to (\alpha+\beta)^2\left(\hat{a}_{0,s}^{\dagger o}\right)^2|0\rangle \tag{6.48}$$

$$\hat{a}_{0,s}^{\dagger i}\hat{a}_{0,a}^{\dagger i}|0\rangle \to (\alpha^2-\beta^2)\hat{a}_{0,s}^{\dagger o}\hat{a}_{0,a}^{\dagger o}|0\rangle \tag{6.49}$$

$$\left(\hat{a}_{0,a}^{\dagger i}\right)^2|0\rangle \to (\alpha-\beta)^2\left(\hat{a}_{0,a}^{\dagger o}\right)^2|0\rangle. \tag{6.50}$$

The result in Eqs. (6.48)-(6.50) indicates that there are three symmetry-protected states built from two photons with $m = 0$. And, in line with what we have discussed in the previous Section, such two photon states are protected only if we post-select on having no losses, i.e. if we just consider the events in which two photons are found in the output port. Experimentally, this is usually implemented by measuring coincidences, i.e. only taking into account events in which two photons arrive simultaneously to the output detectors.

On the other hand, the case of two photon states with $m \neq 0$ is not so straightforward. Indeed, as we have previously shown, there are no symmetry-protected single photon states. This is mainly due to the fact that mirror eigenstates are linear combinations of states with positive and negative angular momentum. As a result, in the single photon regimen, eigenstates of $\hat{M}_y$ operator do not have a well-defined total angular momentum, i.e. they are not eigenstates of $\hat{J}_z$ operator. The situation is radically modified when considering multi photon states because this type of states have total angular momentum $m_{tot} = \sum_{i=1}^{N} m_i$, where N is the number of photons and m_i the angular momentum of each of them. In this line, the space of two photon states $\mathcal{H}_m^{N=2}$ can be split in three subspaces according to the different values of m_{tot}:

$$\mathcal{V}_{2m} = \text{span}\left\{\hat{a}_{m,+}^\dagger \hat{a}_{m,+}^\dagger|0\rangle, \hat{a}_{m,+}^\dagger \hat{a}_{m,-}^\dagger|0\rangle, \hat{a}_{m,-}^\dagger \hat{a}_{m,-}^\dagger|0\rangle\right\} \tag{6.51}$$

$$\mathcal{V}_{-2m} = \text{span}\left\{\hat{a}_{-m,-}^\dagger \hat{a}_{-m,-}^\dagger|0\rangle, \hat{a}_{-m,-}^\dagger \hat{a}_{-m,+}^\dagger|0\rangle, \hat{a}_{-m,+}^\dagger \hat{a}_{-m,+}^\dagger|0\rangle\right\} \tag{6.52}$$

which contain states with $m_{tot} = 2m$ and $m_{tot} = -2m$, respectively. And, then, a subspace with $m_{tot} = 0$:

$$\mathcal{V}_0 = \text{span}\Big\{\hat{a}_{m,+}^\dagger \hat{a}_{-m,-}^\dagger|0\rangle, \hat{a}_{m,-}^\dagger \hat{a}_{-m,+}^\dagger|0\rangle, \hat{a}_{m,+}^\dagger \hat{a}_{-m,+}^\dagger|0\rangle, \hat{a}_{m,-}^\dagger \hat{a}_{-m,-}^\dagger|0\rangle\Big\}. \tag{6.53}$$

Thus, we see that, unlike the single photon regime, the two photon space $\mathcal{H}_m^{N=2}$ contains a subspace with null total angular momentum.

It can be checked that $\mathcal{V}_{2m}$ and $\mathcal{V}_{-2m}$ are mapped into each other by $\hat{M}_y$. $\mathcal{V}_0$ is the only subspsace which maps into itself through the action of the mirror operator. Indeed, in the basis specified by Eq. (6.53), the mirror operator can be expressed as:

$$\hat{M}_y = \begin{pmatrix} 1 & 0 & 0 & 0 \\ 0 & 1 & 0 & 0 \\ 0 & 0 & 0 & 1 \\ 0 & 0 & 1 & 0 \end{pmatrix}. \tag{6.54}$$

This indicates that the first two states of $\mathcal{V}_0$ subspace are mirror symmetric, whereas the last two states are mapped into each other. In other words, the eigenvectors and eigenvalues of the mirror operator in subspace $\mathcal{V}_0$ are:

$$|\psi_1\rangle = \hat{a}^\dagger_{m,+}\hat{a}^\dagger_{-m,-}|0\rangle \quad (\tau = 1) \tag{6.55}$$

$$|\psi_2\rangle = \hat{a}^\dagger_{m,-}\hat{a}^\dagger_{-m,+}|0\rangle \quad (\tau = 1) \tag{6.56}$$

$$|\psi_3\rangle = \left(\hat{a}^\dagger_{m,+}\hat{a}^\dagger_{-m,+} + \hat{a}^\dagger_{m,-}\hat{a}^\dagger_{-m,-}\right)|0\rangle \quad (\tau = 1) \tag{6.57}$$

$$|\psi_4\rangle = \left(\hat{a}^\dagger_{m,+}\hat{a}^\dagger_{-m,+} - \hat{a}^\dagger_{m,-}\hat{a}^\dagger_{-m,-}\right)|0\rangle \quad (\tau = -1). \tag{6.58}$$

In other words, there are three mirror symmetric ($\tau = 1$) and only one mirror antisymmetric ($\tau = -1$) within the $\mathcal{V}_0$ subspace. Moreover, as the total angular momentum, m_{tot}, is also preserved, we reach to the conclusion that $|\psi_4\rangle$ cannot be mixed with any other state through the scattering process.

This can be explicitly checked by applying the transformations given by Eqs. (6.41)-(6.44) to $|\psi_4\rangle$:

$$|\psi_4^i\rangle \to (\eta\gamma - \zeta\epsilon)|\psi_4^o\rangle, \tag{6.59}$$

which confirms that it is left invariant in the scattering process. Also, note that the construction of the state is independent of the scattering coefficients, which implies that $|\psi_4\rangle$ is an eigenstate of *all* post-selected cylindrical scatterers. In other words, the state given in Eq. (6.59) is a two photon symmetry-protected state composed of photons with angular momentum $m \neq 0$. Moreover, $|\psi_4\rangle$ has a feature which differentiates it from the protected states specified by Eqs. (6.48)-(6.50): it cannot be expressed as the product of single photon states. In other words, in the case of $m \neq 0$, symmetry-protection is a consequence of quantum interference and, thus, it is a exclusive feature of the multi photonic nature of the states we are considering. In contrast to the states given by Eqs. (6.48)-(6.50), $|\psi_4\rangle$ is considered an entangled two photon state according to most definitions [91–93].

6.3.2 *Multi photon symmetry-protected states*

Once we have analyzed the single and two photon cases, we may wonder whether there are or not more symmetry-protected states. Up to

now we have inferred the existence of these states in two particular ways. First, by identifying photon states with null total angular momentum and mirror symmetry. If there are states which are uniquely defined by these attributes, i.e. there is only one mirror symmetric or mirror antisymmetric state in the subspace of null total angular momentum, then it must be protected in the interaction with cylindrical samples. As we have explained, this is just because both the total angular momentum and the mirror eigenvalue are conserved in the interaction with this type of samples. Second, symmetry-protected states can also be built from products of previously identified protected states. In the case of $m = 0$, we have shown that the single particle space $\mathcal{H}_0$ can be expanded in terms of symmetry-protected states and, as a result, the space $\mathcal{H}_0^{N=2}$ can also be expanded in terms of two photon protected states.

Following this reasoning, it is clear that there is a systematic way of building multi photon symmetry-protected states with $m = 0$. To construct a N photon protected state we should just consider products as indicated in the previous Section:

$$|\Psi_0\rangle = \left(\hat{a}^\dagger_{0,s}\right)^{n_s} \left(\hat{a}^\dagger_{0,a}\right)^{n_a} |0\rangle, \tag{6.60}$$

where the number of photons is computed as $N = n_s + n_a$. Here, n_s and n_a represent the number of mirror symmetric and antisymmetric states. All these states have null total angular momentum and their mirror eigenvalue is given by $(-1)^{n_a}$. Also, when N is odd there are $(N+1)/2$ mirror symmetric and $(N+1)/2$ mirror antisymmetric states. In the case of the number of photons being even, there are $N/2+1$ mirror symmetric and $N/2$ mirror antisymmetric states. In both cases, the total number of states is $N+1$. One can check that the state given by Eq. (6.60) is protected by explicitly computing the transformation expressed in Eqs. (6.35)-(6.36), which leads to:

$$|\Psi_0^i\rangle \to (\alpha+\beta)^{n_s}(\alpha-\beta)^{n_a}|\Psi_0^o\rangle. \tag{6.61}$$

By construction, it is clear that there are no other multi photon symmetry-protected states for the case $m = 0$.

On the other hand, we may employ exactly the same procedure to build multi photon protected states with $m \neq 0$. In this case, a state of the form:

$$|\Psi_m\rangle = \left(\hat{a}^\dagger_{m,+}\hat{a}^\dagger_{-m,+} - \hat{a}^\dagger_{m,-}\hat{a}^\dagger_{-m,-}\right)^{N/2} |0\rangle \tag{6.62}$$

must be left invariant in the scattering with any cylindrically symmetric sample. Note that this state belongs to the $\mathcal{V}_0$ subspace of the N photon space, $\mathcal{H}_m^N$, and its mirror symmetry depends on whether $N/2$ is even or odd. One can check that $|\Psi_m\rangle$ is left invariant by explicitly applying the transformation given by Eqs. (6.41)-(6.44):

$$|\Psi_m^i\rangle \to (\eta\gamma - \zeta\epsilon)^{N/2}|\Psi_m^o\rangle. \tag{6.63}$$

Interestingly, this is the only protected state for a fixed value of the angular momentum, m, and photon number, N. This can be proved

from the definition of symmetry-protection and exploiting the properties of the **S** matrix for cylindrically symmetric samples. The details are given in Contribution I and the proof rests on the fact that a protected state must be an eigenstate of *all* matrices $\mathbf{S}, \mathbf{S}'$...etc compatible with the group $C_{\infty v}$. The transformations between two infinitesimally distinct matrices **S** and $\mathbf{S}'$ suffice to prove that the symmetry-protected state given by Eq. (6.62) is unique. In other words, for $m \neq 0$ and $N > 2$, there are no other symmetry-protected states which emerge as a consequence of quantum interference. All the protected states are products of the $|\psi_4\rangle$ state identified in the two photon case.

6.3.3 *Construction of decoherence free subspaces*

Note that so far we have discussed the protection of one-dimensional subspaces, namely single N photon states which are preserved in the scattering with cylindrical samples. While this provides an interesting characterization of the scatterer and may be useful for certain applications, it is not sufficient to transmit quantum information. To profit from symmetry-protection, at least a two-dimensional protected subspace is required. In this line, one would like to build superpositions which are robust to the environmental conditions, i.e. subspaces in which the relative amplitudes may remain unchanged through the propagation. This kind of subspaces are most commonly denoted as decoherence free subspaces. In this last Subsection, we show that, with one additional assumption on the scatterer, decoherence free subspaces may be constructed even in the presence of losses.

If the scatterer, and hence the **S** matrix, can be considered to be static, i.e. constant during a time interval $[t_1, t_2]$, then a protected state $\hat{P}_m|0\rangle$ scattered at time t_1 or time t_2 undergoes exactly the same transformation and, therefore, if we can post-select on having no losses, any superposition of the two would be unaffected. Indeed, for the protected states constructed in the previous Sections, the state after scattering is of the form $\lambda_m \hat{P}_m|0\rangle + |\psi_R\rangle$, where λ_m is the eigenvalue of the symmetry-protected state and $|\psi_R\rangle$ is the part in which at least one photon has been scattered into environmental modes. If the scattering is time-independent, sending an input state in a superposition of being in the first or the second time-bin $(c_1\hat{P}_m(t_1) + c_2\hat{P}_m(t_2))|0\rangle$ will be scattered into $\lambda_m(c_1\hat{P}_m(t_1) + c_2\hat{P}_m(t_2))|0\rangle + b_1|\psi_R(t_1)\rangle + b_2|\psi_R(t_2)\rangle$, where b_1 and b_2 are coefficients that account for the losses at times t_1 and t_2. Thus, post-selecting on having the input number of photons, N, either in the first and zero in the second time-bin or vice versa yields the unchanged input state. In principle, this post-selection can be done without affecting the superposition, i.e. by filtering on the correct photon number in the full set of employed modes. This implies that the whole subspace can be transmitted in protected fashion, leading to a two dimensional decoherence free subspace.

Furthermore, one can generalize this to construct d dimensional decoherence free subspaces given by: $\sum_{i=1}^{d} c_i \hat{P}_m(t_i)|0\rangle$, as long as

the scattering matrix remains static in the time interval $[t_1, t_d]$. Since the loss of probability only depends on the total photon number, not on the number of time-bins, these do not suffer larger losses. Note that the simplest realization is the use of single photon symmetry-protected states as given in Eq. (6.38), in which case the qubit is just a suitable angular-momentum choice of the time-bin qubit long used in quantum communications [94] and for which efficient quantum logic has been developed [95].

6.4 SUMMARY

In Section 6.1 we have discussed the second quantization of the electromagnetic field. We have shown that the input-output formalism provided by the quantum beam splitter can be extended to study the scattering of photon states by linear optical samples. In this line, we have seen that in a linear scattering problem the input and output modes are related by the so-called scattering matrix of the system. In Section 6.2 we have introduced the notion of post-selection and we have focused on situations in which photon states may be well-described only by their total angular momentum, m, and helicity, λ. More specifically, we have discussed some general properties of the scattering of these photon states with cylindrically symmetric samples. Indeed, we have shown that the evolution of states with zero ($m = 0$) and non-zero ($m \neq 0$) angular momentum differs in certain important aspects. In Section 6.3 we have discussed the notion of symmetry-protection. We have shown that, unlike $m = 0$ states, symmetry-protection for $m \neq 0$ states is a consequence of quantum interference and the multi photon nature of the input states. Finally, we have discussed the possibility of building decoherence free subspaces with time-bin superpositions of symmetry-protected states.

7

CONCLUSIONS

In this brief Chapter, we discuss the main results and conclusions of our work. We also provide an outlook of the potential applications that our findings may have in different fields of Physics and, particularly, in electromagnetic scattering theory.

MAIN RESULTS AND CONCLUSIONS

In Chapter 2, we have introduced Maxwell's equations both in the conventional form and in terms of different versions of the RS vector. Also, we have shown that the canonical operator form of some fundamental physical magnitudes such as energy, linear momentum, total angular momentum and boosts, generates a representation of the Poincaré group.

In Chapter 3, based on the symmetry breaking principle, we have extended the description of electromagnetic waves in vacuum provided by Wigner and Bargmann to generic homogeneous media. More specifically, we have shown that the description of electromagnetic waves in homogeneous media is naturally related to the $P_{3,1}$ subgroup of the Poincaré group. In this line, we have provided an alternative starting point to study the dynamics of monochromatic electromagnetic waves propagating in this type of environments. Our analysis puts forward the fundamental role that the Casimir operators of $P_{3,1}$, i.e. the helicity operator, $\hat{\Lambda}$, and the square of linear momentum operator, $\hat{\mathbf{P}}^2$, play in the description of monochromatic electromagnetic waves. Moreover, we have also shown that the monochromatic RS vector naturally emerges from the analysis of the unitary irreducible representations of $P_{3,1}$. Our group theoretical analysis sheds light on why the monochromatic RS vector constitutes such a particular (and useful) choice to represent monochromatic electromagnetic fields. Finally, our discussion also clarifies the role of the Euclidean group in electromagnetism and its link with the construction of wave solutions with well-defined helicity.

In Chapter 4, we have shown that the systematic application of the monochromatic RS vector to the study of linear electromagnetic scattering phenomena leads to interesting insights and new results. For instance, we have shown that the use of the monochromatic RS vector reinforces Bohren and Huffman's idea of extinction emerging as an interference between the incident and the scattered fields. Also, it facilitates the link between the scattered power and the scattered helicity with the Stokes parameters. On top of this, we have provided a few substantial contributions. First, we have shown that optical losses in dielectric scatterers preclude the conservation of helicity in many different systems, such as conventional spheres, chiral spheres and core-shell. This implies that lossy systems should be avoided if one seeks the conservation of helicity for applications such as surface-enhanced Circular Dichroism, directional scattering and so on. Second, we have analytically shown that optical gain is a necessary condition to build antidual scatterers of any size, shape and under generic illumination conditions. This closes a long-standing controversy about the implementation of helicity flipping scatterers, while at the same time clarifies where the experimental efforts should be directed instead. Third, we have reported a method to characterize cylindral particles in more favourable experimental conditions, i.e. the Single Characterization Angle method. Potentially, this technique may allow the experimental determination of the scattered power and the scattered helicity

with a single photo-detector placed in the far-field in some particular cases. The method may indeed be useful to characterize cylindrical samples whose multipolar resonances do not overlap spectrally.

In Chapter 5, we have delved into the study of electromagnetic waves propagating through magnetic inhomogeneous media. We have shown that the impedance and refractive index matching conditions naturally emerge from the form that Maxwell's equations acquire in terms of the monochromatic RS vector. In this line, we have shown that, under both the impedance and the refractive index matching conditions, Fresnel and Mie coefficients acquire very specific analytical expressions, some of which had previously been overlooked in the literature. We have also shown that the refractive index matching condition permits the construction of efficient helicity flipping spherical scatterers while respecting the law of energy conservation. In addition, we have identified the mechanism that permits the helicity conversion under the refractive index matching condition. Making a formal analogy with two-level quantum systems, we have shown that the index matching condition leads to the phenomenon of avoided level crossing and, thus, to the resonant mixing of the different helicity components of the electromagnetic field. Finally, we have discussed the conserved quantities associated with the impedance and refractive index matching conditions, i.e. helicity, $\hat{\Lambda}$, and the square of linear momentum, $\hat{\mathbf{P}}^2$, respectively. We have concluded that the emergence of these conserved quantities puts forward an alternative interpretation of the phenomena reported by Kerker, Wang and Giles 40 years ago [70]. In our view, the emergence of such anomalous effects can also be understood in terms of the Casimir operators of $P_{3,1}$ group. We believe that this perspective of the Kerker phenomena is more consistent with the analysis provided in Chapter 3.

In Chapter 6, we have applied the description of electromagnetic waves in terms of modes with well-defined helicity to study the scattering of multi photon states with cylindrically symmetric structures. In this line, we have shown that, within post-selected quantum scattering processes, there are states which are left invariant under the action of arbitrary cylindrical scatterers, i.e. the so-called symmetry-protected states. In our analysis we have identified both single photon and multi photon symmetry-protected states. As we have shown, single photon symmetry-protected states can only be built with modes with null total angular momentum ($m = 0$), whereas multi photon protected states can be built from modes with any value of the total angular momentum. More specifically, we have demonstrated that all of the symmetry protected states built from modes with null total angular momentum can be expressed as products of single photon protected states. On the other hand, we have also shown that symmetry protected states built with modes with $m \neq 0$ are products of two photon protected states. Finally, we have discussed the possible application of symmetry-protected states to build decoherence-free subspaces. We have concluded that time-bin superpositions of symmetry-protected states may serve for this goal, the only experi-

mental requirement is that the response of the scatterers cannot dramatically change in time.

OUTLOOK

Our group theoretical analysis of Chapter 3 opens the way to the application of the symmetry breaking principle in other electromagnetic problems. A systematic study of environments based on such principle may lead to the discovery of new optical phenomena. For instance, the identification of relativistically invariant materials would open the way to a completely new paradigm in which other subgroups of the Poincaré group may be employed to anticipate the properties of novel optical samples.

Also, the discussion in Chapter 4 proves that the monochromatic RS vector constitutes an extremely useful tool for the analysis of electromagnetic scattering problems. Our study has mainly focused on power measurements, but we believe that the potential of the RS vector goes well beyond this magnitude. For instance, the application of the monochromatic RS vector may also be useful to study optical forces and torques in linear electromagnetic scattering problems. On the other hand, the results on dual and antidual scatterers indicate that experimental designs should take into account the conditions under which these types of scatterers may or not be built. Finally, the implementation of the Single Characterization Angle method has a clear potential in simplifying routine optical measurements. Indeed, some research groups are already studying the experimental conditions in which this method may be applied.

The impact of the results reported in Chapter 5 is more conceptual. On the one hand, we have shown that the refractive index matching condition is paired with the impedance matching condition in several contexts of electromagnetism. While the role of the impedance has been analyzed in a wide variety of problems, the refractive index has been quite generally overlooked in the literature. Thus, we believe it would be interesting to check whether the index matching condition provides new insights in systems in which impedance matching has been analyzed in the past. On the other hand, the connection of the refractive index matching condition with the avoided level crossing phenomenon opens the way to explore similarities in the dynamics of other fundamental particles such as neutrinos. One should be cautious when proposing this type of analogies or connections, but we believe that there are elements in our analysis that indicate that the refractive index matching condition is related with other phenomena such as the Mikheyev–Smirnov–Wolfenstein effect. A deeper study in this direction may also be interesting. Finally, we also believe that the inclusion of the refractive index matching condition in the analysis of the Kerker phenomena clarifies the discussion about the conserved quantities in such scenarios.

Regarding the analysis provided in Chapter 6, we believe it may serve to settle the study of the scattering of photon states with cylin-

drically symmetric structures. In this line, there are many optical systems which have cylindrical symmetry, such as circular optical fibers, in which the analysis of helicity states may also lead to new insights and results. Finally, it may be interesting to extend the notion of symmetry-protection to other geometries.

BIBLIOGRAPHY

[1] H. Cavendish. *The electrical researches of the honourable Henry Cavendish*. Ed. by J. C. Maxwell. Frank Cass and Co., Ltd., 1967 (page 3).

[2] C. A. de Coulomb. *Collection de mémoires relatifs à la physique*. Gauthier-Villars, 1884 (page 3).

[3] J. C. Maxwell. "On Faraday's lines of force." In: *Transactions of the Cambridge Philosofical Society* 10 (1864), p. 27 (page 3).

[4] J. C. Maxwell. "A dynamical theory of the electromagnetic field." In: *Philosophical Transactions of the Royal Society of London* 155 (1865), pp. 459–512 (page 3).

[5] E. P. Wigner. "On Unitary Representations of the Inhomogeneous Lorentz Group." In: *Annals of Mathematics* 40.1 (1939), pp. 149–204 (pages 4, 30).

[6] V. Bargmann and E. P. Wigner. "Group Theoretical Discussion of Relativistic Wave Equations." In: *Proceedings of the National Academy of Sciences* 34.5 (1948), pp. 211–223 (pages 4, 30, 32).

[7] E. P. Wigner. "Events, Laws of Nature, and Invariance Principles." In: *Science* 145.3636 (1964), pp. 995–999 (page 4).

[8] I. Bialynicki-Birula. "Photon wave function." In: *Progress in Optics*. Ed. by Emil Wolf. Vol. 36. Elsevier, 1996. Chap. 5, pp. 245–294 (pages 4, 10, 16, 26, 33, 35, 37, 74, 75).

[9] E. P. Wigner. *Group theory and its applications to the quantum mechanics of atomic spectra*. Academic Press, 1959 (page 5).

[10] D. J. Gross. "Symmetry in Physics: Wigner's Legacy." In: *Physics Today* 48.12 (1995), pp. 46–50 (page 5).

[11] E. Yablonovitch, T. J. Gmitter, and K. M. Leung. "Photonic band structure: The face-centered-cubic case employing nonspherical atoms." In: *Physical Review Letters* 67 (1991), pp. 2295–2298 (page 5).

[12] J. D. Jackson. *Classical Electrodynamics*. John Wiley and Sons, Inc., 1999 (pages 8, 10, 35, 45, 46, 51, 52, 54, 56, 57, 64, 67).

[13] M. Born and E. Wolf. *Principles of Optics*. Cambridge University Press, 1999 (pages 8, 13).

[14] C. F. Bohren and D. R. Huffman. *Absorption and scattering of light by small particles*. John Wiley and Sons, Inc., 1998 (pages 9, 55, 58, 59, 61, 79).

[15] I. Fernández-Corbaton, X. Zambrana-Puyalto, and G. Molina-Terriza. "Helicity and angular momentum: A symmetry-based framework for the study of light-matter interactions." In: *Physical Review A* 86 (2012), p. 042103 (pages 10, 36, 42, 43, 69).

[16] I. Bialynicki-Birula and Z. Bialynicka-Birula. "The role of the Riemann–Silberstein vector in classical and quantum theories of electromagnetism." In: *Journal of Physics A: Mathematical and Theoretical* 46.5 (2013), p. 053001 (pages 11, 12).

[17] R. H. Good. "Particle Aspect of the Electromagnetic Field Equations." In: *Physical Review* 105 (1957), pp. 1914–1919 (page 12).

[18] Iwo Bialynicki-Birula and Zofia Bialynicka-Birula. "Quantum-mechanical description of optical beams." In: *Journal of Optics* 19.12 (2017), p. 125201 (pages 13, 30, 37).

[19] W. Tung. *Group Theory in Physics*. World Scientific, 1985 (pages 17, 20, 21, 30, 31, 34–36, 40, 41, 44, 45, 90).

[20] M. Hamermesh. *Group theory and its applications to physical problems*. Addison-Wesley Publishing Company, Inc., 1964 (page 17).

[21] G. Mie. "Beiträge zur Optik trüber Medien, speziell kolloidaler Metallösungen." In: *Annalen der Physik* 330.3 (1908), pp. 377–445 (pages 20, 50).

[22] H. Goldstein. *Classical Mechanics*. Addison-Wesley Publishing Co., 1980 (page 20).

[23] W. Rossmann. *Lie groups: An introduction through linear groups*. Oxford University Press, 2002 (page 21).

[24] J. S. Lomont and H. E. Moses. "Simple Realizations of the Infinitesimal Generators of the Proper Orthochronous Inhomogeneous Lorentz Group for Mass Zero." In: *Journal of Mathematical Physics* 3.3 (1962), pp. 405–408 (pages 21, 26, 31, 32, 37).

[25] I. Bialynicki-Birula and Z. Bialynicka-Birula. "Canonical separation of angular momentum of light into its orbital and spin parts." In: *Journal of Optics* 13.6 (2011), p. 064014 (pages 21, 26).

[26] H. Bacry. "A set of wave equations for massless fields which generalize Weyl and Maxwell's equations." In: *Il Nuovo Cimento A* 32 (1976), pp. 448–460 (pages 21, 31–33).

[27] P. M. Mathews. "Relativistic Schrödinger Equations for Particles of Arbitrary Spin." In: *Physical Review* 143 (1966), pp. 978–985 (pages 21, 26).

[28] A. Messiah. *Quantum Mechanics, Volume 1*. North Holland Publishing Company, 1962 (pages 21, 27).

[29] L. H. Ryder. *Quantum Field Theory*. Cambridge University Press, 1996 (pages 21, 32).

[30] W. Greiner and J. Reinhardt. *Field quantization*. Springer, 1996 (page 26).

[31] P. Woit. *Quantum Theory, Groups and Representations: An Introduction*. 2021 (page 26).

[32] P. A. M. Dirac. "Relativistic wave equations." In: *Proceedings of the Royal Society of London. Series A - Mathematical and Physical Sciences* 155.886 (1936), pp. 447–459 (pages 27, 32).

[33] A. Gersten. "Maxwell's Equations as the One-Photon Quantum Equation." In: *Foundations of Physics Letters* 12.3 (1999), pp. 291–298 (pages 27, 32, 33).

[34] S. Weinberg. *The quantum theory of fields*. Vol. I. Cambridge University Press, 1995 (page 30).

[35] J. Patera, P. Winternitz, and H. Zassenhaus. "Continuous subgroups of the fundamental groups of physics. I. General method and the Poincaré group." In: *Journal of Mathematical Physics* 16.8 (1975), pp. 1597–1614 (pages 30, 39).

[36] V. Bargmann. "Irreducible Unitary Representations of the Lorentz Group." In: *Annals of Mathematics* 48.3 (1947), pp. 568–640 (page 31).

[37] I. Bialynicki-Birula. "On the wave function of the photon." In: *Acta Physica Polonica A* 86 (1994), pp. 97–116 (page 33).

[38] M. Vavilin and I. Fernández-Corbaton. *The Polychromatic T-matrix*. 2023. arXiv: 2306.07776 (pages 34, 36).

[39] M. E. Rose. *Elementary theory of angular momentum*. John Wiley and Sons, Inc., 1957 (page 35).

[40] H. Minkowski. "Die Grundgleichungen für die elektromagnetischen Vorgänge in bewegten Körpern." In: *Nachrichten von der Gesellschaft der Wissenschaften zu Göttingen, Mathematisch sPhysikalische Klasse* (1908), pp. 53–111 (page 39).

[41] A. Einstein. *Collected papers of Albert Einstein, Volume 2: The Swiss Years.* Princeton University Press, 1989 (page 39).

[42] L. D. Landau and E. M. Lifshitz. *Electrodynamics of continuous media*. Pergamon Press, 1984 (page 39).

[43] P. Winternitz. "Subgroups of Lie groups and symmetry breaking." In: *Group Theoretical Methods in Physics*. Ed. by Robert T. Sharp and Bernard Kolman. Academic Press, 1977, pp. 549–572 (page 39).

[44] J. Patera, P. Winternitz, and H. Zassenhaus. "Continuous subgroups of the fundamental groups of physics. II. The similitude group." In: *Journal of Mathematical Physics* 16.8 (1975), pp. 1615–1624 (page 39).

[45] J. Patera, R. T. Sharp, P. Winternitz, and H. Zassenhaus. "Continuous subgroups of the fundamental groups of physics. III. The de Sitter groups." In: *Journal of Mathematical Physics* 18.12 (1977), pp. 2259–2288 (page 39).

[46] L. Gagnon and P. Winternitz. "Lie symmetries of a generalised nonlinear Schrodinger equation: I. The symmetry group and its subgroups." In: *Journal of Physics A: Mathematical and General* 21.7 (1988), pp. 1493–1511 (page 39).

[47] J. Beckers, J. Patera, M. Perroud, and P. Winternitz. "Subgroups of the Euclidean group and symmetry breaking in nonrelativistic quantum mechanics." In: *Journal of Mathematical Physics* 18.1 (1977), pp. 72–83 (page 39).

[48] J. Patera, R. T. Sharp, P. Winternitz, and H. Zassenhaus. "Subgroups of the Poincaré group and their invariants." In: *Journal of Mathematical Physics* 17.6 (1976), pp. 977–985 (pages 39, 91).

[49] G. W. Mackey. *Unitary Group Representations in Physics, Probability and Number Theory*. The Benjamin/Cummings Publishing Company, Inc., 1978 (pages 39–41, 93).

[50] G. Molina-Terriza. "Determination of the total angular momentum of a paraxial beam." In: *Physical Review A* 78 (2008), p. 053819 (page 42).

[51] I. Fernández-Corbaton. "Helicity and duality symmetry in light matter interactions: theory and applications." 2014 (page 44).

[52] J. A. Stratton. *Electromagnetic theory*. McGraw-Hill Book Company, Inc., 1941 (pages 44, 50).

[53] X. Zambrana-Puyalto. "Control and characterization of nanostructures with the symmetries of light." 2014 (page 45).

[54] N. Tischler, X. Zambrana-Puyalto, and G. Molina-Terriza. "The role of angular momentum in the construction of electromagnetic multipolar fields." In: *European Journal of Physics* 33.5 (2012), pp. 1099–1109 (pages 45, 46, 58).

[55] H. Horvath. "Gustav Mie and the scattering and absorption of light by particles: Historic developments and basics." In: *Journal of Quantitative Spectroscopy and Radiative Transfer* 110.11 (2009), pp. 787–799 (page 50).

[56] A. Neves and C. L. Cesar. "Analytical calculation of optical forces on spherical particles in optical tweezers: tutorial." In: *Journal of the Optical Society of America B* 36.6 (2019), pp. 1525–1537 (page 53).

[57] B. Carrascal, G. A. Estevez, P. Lee, and V. Lorenzo. "Vector spherical harmonics and their application to classical electrodynamics." In: *European Journal of Physics* 12.4 (1991), pp. 184–191 (pages 56, 57, 65, 68).

[58] J. H. Crichton and P. L. Marston. "The measurable distinction between the spin and orbital angular momenta of electromagnetic radiation." In: *Electronic Journal of Differential Equations* 4 (2000), pp. 37–50 (page 56).

[59] J. Lasa-Alonso, J. Olmos-Trigo, A. García-Etxarri, and G. Molina-Terriza. "Correlations between helicity and optical losses within general electromagnetic scattering theory." In: *Materials Advances* 3 (2022), pp. 4179–4185 (pages 58, 94).

[60] C. F. Bohren. "Light scattering by an optically active sphere." In: *Chemical Physics Letters* 29.3 (1974), pp. 458–462 (page 58).

[61] I. Fernández-Corbaton, X. Zambrana-Puyalto, N. Tischler, X. Vidal, M. L. Juan, and G. Molina-Terriza. "Electromagnetic Duality Symmetry and Helicity Conservation for the Macroscopic Maxwell's Equations." In: *Physical Review Letters* 111 (2013), p. 06 0401 (pages 60, 64, 82, 91).

[62] X. Zambrana-Puyalto, I. Fernández-Corbaton, M. L. Juan, X. Vidal, and G. Molina-Terriza. "Duality symmetry and Kerker conditions." In: *Optics Letters* 38.11 (2013), pp. 1857–1859 (pages 61, 82).

[63] I. Fernández-Corbaton. "Forward and backward helicity scattering coefficients for systems with discrete rotational symmetry." In: *Optics Express* 21 (2013), pp. 29885–29893 (page 61).

[64] A. Alú and N. Engheta. "How does zero forward-scattering in magnetodielectric nanoparticles comply with the optical theorem?" In: *Journal of Nanophotonics* 4 (2010), p. 041590 (pages 61, 62).

[65] L. Novotny and B. Hetch. *Principles of Nano-optics*. Cambridge University Press, 2006 (pages 61, 77).

[66] X. Zambrana-Puyalto, X. Vidal, and G. Molina-Terriza. "Excitation of single multipolar modes with engineered cylindrically symmetric fields." In: *Optics Express* 20.22 (2012), pp. 24536–24544 (page 69).

[67] I. Bialynicki-Birula. "The Photon Wave Function." In: *Coherence and Quantum Optics VII*. Ed. by J. H. Eberly, L. Mandel, and E. Wolf. Springer, 1996, pp. 313–322 (page 75).

[68] C. L. Giles and W. J. Wild. "Fresnel reflection and transmission at a planar boundary from media of equal refractive indices." In: *Applied Physics Letters* 40.3 (1982), pp. 210–212 (page 78).

[69] A. Lakhtakia. "On pathological conditions and Fresnel coefficients." In: *International Journal of Infrared and Milimiter Waves* 11.12 (1990), pp. 1407–1413 (page 78).

[70] M. Kerker, D. Wang, and C. L. Giles. "Electromagnetic scattering by magnetic spheres." In: *Journal of the Optical Society of America* 73.6 (1983), pp. 765–767 (pages 80, 95, 119).

[71] D. J. Griffiths. *Introduction to Quantum Mechanics*. Pearson Education, Inc., 2005 (page 85).

[72] C. Cohen-Tannoudji, B. Diu, and F. Laloë. *Quantum Mechanics*. John Wiley and Sons, Inc., 1977 (pages 85, 88, 89).

[73] L. D. Landau and E. M. Lifshitz. *Quantum Mechanics: non-relativistic theory*. Pergamon Press, 1991 (page 85).

[74] S. P. Mikheyev and A. Y. Smirnov. "Resonant amplification of ν oscillations in matter and solar-neutrino spectroscopy." In: *Il Nuovo Cimento C* 9 (1986), pp. 17–26 (page 88).

[75] S. P. Mikheyev and A. Y. Smirnov. "Resonant neutrino oscillations in matter." In: *Progress in Particle and Nuclear Physics* 23 (1989), pp. 41–136 (page 88).

[76] M. G. Calkin. "An Invariance Property of the Free Electromagnetic Field." In: *American Journal of Physics* 33.11 (1965), p. 958 (page 91).

[77] J. Patera, R. T. Sharp, P. Winternitz, and H. Zassenhaus. "Subgroups of the Poincaré group and their invariants." In: *Journal of Mathematical Physics* 17.6 (1976), pp. 977–985 (page 93).

[78] J. R. Taylor. *Scattering theory: the quantum theory of nonrelativistic collisions*. John Wiley and Sons, Inc., 1972 (page 93).

[79] S. Liñares Beiras. *Estados Puros e Mestura de Luz Cuántica*. Universidade de Santiago de Compostela, 2016 (page 99).

[80] Á. Nodar. "Theoretical description of light emission in the presence of nanoscale resonators: from classical scattering to phootn states entanglement and statistics." 2023 (pages 99, 106).

[81] R. Loudon. *The quantum theory of light*. Oxford University Press, 2001 (pages 101, 102, 107).

[82] L. Mandel and E. Wolf. *Optical coherence and quantum optics*. Cambridge University Press, 1995 (pages 102, 109).

[83] P. C. Waterman. "Matrix formulation of electromagnetic scattering." In: *Proceedings of the IEEE* 53.8 (1965), pp. 805–812 (page 102).

[84] M. I. Mishchenko, L. D. Travis, and D. W. Mackowski. "T-matrix computations of light scattering by nonspherical particles: A review." In: *Journal of Quantitative Spectroscopy and Radiative Transfer* 55.5 (1996), pp. 535–575 (page 102).

[85] M. Fruhnert, I. Fernández-Corbaton, V. Yannopapas, and C. Rockstuhl. "Computing the T-matrix of a scattering object with multiple plane wave illuminations." In: *Beilstein Journal of Nanotechnology* 8 (2017), pp. 614–626 (page 103).

[86] Á. Nodar, R. Esteban, C. Maciel-Escudero, J. Lasa-Alonso, J. Aizpurua, and G. Molina-Terriza. *Preservation and destruction of the purity of two-photon states in the interaction with a nanoscatterer*. 2022. arXiv: 2211.14244 (page 106).

[87] A. Büse, M. L. Juan, N. Tischler, V. D'Ambrosio, F. Sciarrino, L. Marrucci, and G. Molina-Terriza. "Symmetry protection of photonic entanglement in the interaction with a single nanoaperture." In: *Physical Review Letters* 121 (2018), p. 173901 (pages 106, 107).

[88] N. Tischler, C. Rockstuhl, and K. Słowik. "Quantum Optical Realization of Arbitrary Linear Transformations Allowing for Loss and Gain." In: *Physical Review X* 8 (2018), p. 021017 (pages 107, 110).

[89] S. M. Barnett, J. Jeffers, A. Gatti, and R. Loudon. "Quantum optics of lossy beam splitters." In: *Physical Review A* 57 (1998), pp. 2134–2145 (page 109).

[90] R. Uppu, T. A. W. Wolterink, T. B. H. Tentrup, and P. W. H. Pinkse. "Quantum optics of lossy asymmetric beam splitters." In: *Optics Express* 24.15 (2016), pp. 16440–16449 (page 109).

[91] J. Sperling, A. Perez-Leija, K. Busch, and C. Silberhorn. "Mode-independent quantum entanglement for light." In: *Physical Review A* 100 (6 2019), p. 062129 (page 112).

[92] K. Eckert, J. Schliemann, D. Bruss, and M. Lewenstein. "Quantum Correlations in Systems of Indistinguishable Particles." In: *Annals of Physics* 299 (2002), p. 88 (page 112).

[93] Y. S. Li, B. Zeng, X. S. Liu, and G. L. Long. "Entanglement in a two-identical-particle system." In: *Physical Review A* 64 (5 2001), p. 054302 (page 112).

[94] J. Brendel, N. Gisin, W. Tittel, and H. Zbinden. "Pulsed Energy-Time Entangled Twin-Photon Source for Quantum Communication." In: *Physical Review Letters* 82 (1999), pp. 2594–2597 (page 115).

[95] P. P. Rohde. "Simple scheme for universal linear-optics quantum computing with constant experimental complexity using fiber loops." In: *Physical Review A* 91 (2015), p. 012306 (page 115).